The Thesis Committee for Neeraj Anil Karnik

Certifies that this is the approved version of the following thesis:

Sensitivity Analysis of Impedance-based Fault Location Methods

APPROVED BY

SUPERVISING COMMITTEE:

Supervisor: _____

Surya Santoso

_____

W.Mack Grady

Sensitivity Analysis of Impedance-based Fault Location Methods

by

Neeraj Anil Karnik, B.Tech.

THESIS

Presented to the Faculty of the Graduate School of

of the University of Texas at Austin

in Partial Fulfillment

of the Requirements

for the Degree of

Master of Science in Engineering

THE UNIVERSITY OF TEXAS AT AUSTIN

December 2011

This work is dedicated to my parents and my sister.

Acknowledgments

I consider myself fortunate to have Dr. Surya Santoso as my research advisor. I joined his research group in Fall 2009 and I have been working with him for two years. During this time, he provided me financial support in the form teaching and research assistant positions. He gave me the opportunity to work on a challenging project for this thesis. He offered sound technical advice whenever I faced a problem. Simply put, Dr. Santoso's exemplary guidance, motivation and support made this thesis possible.

I am greatful to Dr. Mack Grady for having graciously agreed to serve as reader for this thesis.

I thank my friend and colleague Swagata Das for being an excellent project partner. I had a great time working with her and I believe we achieved a lot through teamwork.

Lastly, I also thank my parents Mr. Anil and Mrs. Supriya Karnik, my sister Madhura and my fiancée Rujuta for their love, support and encouragement.

Statement of Originality and Academic Integrity

I certify that I have completed the online ethics training modules, particularly the Academic Integrity Module [1] (Completed on 10/09/2011), of the University of Texas at Austin - Graduate School. I fully understand, and I am familiar with the University policies and regulations relating to academic integrity and the academic policies and procedures [2].

I attest that this thesis is the result of my own original work and efforts. Any ideas of other authors, whether or not they have been published or otherwise disclosed, are fully acknowledged and properly referenced.

I acknowledge the thoughts, direction and supervision of my research advisor, Professor Surya Santoso. I give him consent to use the materials presented herein for publication, instructional and research activities.

[1] The University of Texas at Austin - Graduate School's online ethics training on academic integrity, http://www.utexas.edu/ogs/student_services/ethics/academic.html

[2] The Catalog of the University of Texas at Austin, General Information, 2010-2011, Appendix C, Sec. 11 - 402, http://registrar.utexas.edu/docs/catalogs/gi/ut-catalog-gi1011.pdf

Sensitivity Analysis of Impedance-based Fault Location Methods

Neeraj Anil Karnik, MSE
The University of Texas at Austin, 2011

Supervisor: Surya Santoso

Impedance-based methods are used to locate faults on distribution systems because of their simplicity and ease of implementation. These methods require fault voltage and current data along with the positive- and zero-sequence line impedance values (in ohm per unit length) to estimate the reactance or distance to fault location. Inaccuracies in line impedance values, which arise from circuit model errors, have an adverse impact on fault location estimates of the impedance-based methods. Measurement errors in current and voltage transformers can also lead to inaccuracy in estimation. Further, all methods use simplistic models to represent the system load. The load in a practical distribution system does not conform to the oversimplified models leading to errors in estimation of fault location.

This thesis presents sensitivity analysis of four impedance-based methods. It focuses on the Takagi, positive-sequence reactance, loop reactance and balanced-load methods. Amongst these four methods, the first three are commonly used for fault location. The fourth method was developed as a part of this work. The objective of sensitivity analysis is to study and quantify

the effect of circuit model, measurement and load model errors, on the fault location estimates of the four methods. The results of this analysis are used to establish upper and lower bounds on the estimation errors for each method.

The analysis begins with creation of a baseline case using a modified version of the IEEE 34 Node Test Feeder. All the methods estimate the reactance to fault location as a part of this analysis. The baseline case uses accurate line impedances and measurement values in the four methods. The fault location estimates for this case serve as a means of comparison for all subsequent analyzes.

Secondly, various circuit model errors are introduced while computing the line impedance values. These errors include inaccurate modeling of four parameters viz. phase conductor distances, conductor sizes, phase to neutral conductor distances and earth resistivity. The erroneous line impedance values, which arise from these circuit model errors, are used in the four methods. The resultant location estimates are compared with those for the baseline case. It is observed that modeling errors in earth resistivity can cause estimation errors of 2% to 5% in the Takagi and positive-sequence reactance methods. These errors can be positive or negative depending upon whether the modeled earth resistivity value is more than or less than the accurate value. The effect of inaccurate modeling of the other three parameters is marginal. Additionally, the Takagi and positive-sequence reactance methods assume line impedances to be uniform while estimating fault location. Although this assumption is a type of circuit model error, it does not lead to significant errors in estimation. The loop reactance and balanced-load methods are insensitive to circuit model errors as they do not use line impedance values while estimating reactance to fault location.

The next part is analysis of effect of measurement errors on fault location estimates. Ratio and phase angle errors are deliberately introduced in the current and voltage transformers and the erroneous measurements are used to conduct fault location. This causes 5% to 6% errors in estimation for the Takagi and positive-sequence reactance methods. These estimation errors can be positive or negative depending upon the magnitude of the CT and VT ratio errors and the sign of the phase angle errors. For the loop reactance method, erroneous measurements introduce 8% to 30% errors in fault location. This indicates that the loop reactance method is highly sensitive to measurement errors. The balanced-load method is moderately sensitive and experiences 6% to 7% errors in fault location estimates.

Lastly, the effect of load current on fault location estimates is analyzed. When the Takagi and positive-sequence reactance methods are used on a heavily loaded system, they estimate fault location with an error of 5% to 8%. The loop reactance method is severely affected by the level of load current in the system. This method can estimate fault location with nearly 100% accuracy, on a lightly loaded system. However, the estimation errors for this method increase significantly and are in the range of 15% to 30%, as load current in the system increases. In case of the balanced-load method, unbalanced, heavy loads can cause estimation errors of 7% to 25%.

The combined effect of all the error sources is taken into account by creating a confidence interval for each method. For the Takagi and positive-sequence reactance methods, the actual fault location can be expected to lie within $\pm 10\%$ of the estimated value. The fault location estimation error for the loop reactance and balanced-load methods is always positive. The actual reactance-to-fault is within -30% of the value estimated by these methods.

Table of Contents

List of Figures

List of Tables

Chapter 1

Overview of Impedance-based Methods and Objective of Sensitivity Analysis

Transmission and distribution lines in electric power systems are subjected to permanent as well as temporary faults. Permanent faults put the line out of service and lead to sustained interruptions. Temporary faults cause short-duration voltage variations like voltage sags [1]. They leave a residue of damage which must be repaired at the earliest opportunity [2]. In either case, it is important to determine the location of the fault, so that the line can be repaired and restored as soon as possible. A number of methods have been developed to locate faults on transmission and distribution lines. They can be broadly classified into hardware based approaches, impedance-based methods, traveling-wave methods and fuzzy logic/neural network based approaches [3]. This thesis concentrates on impedance-based methods.

Impedance-based methods are commonly used to locate faults on distribution systems because of their simplicity and ease of implementation. The main inputs for these methods are the voltage and current measurements recorded by a power quality monitor or a relay. They also require the positive- and zero-sequence z_1 and z_0 line impedance values (in Ω per unit length) while estimating fault location. The output of these methods is in terms of reactance or distance to fault location.

This Chapter begins with an overview of three popular impedance-

based methods: the Takagi method [2] [4], the positive-sequence reactance method [5] [6] and the loop reactance method [3]. The three methods are briefly reviewed in Section 1.1. This Section also highlights important assumptions made by these methods. A new impedance-based method, called as the balanced-load method, was developed as a part of this thesis. Section 1.2 presents a detailed derivation of this method.

Section 1.3 identifies the main factors which cause fault location estimates of the impedance-based methods to be erroneous [7] [8]. This section points out that inaccurate circuit modeling causes errors in computation of z_1 and z_0 values. The erroneous z_1 and z_0 values in turn have an adverse impact on accuracy of estimation. Errors in voltage and current measurements, which arise from inadequacies of instrument transformers, also affect estimation accuracy. Additionally, the impedance-based methods make a number of simplifying assumptions regarding the system load. These assumptions are not satisfied in a practical distribution system, leading to errors in estimation.

The objective of sensitivity analysis is to study and quantify the effect of each of the factors identified in Section 1.3, on accuracy of the impedance-based methods. Subsequent Chapters build on the foundation created in Chapter 1.

1.1 Commonly Used Impedance Based Methods

The Takagi method, the positive-sequence reactance method and the loop reactance method are three well known fault location methods. These methods make certain assumptions, while deriving the expression for reactance- or distance-to-fault. Although this leads to some loss in accuracy, the resultant expression for fault location is easier to compute. This Section presents the

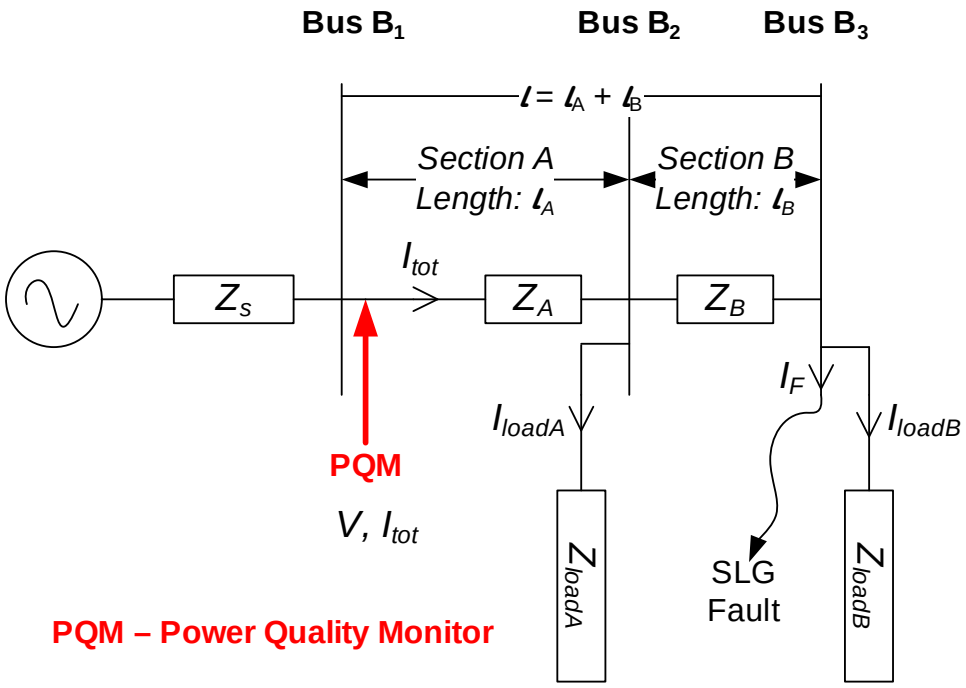

Figure 1.1: Single Line-to-ground Fault on a Distribution System

derivations of the three methods. All the simplifying assumptions made by these methods are highlighted.

The single line diagram for a distribution system is shown in Figure 1.1. There are three buses in the network. Bus B_1 is the substation bus. There is a relay or a power quality monitor (PQM) at this bus which records voltage and current values. There are two sections of distribution lines: Section A is longer and occupies a length l_A whereas Section B has a shorter length l_B. The total length of distribution lines from Bus B_1 to Bus B_3 is $l = l_A + l_B$. The distribution lines are represented by a short transmission line model [9]. Line admittances are neglected and Z_A and Z_B (in Ω) are the positive-sequence impedances of the two sections. The positive-sequence line impedances are z_A

and z_B (in Ω per unit length). Hence $Z_A = l_A z_A$ and $Z_B = l_B z_B$. It is to be noted that adjacent sections of the distribution system may be constructed using different conductor types and pole configurations. As a result, the values of line impedances z_A and z_B, which depend on factors like conductor sizes and distance between phase conductors, may differ for each section. Further, loads are present at buses B_2 and B_3. The load impedances are represented by Z_{loadA} and Z_{loadB}.

A single line-to-ground (SLG) fault occurs at bus B_3. The impedance to fault as measured from the monitoring point is $Z_A + Z_B$. The current I_{tot} recorded by the PQM is given by: $I_{tot} = I_F + I_{loadA} + I_{loadB}$

where, I_F = fault current

I_{loadA} and I_{loadB} = currents drawn by the two loads.

The current I_{tot} flows through Z_A whereas $I_F + I_{loadB}$ flows through Z_B.

While deriving the expression for impedance-to-fault, two assumptions are made.

Lumped Load Assumption:

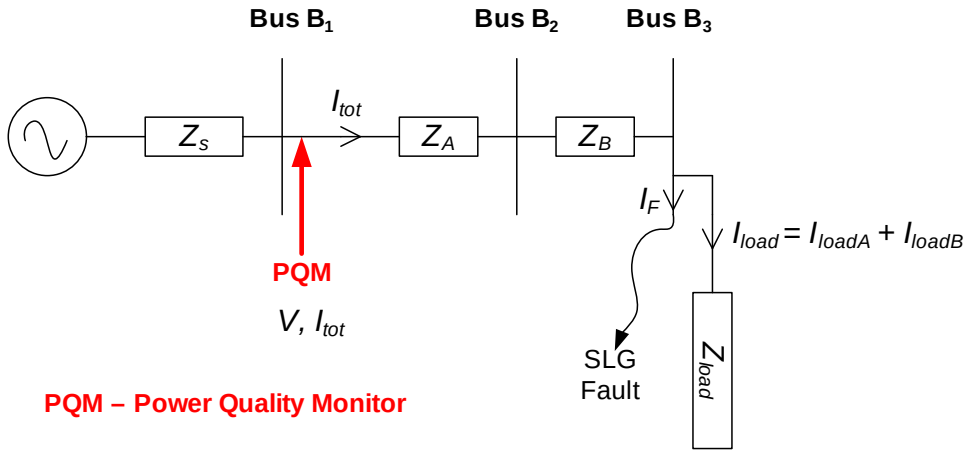

Figure 1.2: System Load Lumped Beyond the Fault Point

In the simplified system shown in Figure 1.2 the distributed load impedances Z_{loadA} and Z_{loadB} are replaced by a single impedance Z_{load}. It is placed at the faulted bus B_3. This impedance draws current I_{load} which is given by $I_{load} = I_{loadA} + I_{loadB}$. In Fig. 1.1 the current $I_F + I_{loadB}$ flows through Z_B. However in the simplified system (Fig. 1.2) the current $I_F + I_{loadA} + I_{loadB}$ flows through Z_B. In effect the voltage drop caused by I_{loadA} across Z_B is ignored leading to an inaccurate circuit representation. The degree of inaccuracy depends upon the magnitude of I_{loadA}. If this magnitude is high, then the lumped load assumption can lead to significant errors in fault location.

As no current is drawn at Bus B_2 in the simplified system, the impedances Z_A and Z_B are in series. They can be represented by a single impedance Z_{actual} which is equal to $Z_A + Z_B$ as shown in Figure 1.3.

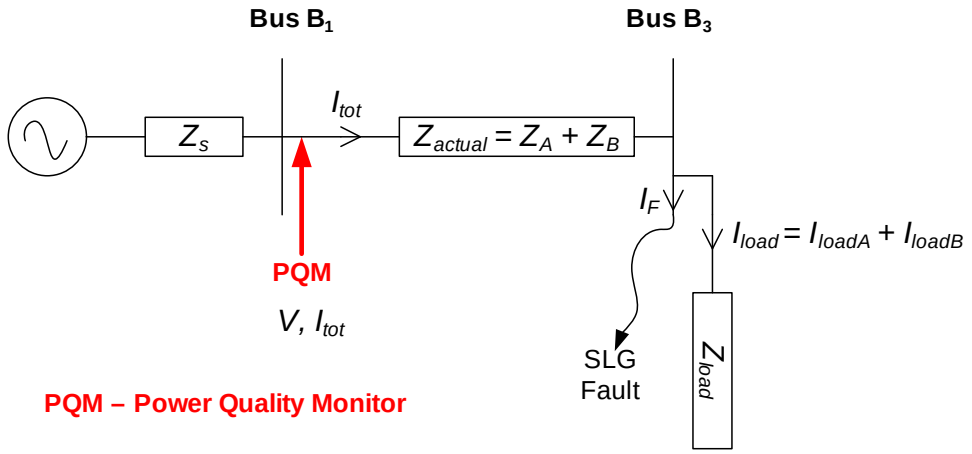

Figure 1.3: System With Lumped Load and Combined Line Impedance

Uniform Line Impedance Assumption:

The system in Figure 1.3 is further simplified by the uniform line impedance assumption. The actual impedance between buses B_1 and B_3 is $Z_{actual} = Z_A + Z_B = l_A z_A + l_B z_B$.

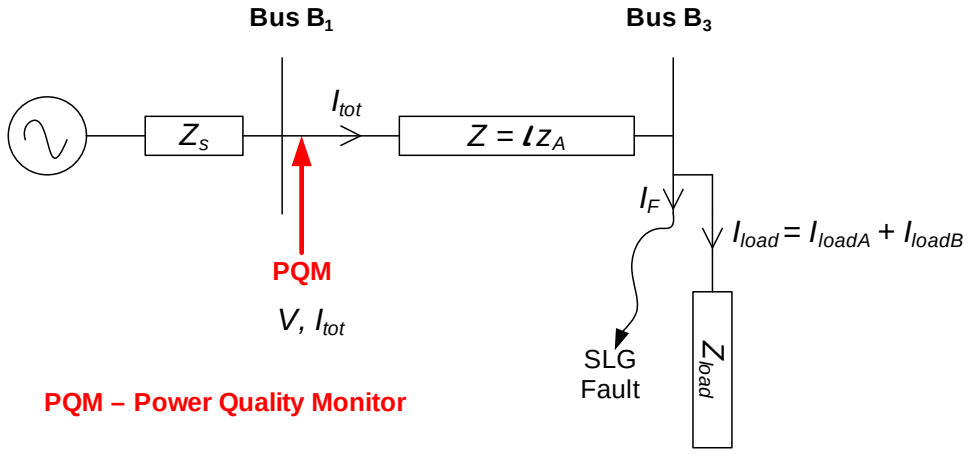

Figure 1.4: SLG Fault on a System with Lumped Load and Uniform Line Impedance

However in the system shown in Figure 1.4 the impedance between these buses is $Z = lz_A$. It is mentioned previously that Section A occupies a larger portion of the total system. Hence the line impedance value corresponding to this section (i.e. z_A) is used to represent the entire system. In short, it is assumed that the system has uniform line impedance of z_A Ω per unit length.

1.1.1 Fundamental Equation for a Single Line-to-ground Fault

The sequence network representation of the system in Figure 1.4 is shown in Figure 1.5. Here Z_1, Z_2 and Z_0 are the positive-, negative- and zero-sequence impedances between the monitoring point and the fault location. The sequence impedances of the load are represented by Z_{L1}, Z_{L2} and Z_{L0}. The total current recorded by the monitor I_{tot}, the fault current I_F and the load current I_{load} are also split into their sequence components. The sequence components of the voltages at the monitoring location are V_1, V_2 and V_0 while V_{F1}, V_{F2} and V_{F0} represent the sequence voltages at the fault point.

Applying Kirchhoff's voltage law to the positive-, negative- and zero-sequence networks:

$$V_1 = I_{tot1}Z_1 + V_{F1} \tag{1.1}$$

$$V_2 = I_{tot2}Z_2 + V_{F2} \tag{1.2}$$

$$V_0 = I_{tot0}Z_0 + V_{F0} \tag{1.3}$$

Adding (1.1), (1.2) and (1.3)

$$V_1 + V_2 + V_0 = I_{tot1}Z_1 + V_{F1} + I_{tot2}Z_2 + V_{F2} + I_{tot0}Z_0 + V_{F0} \tag{1.4}$$

As $V = V_1 + V_2 + V_0$ and $V_F = V_{F1} + V_{F2} + V_{F0}$, (1.4) is simplified to:

$$V = V_F + I_{tot1}Z_1 + I_{tot2}Z_2 + I_{tot0}Z_0 \tag{1.5}$$

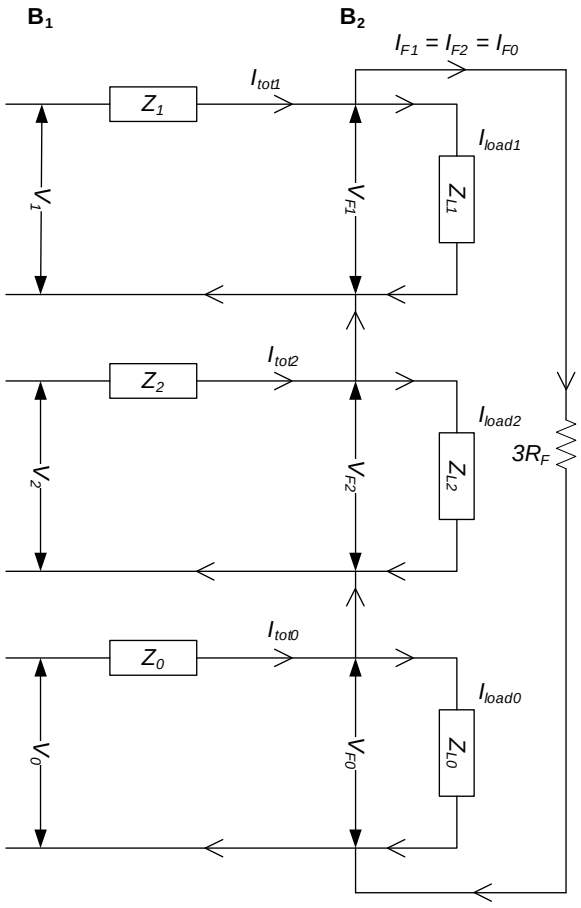

Figure 1.5: Sequence Network Representation for SLG Fault on Bus B_3

When the fault resistance is R_F, $V_F = 3I_0R_F$. Also for an SLG fault, $3I_0 = I_F$ so that $V_F = I_FR_F$. Hence

$$V = I_{tot1}Z_1 + I_{tot2}Z_2 + I_{tot0}Z_0 + I_FR_F \tag{1.6}$$

Further, for static equipment like transmission lines, the positive- and negative-sequence impedances are equal [9]. As $Z_1 = Z_2$, (1.6) can be simplified as:

$$V = (I_{tot1} + I_{tot2})Z_1 + I_{tot0}Z_0 + I_FR_F \tag{1.7}$$

Equation (1.7) is the basic equation for an SLG fault on a radial system. The only simplifications made while deriving (1.7) are lumped load and uniform line impedance assumptions. All three methods use (1.7) and make additional assumptions while deriving the expression for impedance-to-fault.

1.1.2 Expression for the Positive-sequence Reactance Method

The term $I_{tot0}Z_1$ is added and subtracted from the RHS of (1.7) [10]

$$V = (I_{tot1} + I_{tot2})Z_1 + I_{tot0}Z_1 - I_{tot0}Z_1 + I_{tot0}Z_0 + I_F R_F$$

$$\therefore V = (I_{tot1} + I_{tot2} + I_{tot0})Z_1 + I_{tot0}(Z_0 - Z_1) + I_F R_F$$

Now, $I_{tot1} + I_{tot2} + I_{tot0} = I_{tot}$ = current value recorded at the monitoring location.

$$\therefore V = I_{tot}Z_1 + I_{tot0}(Z_0 - Z_1) + I_F R_F$$

$$\therefore V = Z_1 \left(I_{tot} + I_{tot0}\frac{Z_0 - Z_1}{Z_1} \right) + I_F R_F$$

Now l is the distance of the fault from the monitoring location. Also it is assumed that the system has uniform positive- and zero-sequence z_1 and z_0 line impedances. As a result: $Z_1 = lz_1$ and $Z_0 = lz_0$. Hence:

$$V = Z_1 \left(I_{tot} + I_{tot0}\frac{lz_0 - lz_1}{lz_1} \right) + I_F R_F \tag{1.8}$$

The factor k is defined as:

$$k = \frac{z_0 - z_1}{z_1} \tag{1.9}$$

From (1.8) and (1.9)

$$V = Z_1(I_{tot} + kI_{tot0}) + I_F R_F \tag{1.10}$$

The current I_S is defined as:

$$I_S = I_{tot} + kI_{tot0} \tag{1.11}$$

$$\therefore V = Z_1 I_S + I_F R_F \tag{1.12}$$

The positive-sequence reactance method divides (1.12) by I_S

$$\frac{V}{I_S} = Z_1 + \frac{I_F R_F}{I_S} \tag{1.13}$$

To compensate for the effect of fault resistance only the imaginary part of (1.13) is computed.

$$imag\left(\frac{V}{I_S}\right) = imag(Z_1) + imag\left(\frac{I_F R_F}{I_S}\right) \tag{1.14}$$

Now if I_F and I_S are in phase with each other,$\frac{I_F}{I_S}$ is a real number, so that $imag\left(\frac{I_F R_F}{I_S}\right) = 0$.

The positive-sequence reactance-to-fault X_1 is given by:

$$X_1 = imag(Z_1) = imag\left(\frac{V}{I_S}\right) \tag{1.15}$$

Thus the positive-sequence reactance method assumes that I_S and I_F are in phase. For a non-zero fault resistance, phase difference between I_S and I_F can cause errors in estimation of X_1. If the distance to fault location l is desired, it can be computed as:

$$l = \frac{X_1}{imag(z_1)} \tag{1.16}$$

where z_1 = positive-sequence impedance of the line in ohm per unit length.

1.1.3 Expression for the Takagi Method

The Takagi method assumes that the load current during the fault remains constant at its pre-fault value [2] [4]. In essence, the load is represented

by a constant current load model. If $I_{pre-flt}$ is the pre-fault load current, the method then computes the superposition current as follows:

$$I_{sup} = I_{tot} - I_{pre-flt} \tag{1.17}$$

The main assumption is that $I_{sup} = I_F$. Equation (1.12) can now be written as:

$$V = Z_1 I_S + I_{sup} R_F \tag{1.18}$$

Multiplying both sides of (1.18) by the conjugate of I_{sup} i.e. I^*_{sup}:

$$VI^*_{sup} = Z_1 I_S I^*_{sup} + I_{sup} I^*_{sup} R_F$$

$$\therefore imag(VI^*_{sup}) = imag(Z_1 I_S I^*_{sup}) + imag(I_{sup} I^*_{sup} R_F)$$

As $I_{sup} I^*_{sup}$ is a real number, $imag(I_{sup} I^*_{sup} R_F) = 0$

$$\therefore imag(VI^*_{sup}) = imag(Z_1 I_S I^*_{sup})$$

Further, $Z_1 = lz_1$ and l is a real number:

$$\therefore imag(VI^*_{sup}) = l \times imag(z_1 I_S I^*_{sup})$$

$$\therefore l = \frac{imag(VI^*_{sup})}{imag(z_1 I_S I^*_{sup})} \tag{1.19}$$

Thus the Takagi method assumes a constant current load model. The equation $I_{sup} = I_F$ holds true only when the load has constant current characteristics. The positive-sequence reactance to fault location is computed as $X_1 = l \times imag(z_1)$

1.1.4 Expression for the loop reactance method

The loop reactance method entirely neglects load current while deriving the expression for reactance to fault location. When load current is present in the system:

$$I_{tot1} \neq I_{tot2} \neq I_{tot0}$$

However, if the load current is neglected:

$$I_{tot1} = I_{tot2} = I_{tot0} = I_{F1} = I_{F2} = I_{F0}$$

Using this simplifying assumption, (1.7) can be rewritten as:

$$V = (I_{tot0} + I_{tot0})Z_1 + I_{tot0}Z_0 + I_F R_F$$

$$\therefore V = 2I_{tot0}Z_1 + I_{tot0}Z_0 + I_F R_F$$

$$\therefore V = (2Z_1 + Z_0)I_{tot0} + I_F R_F$$

$$\therefore \frac{V}{3I_{tot0}} = \frac{2Z_1 + Z_0}{3} + \frac{I_F R_F}{3I_{tot0}}$$

As the load current is assumed to be 0A, $I_F = 3I_{tot0}$

$$\therefore \frac{V}{3I_{tot0}} = \frac{2Z_1 + Z_0}{3} + R_F \tag{1.20}$$

The term $\frac{2Z_1+Z_0}{3}$ is defined as the loop impedance-to-fault. In this case as well, only the reactive component of (1.20) is computed to overcome the effect of fault resistance.

$$X_t = imag\left(\frac{2Z_1 + Z_0}{3}\right) = imag\left(\frac{V}{3I_{tot0}}\right) \tag{1.21}$$

It is to be noted that the loop reactance method does not use positive- and zero-sequence z_1 and z_0 line impedances to estimate the reactance-to-fault. The distance-to-fault is calculated as follows:

$$l = \frac{X_t}{imag(z_t)} \tag{1.22}$$

where $z_t = \frac{2z_1+z_0}{3}$

1.2 Derivation of the Balanced-load Method

The balanced-load method is a new impedance-based method, which was developed as a part of this work. Unlike the Takagi and positive-sequence reactance methods, the balanced load method does not require values of z_1 and z_0 line impedances to estimate the reactance-to-fault. Also this method does not neglect the load current. The derivation for this method is presented below.

From Figure 1.5 it is seen that:

$$I_{tot1} = I_{F1} + I_{load1} \tag{1.23}$$

$$I_{tot2} = I_{F2} + I_{load2} \tag{1.24}$$

$$I_{tot0} = I_{F0} + I_{load0} \tag{1.25}$$

Adding (1.23),(1.24) and (1.25):

$$I_{tot} = I_F + I_{load} \tag{1.26}$$

If the fault is assumed to be bolted (i.e. $R_F = 0\ \Omega$), then the load current in the faulted phase is 0 A.

$$I_{load} = I_{load1} + I_{load2} + I_{load0} = 0 \tag{1.27}$$

From (1.26) and (1.27):

$$I_{tot} = I_F \tag{1.28}$$

Also for an SLG fault:

$$I_{F_1} = I_{F_2} = I_{F_0} = \frac{I_F}{3} = \frac{I_{tot}}{3} \tag{1.29}$$

The value of I_{tot} is recorded by the power quality monitor. This value can be substituted in (1.29) to compute I_{F1}, I_{F2} and I_{F0}. Substituting (1.29) in (1.23), (1.24) and (1.25), the values of I_{load1}, I_{load2} and I_{load0} are obtained.

Applying Kirchoff's voltage law to the positive- and negative-sequence networks in Figure 1.5:

$$V_1 = I_{tot1}Z_1 + I_{load1}Z_{L1} \tag{1.30}$$

$$V_2 = I_{tot2}Z_2 + I_{load2}Z_{L2} \tag{1.31}$$

Now $Z_1 = Z_2$. Also if the system is serving a balanced three-phase load, the $Z_{L1} = Z_{L2}$ [9]. Substituting these values in (1.31):

$$V_2 = I_{tot2}Z_1 + I_{load2}Z_{L1} \tag{1.32}$$

Equations (1.30) and (1.32) can be written in matrix form as:

$$\begin{bmatrix} V_1 \\ V_2 \end{bmatrix} = \begin{bmatrix} I_{tot1} & I_{load1} \\ I_{tot2} & I_{load2} \end{bmatrix} \begin{bmatrix} Z_1 \\ Z_{load1} \end{bmatrix} \tag{1.33}$$

The values of V_1, V_2, I_{tot1} and I_{tot2} can be obtained from the power quality monitor measurements. The currents I_{load1} and I_{load2} are calculated as discussed previously. The only unknowns in (1.33) are Z_1 and Z_{load1}. Equation (1.33) can be solved to obtain these values.

$$\begin{bmatrix} Z_1 \\ Z_{load1} \end{bmatrix} = \begin{bmatrix} I_{tot1} & I_{load1} \\ I_{tot2} & I_{load2} \end{bmatrix}^{-1} \begin{bmatrix} V_1 \\ V_2 \end{bmatrix} \tag{1.34}$$

The method can thus be used to compute the positive-sequence impedance-to-fault Z_1. It does not require the z_1 and z_0 line impedances values to estimate Z_1. Also it takes load current into account using a balaned-load model. It is also important to note that the Z_1 and Z_0 values in the sequence networks

are the actual positive- and zero sequence impedances to fault location. This method does not make the uniform line-impedance assumption.

The three important assumptions made during the derivation of this method are summarized below:

1. The entire load is lumped beyond the fault point
2. The fault resistance is 0 Ω (i.e. bolted fault)
3. The system serves a perfectly balanced three-phase load

1.3 Error Sources for the Impedance-based Methods

Sections 1.1 and 1.2 mention that the inputs for the four impedance-based methods are voltage and current measurements and values of z_1 and z_0 line impedances. If either voltage and current measurements or the z_1 and z_0 values are erroneous, the reactance-to-fault estimates will be affected. Also the system loads are not accurately represented while deriving the expression for reactance or distance to fault location. Hence level of load current in the system as well as nature of the loads can have an adverse impact on accuracy of estimation. Four factors affecting the accuracy of fault location estimates are described below:

1.3.1 Inaccurate circuit modeling

The values of z_1 and z_0 depend upon four parameters [11]: distance between phase conductors, sizes of phase conductors, distance between phase and neutral conductors and value of earth resistivity. If any of these parameters is modeled inaccurately, it leads to errors in computation of z_1 and z_0. Incorrect

z_1 and z_0 values in turn introduce errors in the reactance-to-fault estimates of the impedance-based methods. The effect of inaccurate modeling of the four parameters on values of z_1 and z_0 is analyzed in the first part of Chapter 4. The second part of Chapter 4 focuses on effect of erroneous z_1 and z_0 values on fault location estimates of impedance-based methods.

1.3.2 Uniform Line Impedance Assumption

In a practical distribution feeder, there is a wide variation in conductor sizes and pole configurations. The distances between the conductors may not be the same for all sections of the feeder. As a result, the values of z_1 and z_0 are different for different sections of the feeder. Such a feeder is called a non-homogeneous feeder. The Takagi and positive-sequence reactance methods described in this Chapter are derived based on assumption that the distribution feeder has uniform z_1 and z_0 values throughout its length. Since this assumption is violated in a practical distribution feeder, fault location estimates of the two methods are affected. Chapter 4 analyzes the effect of this assumption on fault location estimates of both the methods.

1.3.3 Measurement Errors

Errors in current and voltage measurements affect the reactance-to-fault estimates of all the impedance-based methods. Measurement errors arise due to inadequacies of instrument transformers. Current and voltage transformer measurements are affected by ratio and phase angle errors. It is likely that ratio errors in CTs and VTs have opposite effects on fault location estimates. Also the performance of the impedance-based methods may be different for positive and negative phase angle errors. Chapter 5 presents a comprehen-

sive analysis of the effect of measurement errors on fault location estimates of the impedance-based methods.

1.3.4 Load current

The four impedance-based methods make simplifying assumptions regarding the system load. The loop reactance and balanced-load methods have been derived for no-load and balanced-load conditions respectively. The Takagi method assumes a constant current load model. Additionally, the Takagi, positive-sequence reactance and balanced-load methods assume that the entire load is lumped beyond the fault point. In a practical distribution system, the magnitude of fault current for distant faults is relatively comparable to the load current. Hence load current cannot be neglected. Single-phase and three-phase load taps are present along the length of the distribution feeder. Because of this, the lumped load assumption is erroneous. The load may not be balanced nor may it have constant current characteristics. Thus many assumptions made by the impedance-based methods regarding the system load are not satisfied. Chapter 6 deals with the effect of load current on the fault location estimates obtained using the impedance-based methods.

1.4 Technical Contribution

This Section highlights two technical contributions made by this thesis in the field of distribution fault location. Firstly, a new method of locating faults, called as the balanced-load method was developed as a part of this work. The detailed derivation for this method has been presented in Section 1.2. This method is used to conduct fault location on the IEEE 34 Node Test Feeder and detailed results are included in subsequent Chapters. The

performance of this method on the test feeder is promising and with further development and proofing, it can also be applied to real-world fault data.

Secondly, sensitivity analysis of the Takagi, positive-sequence reactance, loop reactance and balanced-load methods is performed. The first three methods are widely popular and commonly used in relays and fault locators. This thesis identifies incorrect circuit modeling, measurement errors and load current as the major factors which cause inaccuracy in fault location. It presents a quantitative analysis of how each of these factors affects the four fault location methods.

The effect of load current on fault location is of particular interest. This topic has been dealt with in Chapter 6 of this thesis. The key findings and results of analysis [12] were accepted for publication and presented in the proceedings of the IEEE Power and Energy Society General Meeting (July 2011, Detroit).

1.5 Organization of the Thesis

Chapter 2 provides a description of the IEEE 34 Node Test Feeder which is used for sensitivity analysis. Chapter 3 develops and presents the analysis approach. Chapters 4 and 5 deal with effects of modeling and measurement errors on estimation accuracy. Chapter 6 analyzes the effect of load current on impedance-based methods and summarizes the results sensitivity analysis.

Chapter 2

Modeling and Utilization of the IEEE 34 Node Test Feeder for Analysis

A realistic test circuit is required to test the performance of the four impedance-based methods discussed in Chapter 1. The IEEE 34 Node Test Feeder [13], which is based on an actual distribution feeder in Arizona, is chosen for analysis.

Section 2.1 presents a detailed description of the IEEE 34 Node Test Feeder. It mentions that the feeder is long, lightly loaded and has a nominal voltage of 24.9 kV. It has multiple three-phase branches and single-phase laterals along with unbalanced loads, voltage regulators and shunt capacitors. Because of these charactersitics, the feeder is considered to be a good representation of a typical distribution system.

Time-domain modeling of the IEEE 34 Node Test Feeder is discussed in Section 2.2. An Electromagnetic Transient Program (EMTP) called PSCAD [14], is used to create a model of the feeder. The PSCAD model of the feeder is used for sensitivity analysis. Section 2.3 summarizes two important modifications which are made in the PSCAD model of the test feeder. The length of the feeder is reduced and the level of load current is increased. These changes are necessary to make the test feeder more suitable for fault location analysis.

2.1 Description of the IEEE 34 Node Test Feeder

The main characteristics [13] of the IEEE 34 Node Test Feeder are:

1. Nominal voltage of 24.9 kV
2. Long and lightly loaded
3. Multiple single and three-phase laterals
4. Two in-line voltage regulators to maintain a good voltage profile
5. An in-line transformer to step down the voltage to 4.16 kV for a short section of feeder
6. Unbalanced loading with 'spot' and 'distributed' loads. Distributed loads are assumed to be connected at the center of the line segment
7. Shunt capacitors

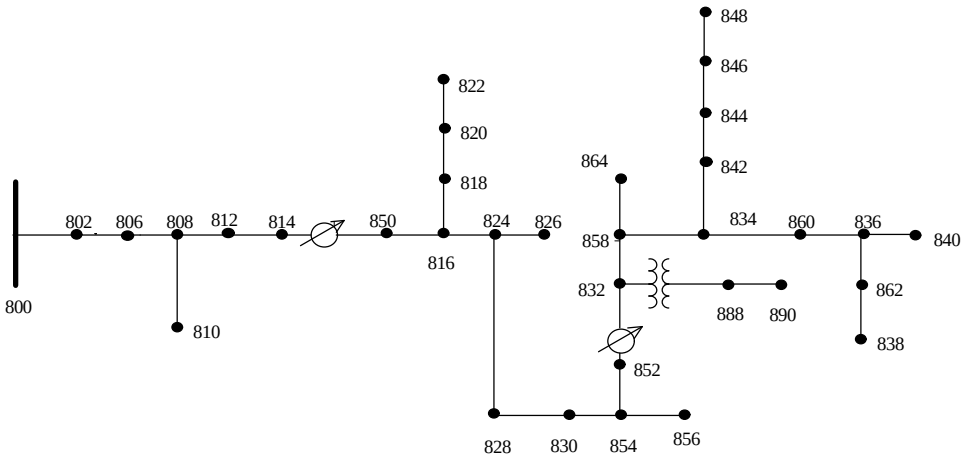

Figure 2.1: IEEE 34 Node Test Feeder

Figure 2.1 shows a single-line diagram of the test feeder. A brief description of the major components in the test feeder is given below:

2.1.1 Overhead Lines

The lengths of all the overhead lines in the IEEE 34 Node Test Feeder are listed in [15]. The feeder has five different configurations of overhead lines. Table 2.1 shows that configurations 300 and 301 represent three-phase feeders while the other three denote single-phase laterals.

Table 2.1: Overhead Line Configurations in the IEEE 34 Node Test Feeder

Configuration	Phasing	Phase (ACSR Conductor)	Neutral (ACSR Conductor)	Spacing ID
300	B A C N	1/0	1/0	500
301	B A C N	#2 6/1	#2 6/1	500
302	A N	#4 6/1	#4 6/1	510
303	B N	#4 6/1	#4 6/1	510
304	B N	#2 6/1	#2 6/1	510

The spacing IDs define the arrangement of phase and neutral conductors in each configuration. Two different types of conductor arrangements, which are used in the test feeder, are shown in Figure 2.2. Spacing 500 is three-phase four wire arrangement while spacing 510 represents a single-phase two wire arrangement.

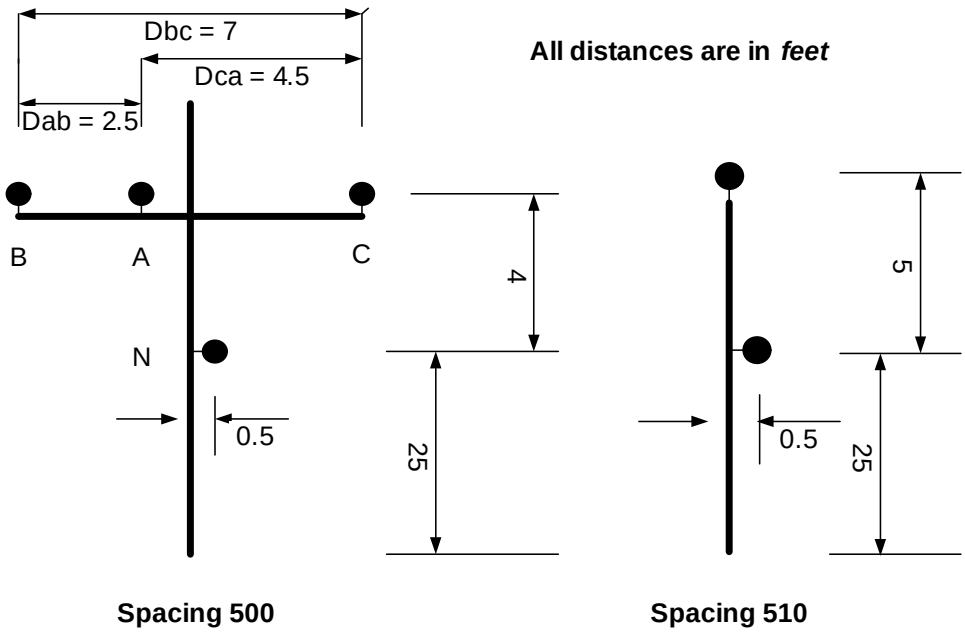

Figure 2.2: Conductor Spacings in the IEEE 24 Node Test Feeder

Aluminium Conductor Steel Reinforced (ACSR) is used for the phase and neutral conductors. The conductor data is listed in Table 2.2

Table 2.2: Phase and Neutral Conductor Data

Size	Stranding	Material	Diameter (inches)	Geometric Mean Radius (feet)	Resistance (Ω/mile)
1/0		ACSR	0.398	0.00446	1.12
2	6/1	ACSR	0.316	0.00418	1.69
4	6/1	ACSR	0.25	0.00437	2.57

Computation of Overhead Line Impedances:

The conductor data and spacing IDs are used to compute the values of positive and zero-sequence z_1 and z_0 line impedances for each configuration. The geometric mean distances between the conductors are defined as [11]:

$$D_{ij} = \sqrt[3]{D_{ab} \times D_{bc} \times D_{ca}} ft \tag{2.1}$$

$$D_{in} = \sqrt[3]{D_{an} \times D_{bn} \times D_{cn}} ft \tag{2.2}$$

The self and mutual inductances can be determined using Carson's equations [11]:

$$z_{ii} = r_i + 0.00158836f + 0.00202237f(ln\frac{1}{GMR_i} + 7.6786 + \frac{1}{2}ln\frac{\rho}{f})\Omega/mile \tag{2.3}$$

$$z_{nn} = r_n + 0.00158836f + 0.00202237f(ln\frac{1}{GMR_n} + 7.6786 + \frac{1}{2}ln\frac{\rho}{f})\Omega/mile \tag{2.4}$$

$$z_{ij} = 0.00158836f + 0.00202237f(ln\frac{1}{D_{ij}} + 7.6786 + \frac{1}{2}ln\frac{\rho}{f})\Omega/mile \tag{2.5}$$

$$z_{in} = 0.00158836f + 0.00202237f(ln\frac{1}{D_{in}} + 7.6786 + \frac{1}{2}ln\frac{\rho}{f})\Omega/mile \tag{2.6}$$

where,

f = frequency = 60 Hz

ρ = earth resistivity = 100 Ωm

i, j denote phase conductors of the feeder

n denotes the neutral conductor

GMR = Geometric Mean Radius

$r_{i/n}$ = resistance of the phase/ neutral conductor

Using (2.3), (2.4), (2.5) and (2.6) all the self and mutual impedances can be computed. These impedances are the elements of the primitive impedance matrix Z_{abcn}. The order of this matrix is $ncond \times ncond$, where $ncond$ is the number of conductors in the configuration. For example, in case of configuration 300, which has three phase conductors and one neutral conductor, the Z_{abcn} matrix is of order 4×4. The Z_{abcn} matrix is partitioned as follows:

$$Z_{abcn} = \begin{bmatrix} Z_{ij} & Z_{in} \\ Z_{nj} & Z_{nn} \end{bmatrix} \tag{2.7}$$

The Kron Reduction Technique [11] is used to reduce the matrix Z_{abcn} to the phase impedance matrix Z_{abc}.

$$Z_{abc} = [Z_{ij}] - [Z_{in}][Z_{nn}]^{-1}[Z_{nj}]\Omega/mile \tag{2.8}$$

The block matrices Z_{ij}, Z_{in}, Z_{nn} and Z_{nj} are defined in (2.7). The phase impedance matrix Z_{abc} can be transformed to the sequence impedance matrix Z_{012} using:

$$Z_{012} = A^{-1} Z_{abc} A\Omega/mile \tag{2.9}$$

where,

$$A = \begin{bmatrix} 1 & 1 & 1 \\ 1 & a^2 & a \\ 1 & a & a^2 \end{bmatrix} \tag{2.10}$$

The factor a in (2.10) is a complex number which is equal to $1\angle 120^0$.

Computation of Shunt Admittances:

The shunt admittances for each line configuration are computed in a similar manner. The method of conductors and their images is used to calculate shunt capacitance [11]. The self and mutual potential coefficients are defined as:

$$P_{ii} = 11.1769 ln \frac{S_{ii}}{RD_i} mile/\mu F \tag{2.11}$$

$$P_{ij} = 11.1769 ln \frac{S_{ij}}{D_{ij}} mile/\mu F \tag{2.12}$$

where,

S_{ii} = Distance from conductor i to its image i' (ft)

S_{ij} = Distance of conductor i to the image of conductor of conductor j (ft)

D_{ij} = Distance from conductor i to conductor j (ft)

RD_i = Radius of conductor i (ft)

P_{ii} = Self potential coefficient (mile/ μ F)

P_{ij} = Mutual potential coefficient (mile/ μ F)

The primitive potential coefficient matrix P_{abcn} is constructed and the Kron Reduction technique is applied to obtain the phase potential coefficient matrix P_{abc}.

$$P_{abc} = [P_{ij}] - [P_{in}][P_{nn}]^{-1}[P_{nj}] mile/\mu F \tag{2.13}$$

The capacitance matrix $[C_{abc}]$ is the inverse of P_{abc}.

$$[C_{abc}] = [P_{abc}]^{-1} \mu F/mile \tag{2.14}$$

The shunt conductance is neglected and the phase shunt admittance matrix Y_{abc} is computed as:

$$[Y_{abc}] = j\omega \times [C_{abc}] \mu S/mile \tag{2.15}$$

2.1.2 Loads

The IEEE 34 Node Test Feeder has 'spot' loads as well as 'distributed' loads. Spot loads are connected at a node. Distributed loads are connected

at the center of the line segment joining two nodes. The loads are three-phase, two-phase or single-phase and connected in wye or delta. They are modeled as constant complex power (PQ), constant current (I) and constant impedance (Z). Table 2.3 lists the codes used to describe different types of loads [15]. Single-phase loads, which are connected line-to-line, are given delta connection code, irrespective of whether the feeder is three-wire delta or four-wire system connected in wye. The kW and kVAR ratings of all the loads in the feeder are listed in [15].

Table 2.3: Load Model Codes

Code	**Connection**	**Model**
Y-PQ	Wye	Constant kW and kVar
Y-I	Wye	Constant Current
Y-Z	Wye	Constant Impedance
D-PQ	Delta	Constant kW and kVar
D-I	Delta	Constant Current
D-Z	Delta	Constant Impedance

2.1.3 Transformers

A three-phase step down transformer, connected in wye-delta, is used to step down the voltage from 24.9kV to 4.16 kV for a small section of the feeder. The specifications of the transformer can be found in [15].

2.1.4 Voltage Regulators

Two three-phase voltage regulators are used to maintain the feeder voltage within acceptable limits. Tap positions of both the regulators are determined by the compensator circuit settings [15].

2.1.5 Shunt Capacitor Banks

Two three-phase capacitor banks are wye-connected. Their ratings are listed in [15].

2.2 Time Domain Modeling of the Feeder

A model of the IEEE 34 Node Test Feeder is created using an Electromagnetic Transient Program (EMTP) called PSCAD. The simulation software PSCAD has a comprehensive library of components, interactive control inputs, meters and online plotting functions and has been widely adopted by utilities as a premier tool for transient simulation [14].

After creating a PSCAD model of the IEEE 34 Node Test Feeder, a load-flow analysis is conducted. The voltage and power flow at each node is measured. The IEEE Distribution System Analysis Subcommittee has published expected results of load-flow analysis for the IEEE 34 Node Test Feeder in [15]. The load-flow results obtained from PSCAD are compared with those in [15]. The PSCAD results are within 1% of the published data indicating that the feeder has been modeled accurately.

The PSCAD model of the IEEE 34 Node Test Feeder is used for sensitivity analysis. Single line-to-ground faults are placed at various nodes in the PSCAD model. Fault current and voltage waveforms are recorded by a power

quality monitor in the model. These measurements and the overhead line impedance values are used to conduct fault location and test the performance of the impedance-based methods.

2.3 Modification of the Feeder

Two important drawbacks of the IEEE 34 Node Test Feeder are that it is exceptionally long and lightly loaded. The load current magnitude is around 40A/ phase. As a result, load current has a marginal effect on accuracy of the impedance-based methods. The original feeder cannot be used to analyze the effect of load current on fault location estimates. Also most of the nodes towards the end of the feeder are located at nearly the same distance from the power quality monitor. Hence it is difficult to analyze how the performance of impedance-based methods is affected when distance from the monitoring location increases.

To make the test feeder more useful for analysis, certain modifications are necessary:

1. Length of the main feeder is decreased from 35 miles to 9.54 miles. This increases the level of fault current in the system. Faults currents are now in the range of 5 kA (for faults closer to the power quality monitor) to 970 A (for distant faults)

2. Lengths of single-phase laterals are reduced. These laterals now have lengths between 1 to 3 miles as compared to 8 to 9 miles in original model

3. The load current magnitude is increased from 40A/phase to 420A/phase

Appendix A lists the lengths of overhead lines, load kW and KVAR ratings for the modified IEEE 34 Node Test Feeder.

2.4 Summary

This Chapter provides a detailed description of the IEEE 34 Node Test Feeder. It discusses time-domain modeling of the feeder using PSCAD. It also describes modification of the feeder. The modified IEEE 34 Node Test Feeder is used for analysis in the rest of the Chapters.

Chapter 3

Approach to Sensitivity Analysis and Construction of Baseline Case

Four factors which adversely affect fault location estimates of the impedance-based method are inaccurate circuit modeling, measurement errors, uniform line impedance assumption and level of load current in the system. Section 3.1 presents a general approach to analyze and quantify the effect of each of these factors on accuracy of estimation.

The first step in the analysis approach is to establish a baseline or reference case. In the baseline case, the Takagi, positive-sequence reactance, loop reactance and balanced-load methods are used to conduct fault location analysis on a PSCAD model of the IEEE 34 Node Test Feeder. This feeder model is short, heavily loaded and has non-uniform positive- and zero-sequence z_1 and z_0 line impedance values. While constructing the baseline case, it is ensured that the main inputs for the four methods (i.e. voltage and current measurements and line impedance values in Ω/mile) are free from errors. All four methods estimate the reactance to fault location for this analysis. The reactance-to-fault estimates obtained in this case are used as a reference against which the results of all subsequent analyzes are compared.

After constructing the baseline case, the effect of circuit model errors on fault location is analyzed. Inaccurate z_1 and z_0 line impedance values are obtained by deliberately introducing modeling errors in computation. These

erroneous values are used in the impedance-based methods and their effect on estimation accuracy is studied. The uniform line impedance assumption made by the Takagi and positive-sequence reactance methods constitutes another type of modeling error. Its effect on accuracy of estimation is studied by conducting fault location analysis on a new feeder model, which has uniform z_1 and z_0 values, and comparing the results with the baseline case. This is followed by analysis of effect of measurement errors on fault location. Ratio and phase angle errors are intentionally introduced in voltage and current transformers and the erroneous measurements are then used in the four methods. To analyze the effect of load current on estimation accuracy, fault location is performed on a no-load model of the test feeder and the results are compared with those for the baseline case.

The development of the baseline case is described in Section 3.2. Although there are no circuit model or measurement errors for this case, none of the methods estimate the reactance-to-fault accurately. Fault location estimates of the Takagi and positive-sequence reactance methods are 5% to 10% lesser than the actual reactance-to-fault. For the balanced-load method the estimates are 7% to 35% higher. The loop reactance method gives highly erroneous estimates which are 10% to 70% higher than the actual value. The main cause of errors in the four methods can be attributed to the nature of loads in the baseline case. The loop reactance method is derived for no-load conditions. The balanced-load method works well when the system load is balanced. The Takagi method assumes a constant current load model. As these assumptions are violated in the baseline case, erroneous fault location estimates are obtained. Another cause of error for the Takagi and positive-sequence reactance methods is that the baseline case does not satisfy the uniform line impedance

assumption made by these methods.

3.1 Approach for Senstivity Analysis of Impedance-based Methods

The approach to sensitivity analysis consists of five parts:

1. Establishing a Baseline (Reference) Case
2. Effect of Circuit Model Errors on Fault Location Estimates
3. Effect of the Uniform Line Impedance Assumption on Fault Location Estimates
4. Effect of Measurement Errors on Fault Location Estimates
5. Effect of Load Current on Fault Location Estimates

The analysis begins with construction of a baseline case using a modified version of the IEEE 34 Node Test Feeder. Subsequently, the effect of modeling errors, measurement errors and load current on fault location estimates is analyzed. The reactance-to-fault estimates for all the analyses are compared with those for the baseline case. This comparison shows how worse the estimates become with respect to the baseline case, when the impedance-based methods are affected by errors. The detailed approach is described below.

Establishing a Baseline (Reference) Case:

The IEEE 34 Node Test Feeder is used to establish a baseline case because it is a good representation of a practical distribution system. The

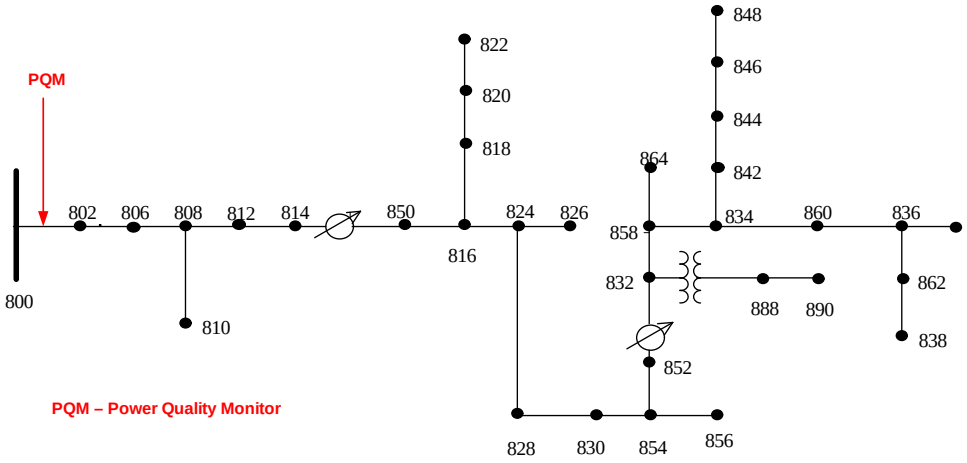

Figure 3.1: IEEE 34 Node Test Feeder

length of this feeder is reduced to less than 10 miles and level of load current is increased to 420 A/phase so that it is better suited for fault location analysis. The single line diagram of this feeder is shown in Fig. 3.1. Node 800 is the monitoring location. A power quality monitor (PQM) samples the voltage and current values at this node at a rate of 128 samples per cycle. Eight bolted ($R_F = 0\Omega$) single line-to-ground (SLG) faults are placed at different locations along the feeder and the values of voltage and current at node 800 are recorded in each case.

The voltage and current measurements are used in the Takagi, positive-sequence reactance, loop reactance and balanced-load methods. In addition to fault currents and voltages, the Takagi and positive-sequence reactance methods require z_1 and z_0 line impedance values to estimate fault location. Configuration 301 is most widely used in the modified IEEE 34 Node Test Feeder. So z_1 and z_0 values corresponding to this configuration are used in these two methods. The reactance-to-fault estimates obtained for this case are used as a means of comparison for sensitivity analysis. Estimation errors are

computed for each fault location as follows:

$$Error(\%) = \frac{Estimated\ reactance - Actual\ reactance}{Actual\ reactance} \times 100 \qquad (3.1)$$

All four methods have been derived to locate single line-to-ground faults on three phase feeders. They cannot be used if faults occur on single-phase laterals. The reactance-to-fault estimates will be highly erroneous for such faults. Hence faults on single-phase laterals are excluded from analysis. The baseline case and rest of the analysis concentrates on SLG faults occurring on three-phase feeders.

Effect of Circuit Model Errors on Fault Location Estimates:

In this part of the analysis, different circuit model errors are introduced while computing the values of z_1 and z_0. Four parameters which affect values of z_1 and z_0 are listed below:

1. Distances between conductors of different phases
2. Sizes of phase conductors
3. Distances between phase and neutral conductors
4. Value of earth resistivity

The effect of inaccurate modeling of each of these parameters is considered separately. Firstly, incorrect values of phase conductor distances are used to compute z_1 and z_0. All the other parameter values are accurate. Erroneous values of z_1 and z_0 are obtained and they are used in the impedance-based methods along with accurate voltage and current measurements. Estimation errors are computed using (3.1). These errors are compared to those for the

baseline case. The analysis is repeated for incorrect values of the other three parameters as well.

Effect of the Uniform Line Impedance Assumption on Fault Location Estimates:

To study the impact of assumption of uniform line impedance on fault location estimates, a homogeneous 34 node feeder is created based on the original test feeder. This feeder has all its distribution lines in configuration 301. Since configuration 301 is an arrangement of three-phase conductor lines, the homogeneous feeder model does not have any single-phase laterals. The distance between adjacent nodes in this model is same as that in the original non-homogeneous test feeder. Thus the distance to fault location is unchanged. However, the positive-sequence reactance to fault location changes. SLG faults are placed at the same eight locations as the baseline case and fault current and voltage values at node 800 are recorded. These measurements are used in the impedance-based methods along with values of z_1 and z_0 corresponding to configuration 301. Estimation errors are computed and compared with those for the baseline case.

Effect of Measurement Errors on Fault Location Estimates:

The voltage and current values recorded by the power quality monitor (PQM) are affected by ratio and phase angle errors in voltage and current transformers (VTs and CTs). Typical values of ratio and phase angle errors are obtained from [16]. These errors are applied to the current and voltage values recorded by the PQM. The following cases are studied:

1. Effect of CT measurement errors (VT measurements are accurate)

2. Effect of VT measurement errors (CT measurements are accurate)

3. Combined effect of CT and VT measurement errors

Erroneous voltage and current measurements and accurate z_1 and z_0 values are used in the four methods to obtain the reactance to fault location.

Effect of Load Current on Fault Location Estimates:

To study the effect of load current on fault location estimates, a new feeder model is constructed in which the level of load current is reduced to 0A. SLG faults are placed at exactly the same locations as the baseline case and the fault current and voltage values are recorded. These measurements are used in the impedance-based methods along with accurate values of z_1 and z_0 and reactance-to-fault estimates are obtained. Estimation errors for the no-load case are compared to those for the baseline case, which uses a heavy-load feeder model.

3.2 Fault Location Estimates for the Baseline Case

Eight bolted ($R_F = 0\Omega$) single line-to-ground (SLG) faults shown in Fig. 3.2 are placed at different nodes along the IEEE 34 Node Test Feeder. These faults are at nodes 808, 814, 830, 832, 840, 844, 848 and 860. The voltage and current values at the monitoring location (node 800) are recorded for faults at each of the eight nodes.

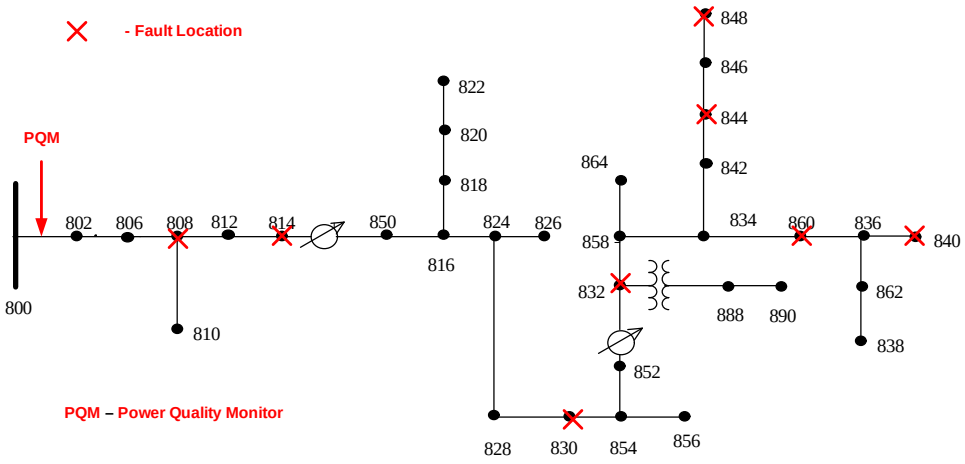

Figure 3.2: Fault Locations Along the IEEE 34 Node Test Feeder

3.2.1 Calculation of Accurate Values of z_1 and z_0

The positive-sequence reactance and the Takagi methods are derived on the basis of the assumption that the values of z_1 and z_0 are uniform throughout the distribution feeder. The IEEE 34 Node Test Feeder has multiple conductor configurations leading to non-uniform z_1 and z_0 values. Hence z_1 and z_0 values of a particular configuration must be selected for use in the two methods. Values corresponding to Configuration 301 are chosen because it occupies 7 of 9.53 miles of the main feeder. In other words, for the methods to work, it is assumed that the IEEE 34 Node Test Feeder has uniform line impedance values. Fig. 3.3 shows distances between phase conductors as well as the phase to neutral conductor distances for configuration 301. In the baseline case, accurate values of conductor sizes, distances between conductors and earth resistivity are used for calculation of z_1 and z_0.

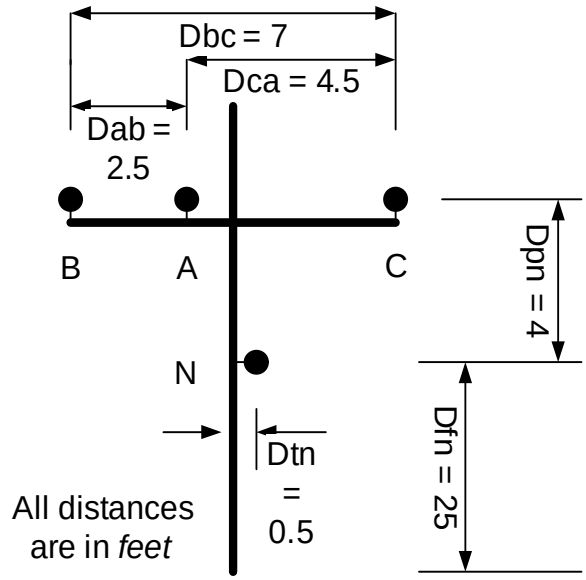

Figure 3.3: Arrangement of Conductors for Configuration 301

The values of z_1 and z_0 are:

$$z_1 = 1.6901 + j0.8412\Omega/\text{mile}$$

$$z_0 = 2.3875 + j2.5782\Omega/\text{mile}$$

These are used in the Takagi and positive-sequence reactance methods.

3.2.2 Performance of the Impedance-based Methods for the Baseline Case

It is mentioned previously that for the baseline case, the main inputs to the impedance-based methods are accurate. The only simplification is the uniform line impedance assumption. Table 3.1 displays the reactance-to-fault estimates for Takagi and positive-sequence reactance methods. The estimation errors for each of the fault locations are computed using (3.1).

Table 3.1: Reactance-to-fault Estimates for the Takagi and Positive-sequence Reactance Methods

A: Takagi Method

Fault at node:	Actual positive seq. reactance (ohm)	Estimated positive seq. reactance (ohm)	Error for reference case (%)
814	2.230	2.081	-6.68
830	3.459	3.294	-4.77
860	5.872	5.589	-4.81
848	7.992	7.230	-9.53
808	1.197	1.123	-6.22
832	4.066	3.893	-4.25
840	7.386	6.813	-7.75
844	6.478	6.109	-5.70

B: Positive-sequence Reactance Method

Fault at node:	Actual positive seq. reactance (ohm)	Estimated positive seq. reactance (ohm)	Error for reference case (%)
814	2.230	2.262	1.42
830	3.459	3.461	0.05
860	5.872	5.692	-3.05
848	7.992	7.303	-8.62
808	1.197	1.219	1.80
832	4.066	4.052	-0.34
840	7.386	6.864	-7.07
844	6.478	6.208	-4.16

For an SLG fault at node 814, the Takagi method gives an estimate of 2.081 Ω which is less than 2.230 Ω where the actual fault is. The estimation error is -6.68%. The negative sign in the estimation error is indicative of an underestimation of fault location as illustrated in Fig. 3.4. The estimated reactance-to-fault is on the left of the actual fault location. On the other hand, for the same fault location, the positive-sequence reactance method gives an estimate of 2.262 Ω which is higher than the actual value. The estimation error is positive indicating an overestimation. Fig. 3.4 shows that the estimate is on the right of the actual fault location.

From Table 3.1, it is obvious that the Takagi method consistently underestimates fault location with estimation errors of -4.77% to -9.53%. On the other hand, estimation errors for the positive-sequence reactance method vary between 1.8% and -8.62%. It is also to be noted that performance of both the methods deteriorates as the distance of the fault from the monitoring location increases.

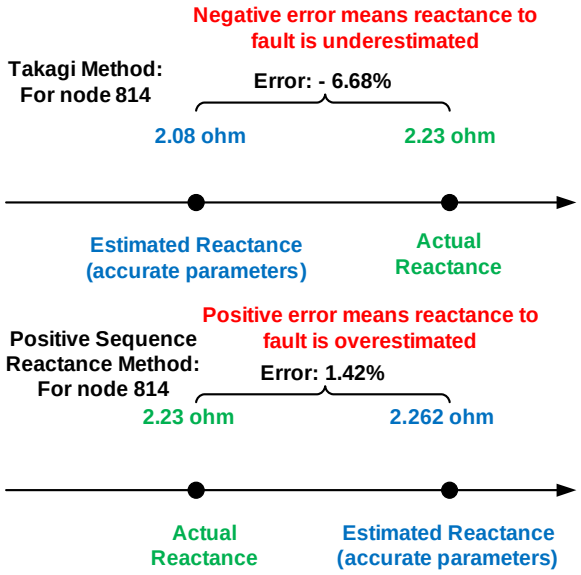

Figure 3.4: Interpretation of Error Percentages

The performance of the loop reactance method is the worst. This is evident from Table 3.2. This method overestimates the loop reactance-to-fault for all the eight fault locations. The estimation errors are in the range 10% to 70%. The accuracy of this method deteriorates with increase in distance from the monitoring location.

The balanced-load method overestimates the reactance-to-fault in all the cases. Table 3.2 shows that estimation errors range from 7% to 35%. This method shows an opposite trend as compared to the other three methods. In this case, accuracy of reactance-to-fault estimates improves as distance from the monitoring location increases. For node 808 which is the closest to the monitoring location, the error is 35.76%. However for node 848 which is the farthest away, the error decreases to 7.41%.

Table 3.2: Reactance-to-fault Estimates for the loop reactance and Balanced-load Methods

A: Loop reactance Method

Fault at node:	Actual loop reactance (ohm)	Estimated loop reactance (ohm)	Error for reference case (%)
814	3.605	4.262	18.22
830	5.684	7.529	32.47
860	9.753	15.860	62.62
848	13.332	23.023	72.69
808	1.935	2.114	9.26
832	6.705	9.386	39.99
840	12.313	21.321	73.16
844	10.780	17.965	66.65

B: Balanced-load Method

Fault at node:	Actual positive seq. reactance (ohm)	Estimated positive seq. reactance (ohm)	Error for reference case (%)
814	2.230	2.881	29.21
830	3.459	4.366	26.22
860	5.872	6.748	14.92
848	7.992	8.584	7.41
808	1.197	1.625	35.76
832	4.066	5.096	25.33
840	7.386	7.949	7.62
844	6.478	7.376	13.87

A comparison of the performance of the four methods shows that, the Takagi and positive-sequence reactance methods work with reasonable accuracy. The balanced-load method is less accurate as compared to these methods. The loop reactance method is the least accurate. However, the loop reactance and the balanced-load methods use only the voltage and current measurements for estimating the reactance-to-fault. The Takagi and positive-sequence reactance methods require positive- and zero-sequence z_1 and z_0 line impedance values in addition to the voltage and current measurements.

It is important to note that none of the methods estimate the reactance-to-fault accurately for the baseline case in spite of the fact that there are no circuit model or measurement errors. The main cause of errors in all the methods can be attributed to the nature of loads in the baseline case. It was mentioned previously that the loop reactance and balanced load methods are derived for no-load and balanced-load conditions respectively. The Takagi method assumes that the load current remains constant during the fault. However in

the baseline case, load current has a considerable magnitude of 420A/phase. Also loads are unbalanced and do not exhibit constant current characteristics. As the assumptions regarding system load are violated, the impedance-based methods give erroneous estimates. The second cause of errors for the Takagi and positive-sequence reactance methods is that they assume the values of positive- and zero-sequence z_1 and z_0 line impedances to be uniform throughout the distribution system. But the reference case uses a non-homogeneous feeder model in which the values of z_1 and z_0 are non-uniform.

3.3 Summary

This Chapter develops a systematic approach for sensitivity analysis. It also describes the construction of a baseline case, which serves as a reference for analysis. Sensitivity analysis is based on comparison of fault location estimates for the baseline case with those obtained in Chapters 4, 5 and 6.

Chapter 4

Effect of Circuit Model Errors on Line Impedances and Fault Location Estimates

One of the goals of sensitivity analysis is to analyze the effect of circuit model errors on fault location estimates of impedance-based methods. However the primary effect of inaccurate circuit modeling is that it leads to errors in computation of values of positive- and zero-sequence z_1 and z_0 line impedances. The erroneous z_1 and z_0 values in turn affect the fault location estimates of the impedance-based methods. Hence the first Section of this Chapter is devoted to analyzing the effect of circuit model errors on values of z_1 and z_0. The second and third Sections extend this analysis by studying the effect of modeling errors on fault location estimates.

It is identified previously, that the values of z_1 and z_0 depend on four parameters: distances between conductors of different phases, sizes of phase conductors, distances between phase and neutral conductors and value of earth resistivity. The analysis conducted in Section 4.1 shows that z_1 is directly proportional to the distance between phase conductors while z_0 is inversely proportional to it. When phase conductor distances are increased by 1 ft, the value of z_1 increases by 0.5% and that of z_0 decreases by 0.8%. Secondly, both z_1 and z_0 are inversely proportional to sizes of phase conductors. Their values decrease by 0.6% when conductor sizes are increased by 24%. Further, z_1 is insensitive to variations in phase to neutral conductor distances while z_0 is

directly proportional to this parameter. It increases by 0.4% for a 50% increase in these distances. Incorrect modeling of earth resistivity does not affect z_1, but z_0 increases by 7% when earth resistivity is increased from 100 Ω-m to 1000 Ω-m. The effect of inaccurate modeling of phase conductor distances, conductor sizes and phase to neutral conductor distances on z_1 and z_0 can be considered insignificant while errors in earth resistivity values can have a considerable influence on z_0.

Section 4.2 investigates how the erroneous z_1 and z_0 values, which arise from modeling errors, affect fault location estimates of the impedance-based methods. It is observed that the Takagi and positive-sequence reactance methods are sensitive to inaccurate modeling of earth resistivity. The estimation errors for these methods increase or decrease by 2% to 5% when value of earth resistivity is increased to 1000 Ω-m or decreased to 10 Ω-m respectively, from its accurate value of 100 Ω-m. Variations in phase conductor distances, conductor sizes and phase to neutral conductor distances do not affect fault location estimates of the Takagi and positive-sequence reactance methods significantly. Further, the Takagi and positive-sequence methods incorrectly assume z_1 and z_0 line impedances to be uniform, while estimating the reactance to fault location. The effect of this assumption on estimation accuracy is analyzed in Section 4.3. It is observed that this assumption causes the estimation errors to increase by 3%.

The loop reactance and balanced-load methods are not analyzed in this Chapter. These methods are insensitive to circuit model errors as they do not use values of z_1 and z_0 while estimating the reactance to fault location.

4.1 Effect of Circuit Model Errors on Values of z_1 and z_0

Four parameters which influence the values of positive- and zero-sequence z_1 and z_0 line impedances are: distances between conductors of different phases, sizes of phase conductors, distances between phase and neutral conductors and value of earth resistivity. Circuit model errors arise from the usage of incorrect values of any or all of the four parameters, to compute z_1 and z_0. The effect of incorrect modeling of each of the four parameters on values of z_1 and z_0 is discussed below:

4.1.1 Phase Conductor Distances: Effect on z_1 and z_0

In the reference case discussed in Chapter 3, accurate values of distances (i.e. $D_{ab} = 2.5$ ft and $D_{bc} = 7$ ft) are used to compute the values of z_1 and z_0.

Figure 4.1 shows the case where distances D_{ab} and D_{bc} are increased by 1 ft. Distance D_{ca} remains constant. Incorrect values of distances (i.e. $D_{ab} = 3.5$ ft and $D_{bc} = 8$ ft) are used to compute values of z_1 and z_0. The boxes adjacent to each figure show the values of z_1 and z_0 obtained using those particular values of phase conductor distances.

Next, the distances D_{ab} and D_{bc} are decreased by 1 ft. Distance D_{ca} remains constant. This is shown in Figure 4.2. Incorrect values of distances (i.e. $D_{ab} = 1.5$ ft and $D_{bc} = 6$ ft) are used to compute values of z_1 and z_0.

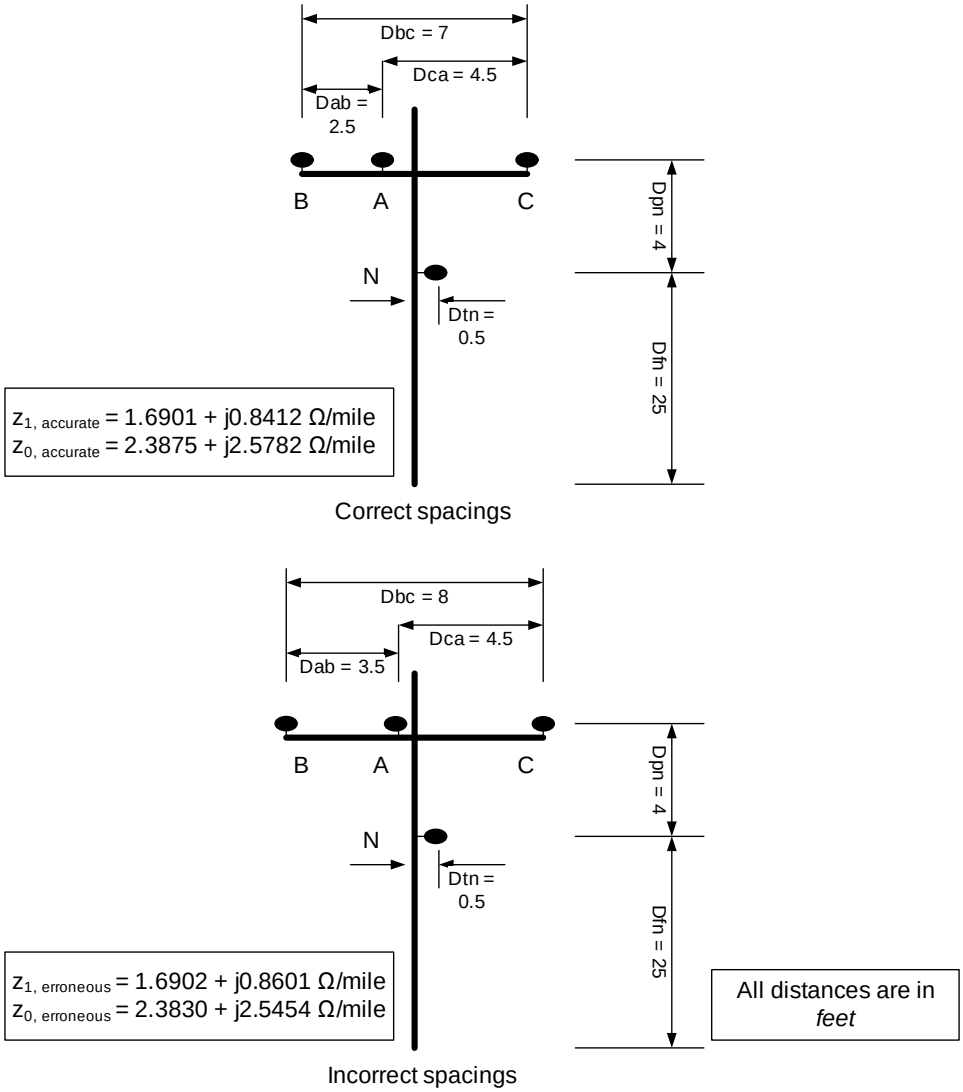

Figure 4.1: Increase in Distances D_{ab} and D_{bc}

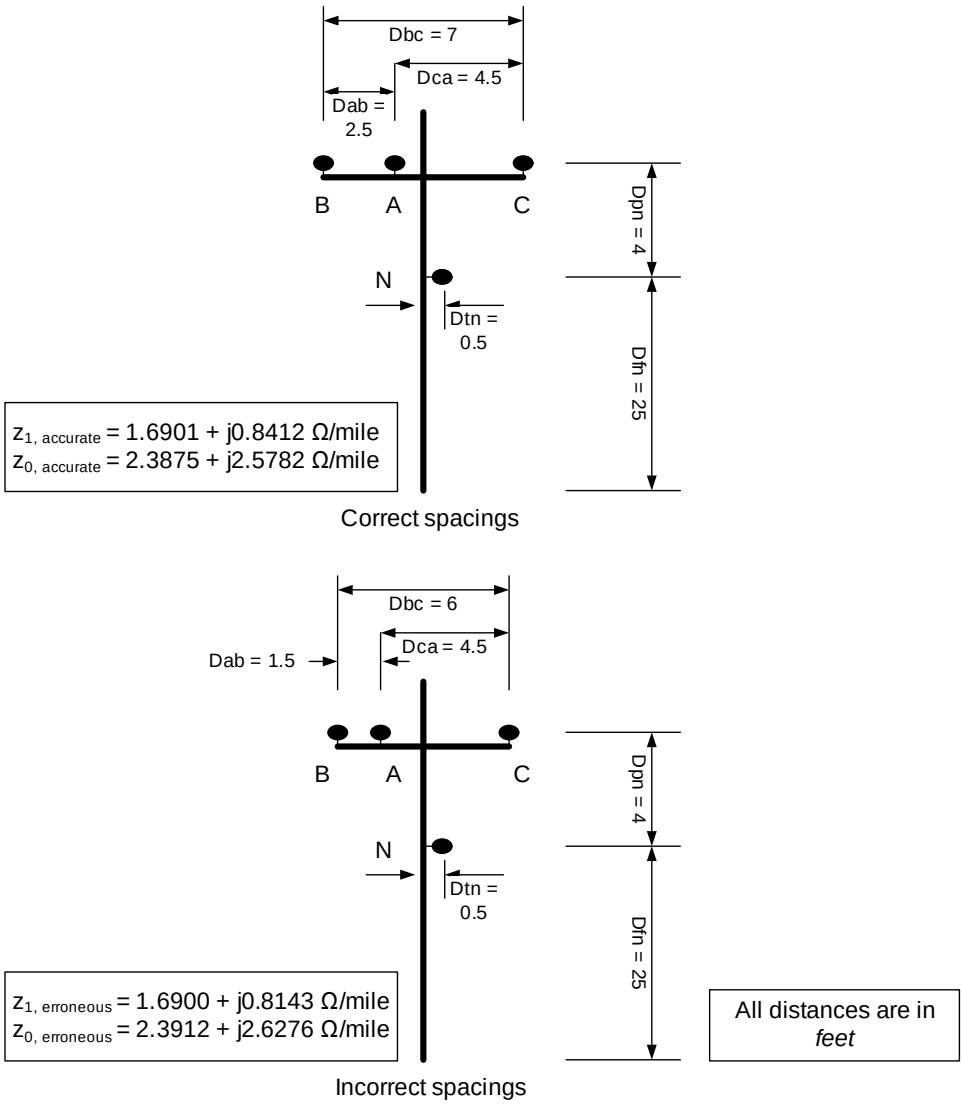

Figure 4.2: Decrease in Distances D_{ab} and D_{bc}

The effect of phase conductor distances on the values of z_1 and z_0 is summarized in Table 4.1 below. When phase conductor distances are increased by 1 ft, the positive-sequence impedance $z_1 = r_1 + jx_1$ increases by 0.47% whereas the zero-sequence impedance $z_0 = r_0 + jx_0$ decreases by 0.8%. On the other hand, when phase conductor distances are decreased by 1 ft, z_1 decreases by 0.6% whereas z_0 increases by 1%. Hence z_1 is directly proportional to distance between phase conductors while z_0 is inversely proportional.

Table 4.1: Summary of Effect of Phase Conductor Distances on Values of z_1 and z_0

Parameter Change	**Effect on r_1**	**Effect on x_1**	**Effect on r_0**	**Effect on x_0**
When phase conductor distances are increased by 1 ft:	Remains unchanged	Increases by 2.25%	Decreases by 0.3%	Decreases by 1.3%
When phase conductor distances are decreased by 1 ft:	Remains unchanged	Decreases by 3%	Increases by 0.15%	Increases by 2%

4.1.2 Phase Conductor Sizes: Effect on z_1 and z_0

The value of phase conductor GMR is increased from 0.00418 ft to 0.00518 ft (a 24% increase). The inaccurate value of conductor GMR (0.00518 ft) is used to compute values of z_1 and z_0. The new (erroneous) values of z_1 and z_0 are:

$$z_{1,erroneous} = 1.6901 + \text{j}0.8151\ \Omega/\text{mile}$$
$$z_{0,erroneous} = 2.3875 + \text{j}2.5522\ \Omega/\text{mile}$$

Next, the value of phase conductor GMR is decreased from 0.00418 ft to 0.00318 ft (a 24% decrease). The corresponding (erroneous) values of z_1 and z_0 are:

$$z_{1,erroneous} = 1.6901 + \text{j}0.8743\ \Omega/\text{mile}$$
$$z_{0,erroneous} = 2.3875 + \text{j}2.6114\ \Omega/\text{mile}$$

The accurate values of z_1 and z_0 computed in Chapter 3 are:

$$z_{1,accurate} = 1.6901 + \text{j}0.8412\ \Omega/\text{mile}$$
$$z_{0,accurate} = 2.3875 + \text{j}2.5782\ \Omega/\text{mile}$$

The effect of phase conductor sizes on the values of z_1 and z_0 is summarized in Table 4.2. It shows that both $z_1 = r_1 + jx_1$ and $z_0 = r_0 + jx_0$ decrease when phase conductor sizes are increased. Hence z_1 and z_0 are inversely proportional to the size of phase conductors.

Table 4.2: Summary of Effect of Phase Conductor Sizes on Values of z_1 and z_0

Parameter Change	**Effect on r_1**	**Effect on x_1**	**Effect on r_0**	**Effect on x_0**
When phase conductor sizes are increased to 0.00518 ft (24% increase)	Remains unchanged	Decreases by 3%	Remains unchanged	Decreases by 1%
When phase conductor sizes are decreased to 0.00318 ft (24% reduction)	Remains unchanged	Increases by 4%	Remains unchanged	Increases by 1.3%

4.1.3 Phase to Neutral Conductor Distances: Effect on z_1 and z_0

Figure 4.3 shows the case where the perpendicular distance between phase and neutral conductors is increased. Distance D_{pn} is increased from 4 ft to 6 ft (a 50% increase). This inaccurate value of D_{pn} (6 ft) is used to compute values of z_1 and z_0.

Figure 4.4 shows the case where the distance D_{pn} is decreased from 4 ft to 2 ft (a 50% decrease). The corresponding z_1 and z_0 values are also shown in the figure.

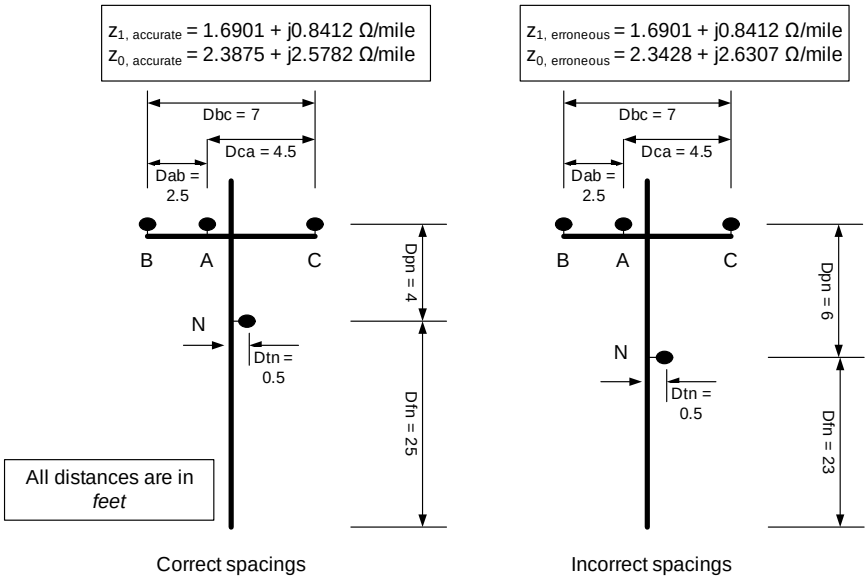

Figure 4.3: Increase in Distance D_{pn}

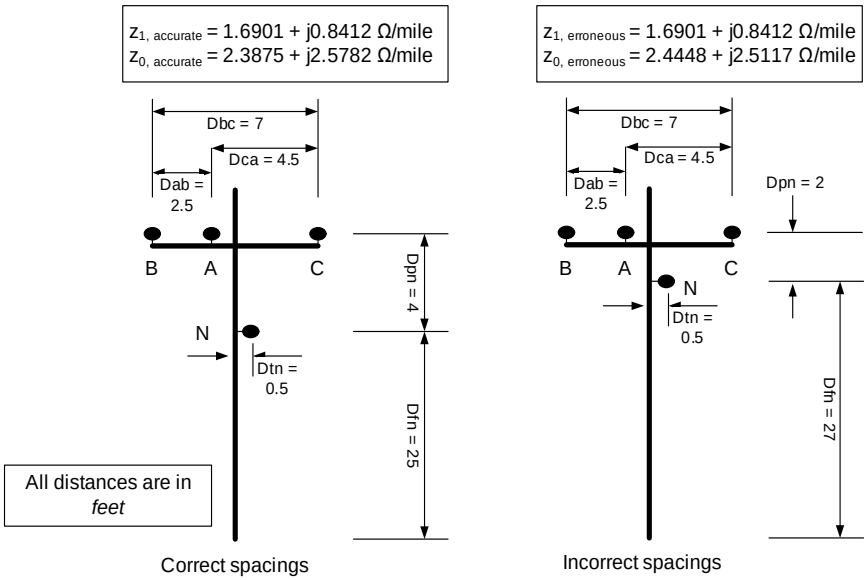

Figure 4.4: Decrease in Distance D_{pn}

The effect of phase to neutral conductor distances on the values of z_1 and z_0 is summarized in Table 4.3. It shows that $z_1 = r_1 + jx_1$ remains unaffected due to change in phase to neutral conductor distances. Also r_0 is inversely proportional to this parameter whereas x_0 is directly proportional.

Table 4.3: Summary of Effect of Phase to Neutral Conductor Distances on Values of z_1 and z_0

Parameter Change	**Effect on r_1**	**Effect on x_1**	**Effect on r_0**	**Effect on x_0**
When phase to neutral conductor distances are increased by 2 ft (50% increase):	Remains unchanged	Remains unchanged	Decreases by 1.8%	Increases by 2%
When phase to neutral conductor distances are decreased by 2 ft (50% reduction):	Remains unchanged	Remains unchanged	Increases by 2.4%	Decreases by 2.6%

4.1.4 Earth Resistivity: Effect on z_1 and z_0

The reference case uses an earth resistivity value of 100 Ω-m to calculate z_1 and z_0. This value is increased to 1000 Ω-m and new (erroneous) values of z_1 and z_0 are computed.

$$z_{1,erroneous} = 1.6901 + \text{j}0.8412\ \Omega/\text{mile}$$
$$z_{0,erroneous} = 2.5233 + \text{j}2.7859\ \Omega/\text{mile}$$

Next, the value of earth resistivity is decreased to 10 Ω-m. This value is used to compute values of z_1 and z_0.

$$z_{1,erroneous} = 1.6901 + \text{j}0.8412\ \Omega/\text{mile}$$
$$z_{0,erroneous} = 2.2603 + \text{j}2.3420\ \Omega/\text{mile}$$

The accurate values of z_1 and z_0 computed earlier are:

$$z_{1,accurate} = 1.6901 + \text{j}0.8412\ \Omega/\text{mile}$$
$$z_{0,accurate} = 2.3875 + \text{j}2.5782\ \Omega/\text{mile}$$

The effect of earth resistivity on the values of z_1 and z_0 is summarized in Table 4.4. It shows that $z_1 = r_1 + jx_1$ remains unchanged and $z_0 = r_0 + jx_0$ increases when earth resistivity is increased. Hence z_0 is directly proportional to earth resistivity.

Table 4.4: Summary of Effect of Earth Resistivity on Values of z_1 and z_0

Parameter Change	**Effect on r_1**	**Effect on x_1**	**Effect on r_0**	**Effect on x_0**
When earth resistivity is increased to 1000 Ω-m:	Remains unchanged	Remains unchanged	Increases by 5.7%	Increases by 8%
When earth resistivity is decreased to 10 Ω-m:	Remains unchanged	Remains unchanged	Decreases by 5.3%	Decreases by 9.2%

4.1.5 Effect of Circuit Model Errors on Values of z_1 and z_0: A Summary

The results of the analysis show that the positive-sequence impedance z_1 is insensitive to any changes in earth resistivity and phase to neutral conductor distances. Variation in phase conductor distances and conductor sizes has a marginal effect on z_1. In a nutshell, incorrect circuit modeling does not affect z_1 significantly.

The zero-sequence impedance z_0 is sensitive to variations in all the four parameters. It increases or decreases by 7% when the earth resistivity value is increased to 1000 Ω-m or decreased to 10 Ω-m from its accurate value of 100 Ω-m. The effect of changes in the other three parameters on the value of z_0 is insignificant. Table 4.5 provides a summary of the analysis presented in previous subsections.

Table 4.5: Summary of Effect of Circuit Model Errors on Values of z_1 and z_0

Parameter	Affects z_1	Affects z_0
Phase Conductor Distance	Yes	Yes
When: Increased by 1 ft.	Increases by 0.25% to 0.6%	Decreases by 0.4% to 0.7%
Decreased by 1 ft.	Decreases by 0.5% to 0.7%	Increases by 0.7% to 1.14%
Phase Conductor Sizes	Yes	Yes
When: Increased by 24%	Decreases by 0.6%	Decreases by 0.57%
Decreased by 24%	Increases by 0.8%	Increases by 0.79%
Phase to Neutral Conductor Distance	No	Yes
When: Increased by 50%	Unchanged	Increases by 0.4%
Decreased by 50%	Unchanged	Decreases by 0.14%
Earth Resistivity	No	Yes
When: Increased to 1000 Ω-m	Unchanged	Increases by 6.83%
Decreased to 10 Ω-m	Unchanged	Decreases by 7.4%

4.2 Effect of Circuit Model Errors on Fault Location Estimates

The effect of incorrect modeling of each of the four parameters on the values of z_1 and z_0 has been discussed in Section 4.1. When incorrect values of z_1 and z_0 are used in the Takagi and positive-sequence reactance methods, their reactance-to-fault estimates are affected. This Section deals with the effect of erroneous z_1 and z_0 values on Takagi and positive-sequence reactance methods. The loop reactance method and the balanced-load method do not use values of z_1 and z_0 while estimating the reactance-to-fault. As these methods are insensitive to variations in z_1 and z_0, they are not analyzed in this Section.

4.2.1 Effect of Phase Conductor Distances on Fault Location Estimates

An important conclusion of the analysis presented in Section 4.1 is that the positive-sequence line impedance z_1 is directly proportional to the distance between phase conductors whereas z_0 is inversely proportional to it. However the effect of variation in phase conductor distances on values of z_1 and z_0 is marginal. As the values of z_1 and z_0 do not change much, it is expected that variation in phase conductor distances will not affect the fault location estimates severely.

In the analysis that follows, phase conductor distances are increased and their effect on fault location estimates is studied. This is followed by analysis of effect of decrease in phase conductor distances.

Increase in phase conductor distances:

Distances D_{ab} and D_{bc} are increased by 1 ft as shown in Figure 4.1 (D_{ca} is the same as that in the reference case). The following values of z_1 and z_0 are obtained:

$$z_{1,erroneous} = 1.6902 + \text{j}0.8601\ \Omega/\text{mile}$$

$$z_{0,erroneous} = 2.3830 + \text{j}2.5454\ \Omega/\text{mile}$$

These values are used in Takagi and positive-sequence reactance methods along with accurate voltage and current measurements and reactance-to-fault estimates are obtained for eight fault locations. Table 4.6 shows representative results for two locations. Estimation errors shown in Table 4.6 are computed using (3.1). Comprehensive results for all the eight locations are included in Appendix B.

Decrease in phase conductor distances:

Next, the distances D_{ab} and D_{bc} are decreased by 1 ft as shown in Figure 4.2 (D_{ca} is the same as that in the reference case). The corresponding z_1 and z_0 values are:

$$z_{1,erroneous} = 1.6900 + \text{j}0.8143\ \Omega/\text{mile}$$

$$z_{0,erroneous} = 2.3912 + \text{j}2.6276\ \Omega/\text{mile}$$

Table 4.6 shows the reactance-to-fault estimates obtained using these values of z_1 and z_0.

Table 4.6: Reactance-to-fault Estimates with Phase Conductor Distance Errors

Fault at node:	**Actual positive-sequence reactance (ohm)**	**Estimated positive seq. reactance (ohm)**	**Error with incorrect circuit model (%)**	**Error for reference case (%)**
Increase in phase conductor distances				
Takagi method:				
848	7.992	7.327	-8.31	-9.53
860	5.872	5.673	-3.39	-4.81
Positive-sequence reactance method:				
848	7.992	7.374	-7.73	-8.62
860	5.872	5.758	-1.94	-3.05
Decrease in phase conductor distances				
Takagi method:				
848	7.992	7.086	-11.33	-9.53
860	5.872	5.466	-6.91	-4.81
Positive-sequence reactance method:				
848	7.992	7.202	-9.89	-8.62
860	5.872	5.598	-4.66	-3.05

The effect of phase conductor distances can be analyzed by examining reactance-to-fault expressions for the positive-sequence reactance and Takagi methods given by (1.15) and (1.19) respectively. Both expressions use the term I_S in the denominator. The current $I_S = I + kI_0$

where,

I = fault current

I_0 = zero-sequence component of fault current

$k = \frac{z_0}{z_1} - 1$

When phase conductor distances are increased, z_1 increases while z_0 decreases leading to decrease in value of k. This in turn causes I_S to decrease. As I_S is in the denominator of (1.15) and (1.19), the reactance-to-fault estimates of both the methods increase. The difference between the actual and estimated reactance-to-fault values reduces and estimation errors become less negative. As an example consider the results for a fault at node 848 in Table 4.6. The actual reactance-to-fault is 7.992 Ω and in the reference case the Takagi method estimates fault location with a -9.53% error. With increase in phase conductor distances the estimated reactance-to-fault is 7.295 Ω. The estimation error decreases to -8.71%. Thus the estimated reactance-to-fault moves closer to the actual value. This is illustrated in Figure 4.5.

The positive-sequence reactance method exhibits the same behavior as the Takagi method. For a fault at node 848, the estimation error is -8.62% for the reference case. It decreases to -8.07% when phase conductor distances are increased. Thus for this method as well, the accuracy of reactance-to-fault estimates improves when distance between phase conductors is increased.

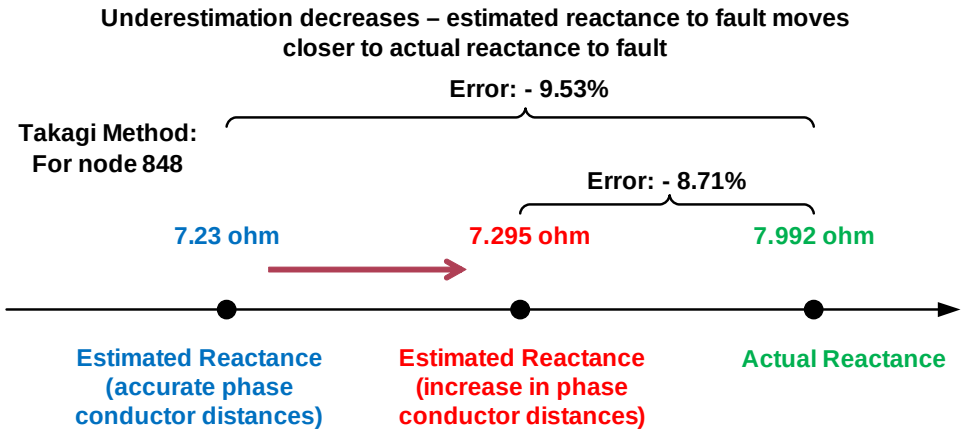

Figure 4.5: Effect of Increase in Phase Conductor Distances on the Takagi Method

Conversely, when phase conductor distances are decreased, the value of k increases thereby increasing I_S. This causes the reactance-to-fault estimates of both the methods to decrease in magnitude. Consequently, the estimation errors become more negative as compared to the reference case (Refer Table 4.6). Thus accuracy of both the methods deteriorates with decrease in phase conductor distances.

The terms 'increase/decrease in underestimation' and 'increase/decrease in overestimation' are convenient for comparing the results with the reference case. They are extensively used henceforth. The interpretation of each of these terms is listed in Table 4.7.

Table 4.7: Interpretation of Terms

Statement	**Interpretation**
Overestimation increases by *x*%	Estimation errors become more positive as compared to reference case. Reactance-to-fault in the reference case is initially overestimated, and becomes more overestimated with a measurement or circuit error. Estimate is now less accurate than that of reference case.
Overestimation decreases by *x*%	Estimation errors become less positive as compared to reference case. Reactance-to-fault in the reference case is initially overestimated, and becomes less overestimated with a measurement or circuit error. Estimate is now more accurate than that of the reference case.
Underestimation increases by *x*%	Estimation errors become more negative as compared to reference case. Reactance-to-fault in the reference case is initially underestimated, and becomes more underestimated with a measurement or circuit error. Estimate is now less accurate than that of reference case.
Underestimation decreases by *x*%	Estimation errors become less negative as compared to reference case. Reactance-to-fault in the reference case is initially underestimated, and becomes less underestimated with a measurement or circuit error. Estimate is now more accurate than that of the reference case.

In conclusion, when phase conductor distances are increased, the value of reactance-to-fault estimates increases as compared to the reference case. In contrast, when these distances are decreased, the estimated reactance-to-fault values decrease. Table 4.8 presents a quantitative summary of the entire analysis.

Table 4.8: Summary of Effect of Phase Conductor Distances on Impedance-based Methods

Parameter Change	**Effect on Takagi Method**	**Effect on Positive-sequence Reactance Method**
When phase conductor distances are increased by 1 ft:	Underestimation decreases by 1 to 2%	Underestimation decreases by 1 to 2%
When phase conductor distances are decreased by 1 ft:	Underestimation increases by 1 to 3%	Underestimation increases by 1 to 3%

4.2.2 Effect of Phase Conductor Sizes on Fault Location Estimates

The approach for analyzing the effect of variations in phase conductor sizes on reactance-to-fault estimates is similar to the one used for analysis of effect of phase conductor distance errors. Initially, phase conductor sizes are increased and the values of positive- and zero-sequence z_1 and z_0 line impedances are computed. These are used to perform fault location and estimation errors are compared with those for the reference case. The analysis is repeated using phase conductor sizes which are smaller than those for the reference case.

Increase in phase conductor sizes:

The value of phase conductor GMR is increased from 0.00418 ft to 0.00518 ft (a 24% increase). The corresponding z_1 and z_0 values are:

$$z_{1,erroneous} = 1.6901 + \text{j}0.8151\ \Omega/\text{mile}$$

$$z_{0,erroneous} = 2.3875 + \text{j}2.5522\ \Omega/\text{mile}$$

The reactance-to-fault estimates obtained using these values are shown in Table 4.9.

Table 4.9: Reactance-to-fault Estimates with Errors in Phase Conductor Sizes

Fault at node:	**Actual positive-sequence reactance (ohm)**	**Estimated positive seq. reactance (ohm)**	**Error with incorrect circuit model (%)**	**Error for reference case (%)**
Increase in conductor GMR				
Takagi method:				
860	5.872	5.524	-5.93	-4.81
848	7.992	7.147	-10.58	-9.53
Positive-sequence reactance method:				
860	5.872	5.673	-3.39	-3.05
848	7.992	7.282	-8.88	-8.62
Decrease in conductor GMR				
Takagi method:				
860	5.872	5.668	-3.47	-4.81
848	7.992	7.331	-8.27	-9.53
Positive-sequence reactance method:				
860	5.872	5.720	-2.59	-3.05
848	7.992	7.332	-8.26	-8.62

Decrease in phase conductor sizes:

Next, the value of phase conductor GMR is decreased to 0.00318 ft (a 24% decrease) and following z_1 and z_0 values are obtained:

$$z_{1,erroneous} = 1.6901 + \text{j}0.8743\ \Omega/\text{mile}$$

$$z_{0,erroneous} = 2.3875 + \text{j}2.6114\ \Omega/\text{mile}$$

These values are used in the Takagi and positive-sequence reactance methods and the fault location estimates are shown in Table 4.9.

It is mentioned in Section 4.1 that a 24% increase in phase conductor sizes causes z_1 and z_0 to decrease by 0.6% and 0.57% respectively. As percent decrease in z_0 is less than that in z_1 the factor $k = \frac{z_0}{z_1} - 1$ increases. This increase in k is marginal as the changes in z_1 and z_0 are insignificant. Hence $I_S = I + kI_0$ increases by a small amount leading to decrease in reactance-to-fault estimates of both the methods. The extent of underestimation increases for both the methods and accuracy of reactance-to-fault estimates deteriorates. The definition of underestimation is given in Table 4.8.

On the other hand, when phase conductor sizes are reduced, the percent increase in z_0 is less than that in z_1 which causes k to decrease. This causes reduction in the value of I_S and the magnitude of reactance-to-fault estimates increases. As a result the estimation errors become less negative and accuracy of both the methods improves.

Table 4.10 provides a quantitative summary of the effect of phase conductor sizes on fault location estimates.

Table 4.10: Summary of Effect of Phase Conductor Sizes on Fault Location Estimates

Parameter Change	Effect on Takagi Method	Effect on Positive-sequence Reactance Method
When phase conductor sizes are increased to 0.00518 ft (24% increase)	Underestimation increases by 1 to 2%	Underestimation increases by 0.4 to 0.8%
When phase conductor sizes are decreased to 0.00318 ft (24% reduction)	Underestimation decreases by 1 to 2%	Underestimation decreases by 0.4 to 0.8%

4.2.3 Effect of Phase to Neutral Conductor Distances on Fault Location Estimates

Any variation in phase to neutral conductor distances does not affect positive-sequence line impedance z_1. The zero-sequence line impedance z_0 is directly proportional to this distance. Any change in z_0 affects the fault location estimates of the Takagi method and the positive-sequence reactance method. The following analysis quantifies the effect of change in phase to neutral conductor distances on fault location estimates.

Increase in phase to neutral conductor distances:

The distance D_{pn} is increased from 4 ft to 6 ft (a 50% increase) and following values of z_1 and z_0 are obtained:

$$z_{1,erroneous} = 1.6901 + \text{j}0.8412\ \Omega/\text{mile}$$

$$z_{0,erroneous} = 2.3428 + \text{j}2.6307\ \Omega/\text{mile}$$

The reactance-to-fault estimates obtained using these values are shown in Table 4.11

Table 4.11: Reactance-to-fault Estimates with Errors in Phase to Neutral Conductor Distances

Fault at node:	**Actual positive-sequence reactance (ohm)**	**Estimated positive seq. reactance (ohm)**	**Error with incorrect circuit model (%)**	**Error for reference case (%)**
Increase in phase to neutral conductor distances				
Takagi method:				
860	5.872	5.553	-5.44	-4.81
848	7.992	7.195	-9.98	-9.53
Positive-sequence reactance method:				
860	5.872	5.637	-4.00	-3.05
848	7.992	7.245	-9.34	-8.62
Decrease in phase to neutral conductor distances				
Takagi method:				
860	5.872	5.635	-4.04	-4.81
848	7.992	7.274	-8.99	-9.53
Positive-sequence reactance method:				
860	5.872	5.764	-1.84	-3.05
848	7.992	7.378	-7.68	-8.62

Decrease in phase to neutral conductor distances:

The distance D_{pn} is decreased to 2 ft (a 50% decrease). The corresponding values of z_1 and z_0 are:

$$z_{1,erroneous} = 1.6901 + \text{j}0.8412\ \Omega/\text{mile}$$

$$z_{0,erroneous} = 2.4448 + \text{j}2.5117\ \Omega/\text{mile}$$

These values are used in the Takagi and positive-sequence reactance methods.

It is mentioned in Section 4.1 that increase in phase to neutral conductor distances causes z_0 to increase whereas z_1 is unaffected. This causes the value of k to increase, thereby increasing I_S. As the denominator of (1.15) and (1.19) increases, the value of reactance-to-fault estimates decreases. Table 4.11 shows that the error percentages are 0.4% to 1% more negative as compared to the reference case. As this variation is not significant, it can be concluded that increase in phase to neutral conductor distances does not impact fault location estimates severely.

The effect of decrease in phase to neutral conductor distances is exactly opposite. The value of k and hence I_S decreases in this case. This leads to an increase in value of fault location estimates. Estimation errors become less negative and the accuracy of reactance-to-fault estimates improves. In this case as well, the errors for both the methods are almost identical to those for the reference case. Thus inaccurate modeling of phase to neutral conductor distances has a marginal effect on fault location estimates.

Table 4.12: Summary of Effect of Phase to Neutral Conductor Distances on Impedance Based Methods

Parameter Change	**Effect on Takagi Method**	**Effect on Positive-sequence Reactance Method**
When phase to neutral conductor distances are increased by 2 ft (50% increase):	Underestimation increases by 0.5 to 1.5%	Underestimation increases by 0.5 to 1.5%
When phase to neutral conductor distances are decreased by 2 ft (50% reduction):	Underestimation decreases by 0.5 to 1.5%	Underestimation decreases by 0.5 to 1.5%

4.2.4 Effect of Earth Resistivity on Fault Location Estimates

Amongst the four parameters which affect line impedances, earth resistivity has the most significant impact on the value of zero-sequence z_0 line impedance. Hence it is expected that this parameter will have a considerable influence on the reactance-to-fault estimates of the Takagi and positive-sequence reactance methods.

Increase in earth resistivity:

The value of earth resistivity is increased from 100 Ω-m to 1000 Ω-m. The corresponding values of z_1 and z_0 are as follows:

$$z_{1,erroneous} = 1.6901 + \text{j}0.8412\ \Omega/\text{mile}$$

$$z_{0,erroneous} = 2.5233 + \text{j}2.7859\ \Omega/\text{mile}$$

These are used in the Takagi method and the positive-sequence reactance method to obtain the reactance-to-fault estimates (Refer Table 4.13).

Table 4.13: Reactance-to-fault Estimates with Errors in Earth Resistivity

Fault at node:	Actual positive-sequence reactance (ohm)	Estimated positive seq. reactance (ohm)	Error with incorrect circuit model (%)	Error for reference case (%)
Increase in earth resistivity				
Takagi method:				
860	5.872	5.436	-7.41	-4.81
848	7.992	7.064	-11.61	-9.53
Positive-sequence reactance method:				
860	5.872	5.513	-6.12	-3.05
848	7.992	7.102	-11.14	-8.62
Decrease in earth resistivity				
Takagi method:				
860	5.872	5.772	-1.70	-4.81
848	7.992	7.425	-7.09	-9.53
Positive-sequence reactance method:				
860	5.872	5.913	0.70	-3.05
848	7.992	7.546	-5.58	-8.62

Decrease in earth resistivity:

Now the value of earth resistivity is decreased from 100 Ω-m to 10 Ω-m and following values of z_1 and z_0 are obtained:

$$z_{1,erroneous} = 1.6901 + \text{j}0.8412\ \Omega/\text{mile}$$

$$z_{0,erroneous} = 2.2603 + \text{j}2.3420\ \Omega/\text{mile}$$

Table 4.13 shows the reactance-to-fault estimates obtained using these values.

Although increase in earth resistivity does not affect z_1, the value of z_0 increases leading to increase in value of k and I_S. As a result the magnitude of fault location estimates decreases. Table 4.13 shows that estimation errors for both methods are 2% to 4% more negative as compared to the reference case. Thus underestimation increases and accuracy of reactance-to-fault estimates deteriorates. With decrease in value of earth resistivity, z_0 decreases leading to reduction in values of k and I_S. The magnitude of reactance-to-fault estimates increases and accuracy of reactance-to-fault estimates improves. Table 4.14 summarizes the results of analysis.

Table 4.14: Summary of Effect of Earth Resistivity on Impedance-based Methods

Parameter Change	**Effect on Takagi Method**	**Effect on Positive-sequence Reactance Method**
When earth resistivity is increased to 1000 Ω-m:	Underestimation increases by 2 to 4%	Underestimation increases by 2 to 4%
When earth resistivity is decreased to 10 Ω-m:	Underestimation decreases by 2 to 5%	Underestimation decreases by 2 to 5%

4.2.5 Summary of Effect of Circuit Model Errors on Fault Location Estimates

Table 4.15 provides a comprehensive summary of the effects of circuit model errors on the fault location estimates. It can be concluded that

reactance-to-fault estimates of the Takagi and positive-sequence reactance methods are not significantly affected by circuit model errors. Amongst the four parameters considered for analysis, variation in earth resistivity has the most pronounced effect on the reactance-to-fault estimates. The effect of the other three parameters is marginal.

Table 4.15: Effect of Circuit Model Errors on Fault Location Estimates

Parameter	Takagi Method	Positive-sequence Reactance Method	Loop Reactance Method	Balanced-load Method
Phase Conductor Distance	Slightly Sensitive	Slightly Sensitive	Insensitive	Insensitive
Increased by 1 ft.	Underestimation decreases by 1% to 2%	Underestimation decreases by 1% to 2%	Estimates Remain unchanged	Estimates Remain unchanged
Decreased by 1 ft.	Underestimation increases by 1% to 3%	Underestimation increases by 1% to 3%		
Phase Conductor Sizes	Slightly Sensitive	Slightly Sensitive	Insensitive	Insensitive
Increased by 24%	Underestimation increases by 1% to 2%	Underestimation increases by 0.4% to 0.8%	Estimates Remain unchanged	Estimates Remain unchanged
Decreased by 24%	Underestimation decreases by 1% to 2%	Underestimation decreases by 0.4% to 0.8%		
Phase to Neutral Conductor Distance	Slightly Sensitive	Slightly Sensitive	Insensitive	Insensitive
Increased by 50%	Underestimation increases by 0.5% to 1.5%	Underestimation increases by 0.5% to 1.5%	Estimates Remain unchanged	Estimates Remain unchanged
Decreased by 50%	Underestimation decreases by 0.5% to 1.5%	Underestimation decreases by 0.5% to 1.5%		
Earth Resistivity	Moderately Sensitive	Moderately Sensitive	Insensitive	Insensitive
Increased to 1000 Ω-m	Underestimation increases by 2% to 4%	Underestimation increases by 2% to 4%	Estimates Remain unchanged	Estimates Remain unchanged
Decreased to 10 Ω-m	Underestimation decreases by 2% to 5%	Underestimation decreases by 2% to 5%		

4.3 Effect of the Uniform Line Impedance Assumption on Fault Location Estimates

The Takagi and positive-sequence reactance method use values of positive- and zero-sequence z_1 and z_0 line impedances (in Ω/mile) to estimate the reactance to fault location. In a practical, non-homogeneous, distribution feeder the values of z_1 and z_0 are different for different segments of the feeder. Both the methods make a simplifying assumption and use values of z_1 and z_0 corresponding to the longest segment of the feeder while estimating the reactance-to-fault. This Section investigates the effect of this assumption on fault location estimates.

4.3.1 Construction of a System Model with Uniform Line Impedances

In the reference case, a non-homogeneous IEEE 34 Node Test Feeder is used for analysis. It has five different conductor configurations viz. 300, 301, 302, 303 and 304. Configurations 300, 301 represent three-phase feeders, while the other three denote single phase laterals. Since configuration 301 is most widely used, the Takagi and positive-sequence reactance methods compute the reactance-to-fault using values of z_1 and z_0 corresponding to this configuration.

To study the effect of the uniform line impedance assumption, a new homogeneous IEEE 34 Node Test Feeder model is created in PSCAD. All sections of the main feeder as well as the laterals are constructed using configuration 301. Since configuration 301 is an arrangement of three-phase conductors, this new model does not have any single-phase laterals. Single-phase laterals are replaced by three-phase lines (in configuration 301) of the same length. As the length of the lines between adjacent nodes is unchanged, the distance-to-fault as measured from the monitoring location (node 800) is the

same as the reference case. However as the line configuration has changed, the reactance-to-fault as measured from the monitoring location (node 800) changes.

4.3.2 Fault Location Using System Model with Uniform Line Impedances

Single line-to-ground faults are placed in the new homogeneous model at the same eight locations as the reference case. Fault location is carried out using the voltage and current measurements obtained from this feeder. Since this feeder has uniform line impedances, using z_1 and z_0 values corresponding to configuration 301 for fault location is justified. In contrast, for the reference case, where there are multiple conductor configurations, using values corresponding to a single configuration is erroneous. Reactance-to-fault estimates for two fault locations are shown in Table 4.16. Appendix C lists the fault location estimates for all eight locations.

Table 4.16: Effect of System Non-homogeneity on Fault Location Estimates

Fault at node:	**Actual positive-sequence reactance (ohm)**	**Estimated positive seq. reactance (ohm)**	**Error for homogeneous system model (%)**	**Error for reference (non-homogeneous) case (%)**
Takagi method:				
860	5.897	5.790	-1.81	-4.81
848	8.017	7.462	-6.92	-9.53
Positive-sequence reactance method:				
860	5.897	5.689	-3.52	-3.05
848	8.017	7.318	-8.71	-8.62

It is to be noted that the reactance-to-fault as measured from the monitoring location (node 800) for the homogeneous feeder is different from that for the reference case. Hence the actual positive-sequence reactance-to-fault (column 2 in Table 4.16) has to be recomputed for each fault location. This new value of actual reactance-to-fault is used to calculate estimation errors for the homogeneous feeder case.

When the Takagi method is used to conduct fault location on the homogeneous feeder with uniform line impedances, the estimation errors are less negative as compared to the reference case (Refer Table 4.16). Thus underestimation decreases and accuracy of reactance-to-fault estimates improves. For a fault at node 860, when the system is non-homogeneous (reference case), the Takagi method estimates the reactance-to-fault with a -4.81% error. For the homogeneous system, with uniform line impedances, the estimation error is - 1.81%. Thus the assumption of uniform line impedances for a non-homogeneous system increases the estimation errors by 3%. For the positive-sequence reactance method, the error percentages for the two cases are almost identical.

To summarize, for both the methods, the difference between error percentages for the homogeneous and non-homogeneous cases is marginal. It is reasonable to assume that a distribution feeder has uniform line impedances, while estimating the reactance-to-fault. This assumption does not have a significant effect on the accuracy of estimation.

Chapter 5

Effect of Measurement Errors on Fault Location Estimates

All the impedance-based methods use voltage and current measurements to estimate the reactance to fault location. If these measurements are inaccurate, the reactance-to-fault estimates are affected. Section 5.1 in this Chapter points out that inaccurate voltage and current measurements arise from ratio and phase angle errors in instrument transformers. This Section also identifies transformer excitation current as the main cause of ratio and phase angle errors.

Section 5.2 focuses on the effect of current transformer (CT) ratio and phase angle errors on fault location estimates and assumes that the voltage transformer (VT) measurements are accurate. It is observed that when CT measurements are affected by 6% ratio errors and phase angle errrors of $\pm 1^0$, the magnitude of estimated reactance to fault location increases. This increase in magnitude has different effects on the estimation accuracy of the four impedance-based methods. It should be recalled that for the reference case, the Takagi and positive-sequence reactance methods underestimate the reactance to fault location leading to negative estimation errors. As CT measurement errors increase the magnitude of fault location estimates, the estimated reactance-to-fault value moves closer to the actual value. As a result, the error percentages for both the methods decrease by 4% to 10% and accu-

racy of estimation improves. The loop reactance and balanced-load methods have positive estimation errors and overestimate fault location in the reference case. With erroneous CT measurements, accuracy of both the methods deteriorates. The estimation errors for the balanced-load method increase by 6% to 11%. The loop reactance method is most severely affected with 10% to 40% increase in estimation errors.

Section 5.3 analyzes the effect of erroneous VT measurements and assumes CT measurements to be accurate. When VT measurements are affected by 5% ratio errors and phase angle errrors of $\pm 1^0$, they tend to decrease the magnitude of estimated reactance to fault location. This has an unfavorable impact on the accuracy of Takagi and positive-sequence reactance methods. The estimation errors for these methods increase by 4% to 8%. In contrast, the errors for loop reatance and balanced-load methods reduce by 6% to 12% and their accuracy improves.

The combined effect of CT and VT measurement errors is analyzed in Section 5.4. CT and VT measurements are affected by ratio errors of 6% and 5% respectively. Additionally, phase angle errors of $\pm 1^0$ are present in both CT and VT measurements. It is oberved that ratio errors in CTs and VTs nullify the effect of each other. In such a scenario, the sign of the phase angle errors determines the effect on estimation accuracy. When the phase angle error in CTs is -1^0 and that in VTs is 1^0, accuracy of the Takagi and positive-sequence reactance methods improves. Estimation errors for these methods reduce by 5% to 6% as compared to the reference case. However error percentages for the balanced-load method increase by 6% to 7% indicating deterioration in performance. The loop reactance method is severely affected with 8% to 30% increase in estimation errors. As opposed to this, when the VT phase angle

error is -1^0 and that in CTs is 1^0, errors for the Takagi and positive-sequence reactance methods increase by 2% to 3% and their accuracy deteriorates. The loop reactance and balanced-load methods show improved accuracy with 5% to 6% reduction in error percentages.

5.1 Types of Measurement Errors

Instrument transformers are prone to 2 types of errors - ratio errors and phase angle errors. The cause of these errors and their effect on current and voltage transformer measurements is discussed below.

Ratio errors in current transformers (CTs) cause the secondary current value to differ from the rated value. For example, for a 200/1 CT, when a current of 200 A circulates in the primary winding, the secondary current is expected to be 1 A. However in a practical transformer, the secondary current is around 0.95 A to 0.97 A. This error arises because of the excitation current drawn by the CT.

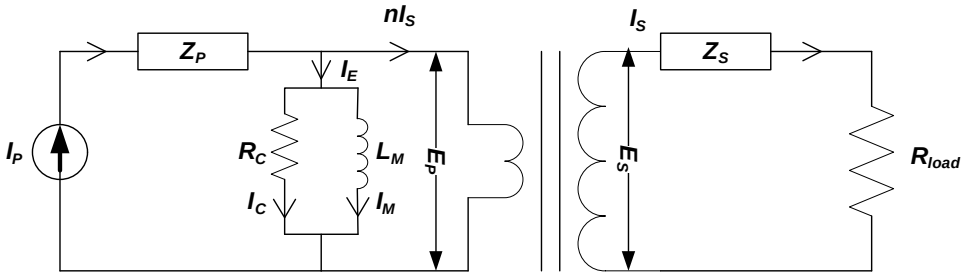

Figure 5.1: Equivalent Circuit of a Current Transformer (CT)

The equivalent circuit for a current transformer is shown in Figure 5.1. The turns ratio of the transformer is denoted by n. The primary current is represented by I_P while I_S is the secondary current. The secondary current

reflected on the primary side of the transformer is nI_S. The excitation current drawn by the CT is denoted by I_E. It has two components:

1. I_C is the core loss component - It is required to supply losses in the CT core

2. I_M is the magnetizing component - It is required to set up magnetic flux in the CT core

It can be seen from Figure 5.1 that $I_P = nI_S + I_E$. Further, in an ideal CT $I_E = 0$ A. Hence,

$$I_P = nI_S \tag{5.1}$$

$$\therefore \frac{I_P}{I_S} = n \tag{5.2}$$

As a result, there is no ratio error. However a practical CT draws finite excitation current. Hence,

$$\therefore I_P > nI_S \tag{5.3}$$

$$\frac{I_P}{I_S} \neq n \tag{5.4}$$

Thus the excitation current I_E causes a ratio error in CTs.

The simplified phasor diagram for a CT is shown in Figure 5.2. Voltage phasors are not shown in the diagram. It is assumed that the load in the CT secondary is purely resistive. Hence I_S lags flux ϕ by 90^0. Figure 5.2 shows that I_P is the phasor addition of nI_S and I_E. In an ideal CT, $I_E = 0$A so that I_P and nI_S are in phase. However for a practical CT, $I_E \neq 0$. Hence there is a phase difference θ between I_P and nI_S. Thus the excitation current I_E also causes a phase angle error θ in CTs.

In a similar manner, the excitation current causes ratio and phase angle errors in voltage transformers (VTs).

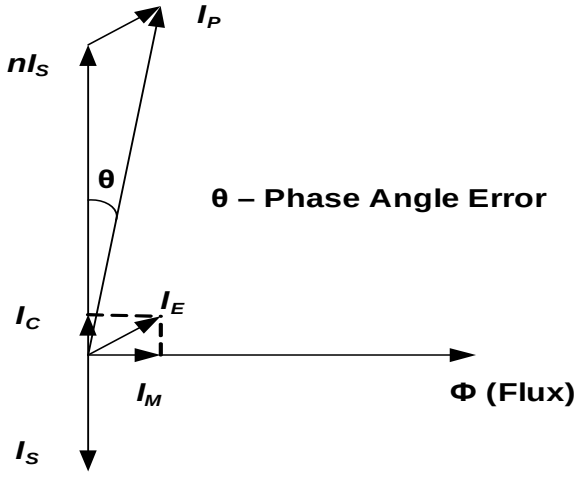

Figure 5.2: Phasor Diagram for a Current Transformer (CT)

5.2 Effect of Errors in Current Measurement on Fault Location

This Section analyzes the effect of ratio and phase angle errors in current transformers, on the four impedance-based methods. It is assumed that voltage measurements are accurate. Typical values of ratio and phase angle errors are obtained from [16]. Ratio errors of 6% and phase angle errors of $\pm 1^0$ are introduced in the CTs. The erroneous current measurements are used in the four impedance-based methods. Estimation errors are computed using (3.1) and labeled as 'Error with inaccurate current measurements'. These errors are compared with those for the reference case. The analysis is presented in five parts.

1. 6% ratio error in CTs but no phase angle error
2. 1^0 phase angle error in CTs but no ratio error
3. -1^0 phase angle error in CTs but no ratio error

4. 6% ratio error and 1^0 phase angle error in CTs

5. 6% ratio error and -1^0 phase angle error in CTs

Six percent ratio error in CTs but no phase angle error:

A ratio error of 6% implies that the CT secondary current is 6% less than the rated value, e.g. for a 200/1 CT, when the primary current is 200, a ratio error of 6% causes the secondary current to be 0.94 A instead of 1 A. The IEEE 34 Node Test Feeder provides fault voltage and current values for this analysis. The fault current value obtained from the IEEE 34 Node Test Feeder is multiplied by a factor of 0.94. The erroneous current value is used in the four impedance-based methods. The voltage measurements and z_1 and z_0 values used in the four methods are accurate. Reactance-to-fault estimates for two representative locations are shown in Table 5.1. Comprehensive results for all eight fault locations are included in Appendix D.

A ratio error of 6% decreases the magnitude of fault current. As all impedance-based methods use phasor value of current in the denominator, it is expected that fault location estimates will increase in magnitude. Table 5.1 shows that for the Takagi and positive-sequence reactance methods, underestimation decreases for a fault at node 848. At node 860, where the reactance-to-fault is underestimated in the reference case, it is now overestimated. This indicates that the magnitude of estimated reactance-to-fault has increased. For the loop reactance and balanced-load methods, overestimation increases and the value of estimated reactance-to-fault moves further away from the actual value. To summarize, the reactance-to-fault estimates of all the methods increase in magnitude when ratio errors are present in current measurements.

Table 5.1: Reactance-to-fault Estimates with 6% Ratio Error in CTs

Fault at node:	Actual reactance-to-fault (ohm)	Estimated reactance-to-fault (ohm)	Error with inaccurate current measurements (%)	Error for reference case (%)
Takagi method:				
860	5.872	6.026	2.65	-4.81
848	7.992	7.821	-2.12	-9.53
Positive-sequence reactance method:				
860	5.872	6.164	5.01	-3.05
848	7.992	7.944	-0.57	-8.62
Balanced-load method:				
860	5.872	7.179	22.30	14.92
848	7.992	9.132	14.29	7.41
Loop Reactance method:				
860	9.753	18.078	85.36	62.62
848	13.332	27.034	102.77	72.69

Phase angle error of one degree in CTs but no ratio error:

Phase angle error of 1^0 is introduced in the fault current value obtained from the IEEE 34 Node Test Feeder. To simulate this phase angle error, the phasor value of current obtained from the IEEE 34 Node Test Feeder is multiplied by a factor of $1\angle 1^0$. The reactance-to-fault estimates obtained using the erroneous value of current are shown in Table 5.2.

Table 5.2 shows that for the Takagi and positive-sequence reactance methods underestimation increases and the accuracy of reactance-to-fault estimates deteriorates. For the loop reactance and balanced-load methods, overes-

Table 5.2: Reactance-to-fault Estimates with 1^0 Phase Angle Error in CTs

Fault at node:	Actual reactance-to-fault (ohm)	Estimated reactance-to-fault (ohm)	Error with inaccurate current measurements (%)	Error for reference case (%)
Takagi method:				
860	5.872	5.466	-6.88	-4.81
848	7.992	7.066	-11.56	-9.53
Positive-sequence reactance method:				
860	5.872	5.494	-6.41	-3.05
848	7.992	7.033	-11.97	-8.62
Balanced-load method:				
860	5.872	6.568	11.90	14.92
848	7.992	8.346	4.45	7.41
Loop Reactance method:				
860	9.753	15.140	55.24	62.62
848	13.332	21.494	61.22	72.69

timation decreases at all the fault locations. Thus a positive phase angle error in current measurements leads to decrease in value of estimated reactance-to-fault for all the methods. It is to be noted that the effect of positive phase angle errors in CTs is exactly opposite to that of ratio errors.

Phase angle error of minus one degree in CTs but no ratio error:

The fault current value is now affected by a phase angle error of -1^0. This is simulated by multiplying the phasor value of current by a factor of $1\angle -1^0$. The corresponding reactance-to-fault estimates are shown in Table 5.3.

Table 5.3: Reactance-to-fault Estimates with -1^0 Phase Angle Error in CTs

Fault at node:	Actual reactance-to-fault (ohm)	Estimated reactance-to-fault (ohm)	Error with inaccurate current measurements (%)	Error for reference case (%)
Takagi method:				
860	5.872	5.705	-2.81	-4.81
848	7.992	7.381	-7.62	-9.53
Positive-sequence reactance method:				
860	5.872	5.890	0.34	-3.05
848	7.992	7.570	-5.26	-8.62
Balanced-load method:				
860	5.872	6.926	17.99	14.92
848	7.992	8.819	10.38	7.41
Loop Reactance method:				
860	9.753	16.511	69.30	62.62
848	13.332	24.501	83.78	72.69

Negative phase angle errors lead to decrease in underestimation for the Takagi and positive-sequence reactance methods. For the loop reactance and balanced-load methods, overestimation increases at all the fault locations. Comparison of results in Table 5.1 and Table 5.3 shows that the effect of negative phase angle errors is similar to ratio errors as both of them cause the magnitude of reactance-to-fault estimates to increase.

Six percent ratio error and one degree phase angle error in CTs:

In this analysis there is a ratio error of 6% as well as a phase angle error of 1^0 in the CT measurements. The phasor value of current, obtained from the

Table 5.4: Reactance-to-fault Estimates with 6% Ratio Error 1^0 Phase Angle Error in CTs

Fault at node:	Actual reactance-to-fault (ohm)	Estimated reactance-to-fault (ohm)	Error with inaccurate current measurements (%)	Error for reference case (%)
Takagi method:				
860	5.872	5.705	-2.81	-4.81
848	7.992	7.381	-7.62	-9.53
Positive-sequence reactance method:				
860	5.872	5.890	0.34	-3.05
848	7.992	7.570	-5.26	-8.62
Balanced-load method:				
860	5.872	6.926	17.99	14.92
848	7.992	8.819	10.38	7.41
Loop Reactance method:				
860	9.753	16.511	69.30	62.62
848	13.332	24.501	83.78	72.69

the IEEE 34 Node Test Feeder, is multiplied by a factor of $0.94\angle 1^0$. This value is used in the four impedance-based methods and the reactance-to-fault estimates are shown in Table 5.4.

Table 5.4 shows that for the Takagi and positive-sequence reactance methods, underestimation decreases for a fault at node 848. Also for node 860, the reactance-to-fault is overestimated. For the loop reactance and balanced-load methods, overestimation increases at all the fault locations. These results are similar to those shown in Table 5.1. However the estimation errors in Table 5.4 are closer to the reference case. This is because ratio errors increase the

magnitude of estimated reactance-to-fault while positive phase angle errors decrease it. When these errors occur simultaneously, their effects are compensated. The effect of ratio errors dominates over that of positive phase angle errors. Hence the magnitude of fault location estimates increases.

Six percent ratio error and minus one degree phase angle error in CTs:

To simulate a 6% ratio error and a phase angle error of -1^0, the fault current phasor is multiplied by a factor of $0.94\angle -1^0$. Table 5.5 shows the reactance-to-fault estimates obtained using erroneous fault current measurements.

Since ratio errors and negative phase angle errors tend to increase the magnitude of fault location estimates, when these errors occur simultaneously, the value of estimated reactance-to-fault increases considerably. As a result the Takagi and positive-sequence reactance methods, which underestimate the reactance-to-fault in the reference case, now overestimate it. For the loop-reactance and balanced-load methods, the errors become more positive and the extent of overestimation increases.

Table 5.5: Reactance-to-fault Estimates with 6% Ratio Error and -1^0 Phase Angle Error in CTs

Fault at node:	**Actual reactance-to-fault (ohm)**	**Estimated reactance-to-fault (ohm)**	**Error with inaccurate current measurements (%)**	**Error for reference case (%)**
Takagi method:				
860	5.872	6.146	4.68	-4.81
848	7.992	7.976	-0.19	-9.53
Positive-sequence reactance method:				
860	5.872	6.375	8.56	-3.05
848	7.992	8.229	2.97	-8.62
Balanced-load method:				
860	5.872	7.368	25.48	14.92
848	7.992	9.382	17.39	7.41
Loop Reactance method:				
860	9.753	18.870	93.48	62.62
848	13.332	28.912	116.86	72.69

On the basis of the analysis presented in Section 5.2, it can be concluded that ratio errors in CTs cause the reactance-to-fault estimates of all the methods to increase. For the Takagi and positive-sequence reactance methods, underestimation decreases by 6% to 8%. Estimation errors for the loop reactance method increase by 8% to 30% as compared to the reference case. For the balanced-load method as well, overestimation increases by 8% to 9%.

When CT ratio errors and positive phase angle errors occur simultaneously, they mitigate the effects of each other. The effect of CT ratio errors dominates leading to increase in magnitude of fault location estimates. Estima-

tion errors for the Takagi and positive-sequence reactance methods decrease by 4% to 5%. It is evident that decrease in underestimation for these two methods is less pronounced as compared to the scenario in which CT measurements are affected by ratio errors only. For the loop reactance method, overestimation increases by 6% to 15% and for the balanced-load method estimation errors become 4% to 6% more positive. It should be noted that error percentages do not increase as significantly as they do with only CT ratio errors. Thus positive phase angle errors compensate for the effect of ratio errors and reduce the sensitivity of the four methods to CT measurement errors.

When CT measurements are affected by ratio errors and negative phase angle errors, fault location estimates of all the methods are severely impacted. Negative phase angle errors amplify the effect of ratio errors leading to significant increase in magnitude of fault location estimates. As a result of this the Takagi and positive-sequence reactance methods overestimate the reactance-to-fault by 1% to 4%. For the loop reactance method overestimation increases by 10% to 40% and for the balanced load method estimation errors become 10% to 11% more positive. Thus the combination of ratio errors and negative phase angle errors in CT measurements has the most pronounced effect on fault location estimates of the impedance-based methods.

5.3 Effect of Errors in Voltage Measurement on Fault Location

This Section analyzes the effect of ratio and phase angle errors in voltage transformers, on the impedance-based methods. It is assumed that current measurements are accurate. The analysis approach is the same as that used for CT measurement errors. Ratio errors of 5% and phase angle errors of $\pm 1^0$ are introduced in the VTs. The erroneous voltage measurements are used in the four impedance-based methods. Estimation errors are computed using (3.1) and labeled as 'Error with inaccurate voltage measurements'. The analysis is presented in five different parts.

1. 5% ratio error in VTs but no phase angle error
2. 1^0 phase angle error in VTs but no ratio error
3. -1^0 phase angle error in VTs but no ratio error
4. 5% ratio error and 1^0 phase angle error in VTs
5. 5% ratio error and -1^0 phase angle error in VTs

Five percent ratio error in VTs but no phase angle error:

A ratio error of 5% implies that the VT secondary voltage is 0.95 times the rated value. The faulted phase voltage value obtained from the IEEE 34 Node Test Feeder is multiplied by a factor of 0.95. This causes the voltage magnitude to decrease. Reactance-to-fault estimates obtained using erroneous voltage measurements are shown in Table 5.6.

Table 5.6: Reactance-to-fault Estimates with 5% Ratio Error in VTs

Fault at node:	Actual reactance-to-fault (ohm)	Estimated reactance-to-fault (ohm)	Error with inaccurate voltage measurements (%)	Error for reference case (%)
Takagi method:				
860	5.872	5.309	-9.55	-4.81
848	7.992	6.868	-14.04	-9.53
Positive-sequence reactance method:				
860	5.872	5.409	-7.86	-3.05
848	7.992	6.939	-13.15	-8.62
Balanced-load method:				
860	5.872	6.368	8.48	14.92
848	7.992	8.117	1.59	7.41
Loop Reactance method:				
860	9.753	15.049	54.30	62.62
848	13.332	21.880	64.12	72.69

Since all four methods use phasor value of voltage in the numerator, decrease in voltage magnitude is accompanied by decrease in value of estimated reactance-to-fault. Table 5.6 shows that for the Takagi and positive-sequence reactance methods, underestimation increases and the accuracy of reactance-to-fault estimates deteriorates. For the loop reactance and balanced-load methods, overestimation decreases at all the fault locations leading to improvement in accuracy.

Phase angle error of one degree in VTs but no ratio error:

Phase angle error of 1^0 is introduced by multiplying the faulted phase voltage phasor by a factor of $1\angle 1^0$. The erroneous fault voltage value is used in the four methods and the reactance-to-fault estimates are shown in Table 5.7

Table 5.7: Reactance-to-fault Estimates with 1^0 Phase Angle Error in VTs

Fault at node:	**Actual reactance-to-fault (ohm)**	**Estimated reactance-to-fault (ohm)**	**Error with inaccurate voltage measurements (%)**	**Error for reference case (%)**
Takagi method:				
860	5.872	5.706	-2.79	-4.81
848	7.992	7.381	-7.62	-9.53
Positive-sequence reactance method:				
860	5.872	5.880	0.16	-3.05
848	7.992	7.551	-5.50	-8.62
Balanced-load method:				
860	5.872	6.949	18.37	14.92
848	7.992	8.844	10.69	7.41
Loop Reactance method:				
860	9.753	16.212	66.22	62.62
848	13.332	23.656	77.44	72.69

This measurement error leads to improvement in accuracy for the Takagi and positive-sequence reactance methods. The extent of underestimation

for these methods decreases as compared to the reference case. For the loop reactance and balanced-load methods, overestimation increases at all the fault locations. Comparison of results in Table 5.6 and Table 5.7 shows that ratio errors and positive phase angle errors have opposite effects on the fault location estimates.

Phase angle error of minus one degree in VTs but no ratio error:

In this analysis, VT measurements are affected by a phase angle error of -1^0. Table 5.8 shows the reactance-to-fault estimates obtained using the erroneous voltage measurements.

The effect of negative phase angle errors is similar to that of ratio errors. These errors lead to increase in underestimation for the Takagi and positive-sequence reactance methods. For the loop reactance and balanced-load methods, overestimation decreases at all the fault locations.

Table 5.8: Reactance-to-fault Estimates with -1^0 Phase Angle Error in VTs

Fault at node:	Actual reactance-to-fault (ohm)	Estimated reactance-to-fault (ohm)	Error with inaccurate voltage measurements (%)	Error for reference case (%)
Takagi method:				
860	5.872	5.470	-6.81	-4.81
848	7.992	7.076	-11.44	-9.53
Positive-sequence reactance method:				
860	5.872	5.506	-6.21	-3.05
848	7.992	7.056	-11.70	-8.62
Balanced-load method:				
860	5.872	6.545	11.50	14.92
848	7.992	8.321	4.14	7.41
Loop Reactance method:				
860	9.753	15.466	58.58	62.62
848	13.332	22.400	68.02	72.69

Five percent ratio error and phase angle error of one degree in VTs:

In this part of the analysis there is a ratio error of 5% as well as a phase angle error of 1^0 in the VT measurements. The phasor value of fault voltage is multiplied by a factor of $0.95\angle 1^0$, to simulate this measurement error.

Ratio errors and positive phase angle errors have opposite effects on fault location estimates. When these errors occur simultaneously, the effect of ratio errors dominates. As a result the magnitude of reactance-to-fault estimates decreases. This leads to increase in underestimation for the Takagi

Table 5.9: Reactance-to-fault Estimates with 5% Ratio Error and 1^0 Phase Angle Error in VTs

Fault at node:	Actual reactance-to-fault (ohm)	Estimated reactance-to-fault (ohm)	Error with inaccurate voltage measurements (%)	Error for reference case (%)
Takagi method:				
860	5.872	5.421	-7.68	-4.81
848	7.992	7.012	-12.26	-9.53
Positive-sequence reactance method:				
860	5.872	5.586	-4.87	-3.05
848	7.992	7.173	-10.24	-8.62
Balanced-load method:				
860	5.872	6.558	11.69	14.92
848	7.992	8.365	4.67	7.41
Loop Reactance method:				
860	9.753	15.400	57.90	62.62
848	13.332	22.470	68.54	72.69

and positive-sequence reactance methods and decrease in overestimation for the loop reactance and balanced-load methods.

Five percent ratio error and phase angle error of minus one degree in VTs:

In this case, a multiplying factor of $0.95\angle -1^0$ is used to simulate a ratio error of 5% and a phase angle error of -1^0. The corresponding reactance-to-fault estimates are shown in Table 5.10.

Table 5.10: Reactance-to-fault Estimates with 5% Ratio Error and -1^0 Phase Angle Error in VTs

Fault at node:	**Actual reactance-to-fault (ohm)**	**Estimated reactance-to-fault (ohm)**	**Error with inaccurate voltage measurements (%)**	**Error for reference case (%)**
Takagi method:				
860	5.872	5.197	-11.50	-4.81
848	7.992	6.722	-15.88	-9.53
Positive-sequence reactance method:				
860	5.872	5.230	-10.93	-3.05
848	7.992	6.703	-16.13	-8.62
Balanced-load method:				
860	5.872	6.175	5.17	14.92
848	7.992	7.867	-1.56	7.41
Loop Reactance method:				
860	9.753	14.693	50.65	62.62
848	13.332	21.280	59.62	72.69

Since ratio errors and negative phase angle errors tend to decrease the magnitude of fault location estimates, when these errors occur simultaneously, the value of estimated reactance-to-fault decreases considerably. Table 5.10 shows that underestimation increases significantly for the Takagi and positive-sequence reactance methods. For the loop reactance and balanced-load methods, the extent of overestimation decreases.

The results of the analysis presented in Section 5.3 can be summarized as follows:

Ratio errors in VTs cause the magnitude of reactance-to-fault estimates to decrease. This leads to 5% to 6% increase in underestimation for the Takagi and positive-sequence methods. For the loop reactance and balanced-load methods, overestimation decreases by 6% to 8%.

When ratio errors and positive phase angle errors occur simultaneously, they attempt to cancel out the effect of each other. The effect of ratio errors dominates, leading to decrease in magnitude of fault location estimates. For the Takagi and positive-sequence reactance methods, underestimation increases by 3% to 4%. Estimation errors for the loop reactance and balanced-load methods become 5% to 6% less positive.

Negative phase angle errors intensify the effect of ratio errors leading to considerable decrease in magnitude of reactance-to-fault estimates of all the methods. The extent of underestimation for the Takagi and positive-sequence reactance methods increases by 6.5% to 7%. For the loop reactance and balanced-load methods, overestimation decreases by 8% to 12%. It can be concluded that simultaneous occurrence of VT ratio errors and negative phase angle errors has the most significant impact on fault location estimates.

5.4 Effect of Errors in Current and Voltage Measurement on Fault Location

The analysis presented in Section 5.2 and Section 5.3 shows that CT measurement errors tend to increase the value of fault location estimates of impedance-based methods while VT measurement errors decrease this value.

Since in a practical distribution system, both CT and VT measurements are likely to be erroneous, it is essential to analyze their combined effect on the reactance-to-fault estimates. In this Section, CT measurements are affected by 6% ratio errors and phase angle errors of $\pm 1^0$. Additionally, 5% ratio errors and phase angle errors of $\pm 1^0$ are present in the VTs. The analysis is presented in three parts.

1. 6% ratio error and 1^0 phase angle error in CTs

   5% ratio error and 1^0 phase angle error in VTs

2. 6% ratio error and 1^0 phase angle error in CTs

   5% ratio error and -1^0 phase angle error in VTs

3. 6% ratio error and -1^0 phase angle error in CTs

   5% ratio error and 1^0 phase angle error in VTs

The erroneous current and voltage measurements are used in the impedance-based methods along with accurate z_1 and z_0 values. Estimation errors are computed using (3.1) and labeled as 'Error with inaccurate current and voltage measurements'.

Six percent ratio error and phase angle error of one degree in CTs Five percent ratio error and phase angle error of one degree in VTs :

The fault current phasor value obtained from the IEEE 34 Node Test Feeder is multiplied by a factor of $0.94\angle 1^0$. Additionally, the faulted phase voltage phasor is multiplied by a factor of $0.95\angle 1^0$. Reactance-to-fault estimates are shown in Table 5.11.

Table 5.11: Reactance-to-fault Estimates with 6% Ratio Error, 1^0 Phase Angle Error in CTs and 5% Ratio Error, 1^0 Phase Angle Error in VTs

Fault at node:	**Actual reactance-to-fault (ohm)**	**Estimated reactance-to-fault (ohm)**	**Error with inaccurate current and voltage measurements (%)**	**Error for reference case (%)**
Takagi method:				
860	5.872	5.724	-2.53	-4.81
848	7.992	7.426	-7.08	-9.53
Positive-sequence reactance method:				
860	5.872	5.844	-0.48	-3.05
848	7.992	7.524	-5.85	-8.62
Balanced-load method:				
860	5.872	6.799	15.79	14.92
848	7.992	8.662	8.39	7.41
Loop Reactance method:				
860	9.753	16.789	72.15	62.62
848	13.332	24.516	83.89	72.69

Table 5.11 shows that for the Takagi and positive-sequence reactance methods, underestimation decreases. For the loop reactance and balanced-load methods, overestimation increases. Thus the effect of CT ratio errors dominates and magnitude of reactance-to-fault estimates increases. However this increase is not significant as CT ratio errors are partly compensated by ratio errors in VTs.

Six percent ratio error and phase angle error of one degree in CTs Five percent ratio error and phase angle error of minus one degree in VTs :

In this part, sign of the phase angle errors is different for CTs and VTs. CTs have a positive phase angle error of 1^0. VTs have a negative phase angle error of -1^0.

Table 5.12: Reactance-to-fault Estimates with 6% Ratio Error, 1^0 Phase Angle Error in CTs and 5% Ratio Error, -1^0 Phase Angle Error in VTs

Fault at node:	**Actual reactance-to-fault (ohm)**	**Estimated reactance-to-fault (ohm)**	**Error with inaccurate current and voltage measurements (%)**	**Error for reference case (%)**
Takagi method:				
860	5.872	5.479	-6.69	-4.81
848	7.992	7.108	-11.05	-9.53
Positive-sequence reactance method:				
860	5.872	5.460	-7.02	-3.05
848	7.992	7.015	-12.22	-8.62
Balanced-load method:				
860	5.872	6.387	8.77	14.92
848	7.992	8.128	1.70	7.41
Loop Reactance method:				
860	9.753	15.971	63.75	62.62
848	13.332	23.083	73.14	72.69

Table 5.12 shows that underestimation increases for the Takagi and positive-sequence reactance methods whereas overestimation decreases for the balanced-load method. This indicates that the magnitude of estimated reactance-to-fault decreases. For the loop reactance method, the estimation errors do not change significantly as compared to the reference case. It is essential to compare the results in Table 5.11 and Table 5.12. Ratio errors are identical in both these cases. In Table 5.11 where phase angle errors in CTs and VTs are of the same sign, the value of fault location estimates increases. As opposed to this in Table 5.12, where sign of phase angle errors in CTs and VTs differs, the value of fault location estimates decreases. Thus sign of phase angle errors has a considerable influence on the results of impedance-based methods.

Six percent ratio error and phase angle error of minus one degree in CTs Five percent ratio error and phase angle error of one degree in VTs :

In this part, in addition to the ratio errors, CTs have a phase angle error of -1^0 while VTs have an error of 1^0. The reactance-to-fault estimates obtained using these measurements are shown in Table 5.13

This measurement error causes increase in magnitude of the reactance-to-fault estimates. As a result, the Takagi and positive-sequence reactance methods overestimate the reactance-to-fault. Also for the loop reactance and balanced-load methods, the extent of overestimation increases as compared to the reference case.

Table 5.13: Reactance-to-fault Estimates with 6% Ratio Error, -1^0 Phase Angle Error in CTs and 5% Ratio Error, 1^0 Phase Angle Error in VTs

Fault at node:	**Actual reactance-to-fault (ohm)**	**Estimated reactance-to-fault (ohm)**	**Error with inaccurate current and voltage measurements (%)**	**Error for reference case (%)**
Takagi method:				
860	5.872	5.952	1.37	-4.81
848	7.992	7.721	-3.38	-9.53
Positive-sequence reactance method:				
860	5.872	6.243	6.31	-3.05
848	7.992	8.065	0.92	-8.62
Balanced-load method:				
860	5.872	7.153	21.82	14.92
848	7.992	9.132	14.27	7.41
Loop Reactance method:				
860	9.753	18.310	87.74	62.62
848	13.332	28.136	111.04	72.69

On the basis of the analysis presented in Section 5.4 it can be concluded that the combined effect of CT and VT measurement errors on the impedance-based methods is less intense as compared to the situation where only one of these errors is present. Moreover since the magnitude of ratio errors in CTs and VTs is nearly the same, sign of the phase angle errors has a significant influence on fault location estimates.

If phase angle errors are of the same sign, underestimation increases by 2% to 3% for the Takagi and positive-sequence reactance methods. For the

loop reactance method, estimation errors increase by 5% to 11%. In case of the balanced-load method, overestimation increases by 1% to 2%. Besides the loop reactance method, none of the methods is significantly affected by this measurement error.

When CT and VT phase angle errors are positive and negative respectively, the magnitude of fault location estimates decreases for all the methods. For the Takagi and positive-sequence reactance methods, underestimation increases by 2% to 3%. For the loop reactance and balanced-load methods, overestimation decreases by 5% to 6%. This measurement error causes deterioration in performance of the Takagi and positive-sequence reactance methods. It improves the accuracy of loop reactance and balanced-load methods.

The magnitude of estimated reactance-to-fault increases when CT phase angle errors are negative and VT phase angle errors are positive. As a result, the extent of underestimation decreases by 5% to 6% for the Takagi and positive-sequence reactance methods. For the loop reactance method, overestimation increases by 8% to 30%. Estimation errors for the balanced-load method increase by 6% to 7% as compared to the reference case. This measurement error leads to improvement in accuracy of the Takagi and positive-sequence reactance methods. It causes deterioration in performance of the loop reactance and balanced-load methods

Chapter 6

Effect of Load Current and Summary of Sensitivity Analysis

The impedance-based methods which are discussed in this thesis, use simple load models while estimating fault location. However the load in a practical system does not conform to the simplified models leading to an adverse impact on accuracy of estimation. The first part of this Chapter focuses on the effect of load current on fault location estimates of the four methods. The goal is to investigate which method is least affected by variations in system load and hence suitable for use under all load conditions. The four methods are used to conduct fault location analysis on a no-load model of the IEEE 34 Node Test Feeder. The performance under no-load conditions is compared to that for the reference case which uses a heavily loaded model of the feeder.

Section 6.1 shows that under no-load conditions, fault location estimates of all four methods are highly accurate. Increase in level of load current does not affect the accuracy of the Takagi and positive-sequence reactance methods severely. They can be used to locate faults on heavily loaded systems. The estimation errors for the balanced-load method increase moderately under full-load conditions. The loop reactance method gives highly erroneous fault location estimates when it is used on heavily loaded systems.

Section 6.2 summarizes the results of sensitivity analysis. It determines the cumulative effect of modeling errors, measurement errors and load current

on the four impedance-based methods. It establishes upper and lower bounds on estimation errors of each method by combining the results of Chapters 4, 5 and Section 6.1. The actual reactance to fault location can be expected to lie within ±10% of the value estimated by the Takagi and positive-sequence reactance methods. For the loop reactance and balanced load methods, the actual fault location is within -30% of the estimated value. Negative sign indicates that the actual reactance to fault location is always lesser than the value estimated by these methods.

6.1 Effect of Load Current on Fault Location Estimates

While deriving the impedance-based methods in Chapter 1, all the assumptions regarding the system load have been highlighted. The Takagi, positive-sequence reactance and balanced-load methods assume that the entire load is lumped beyond the fault point. Additionally, the Takagi method uses a constant current load model to estimate fault location. The positive-sequence reactance method assumes that the current I_S as defined in (1.11) is in phase with the fault current I_F. The balanced-load method is derived on the basis of the assumption that the distribution system serves a perfectly balanced three-phase load. The load current is entirely neglected in the derivation of the loop reactance method.

The IEEE 34 Node Test Feeder used for analysis in the reference case violates most of the assumptions made by the four methods. Unbalanced heavy loads are present throughout the length of this feeder. The load current magnitude recorded at the monitoring location (node 800) is 420 A/phase. Further, there is an equal proportion of constant power, constant current and constant impedance loads.

To quantify the effect of load current on estimation accuracy, a no-load model of the IEEE 34 Node Test Feeder is created. SLG faults with zero fault resistance are placed on this feeder at the same eight locations as the reference case. The voltage and current measurements obtained from this feeder and accurate z_1 and z_0 values are used in the four methods. The estimation errors for the no-load case are compared to those for the baseline case. Table 6.1 shows the reactance-to-fault estimates for two fault locations. Appendix E lists the reactance-to-fault estimates for all the locations.

Table 6.1: Comparison of Reactance-to-fault Estimates for No-load and Full-load Conditions

Fault at node:	**Actual reactance-to-fault (ohm)**	**Estimated reactance-to-fault (ohm)**	**Error for no-load case (%)**	**Error for reference (full-load) case (%)**
Takagi method:				
860	5.872	5.726	-2.45	-4.81
848	7.992	7.833	-1.97	-9.53
Positive-sequence reactance method:				
860	5.872	5.897	0.45	-3.05
848	7.992	7.999	0.12	-8.62
Balanced-load method:				
860	5.872	6.240	6.30	14.92
848	7.992	8.249	3.24	7.41
Loop reactance method:				
860	9.753	9.752	-0.01	62.62
848	13.332	13.389	0.43	72.69

For a fault at node 860, the Takagi method estimates fault location to

be 5.726 Ω under no-load conditions. Since this value is less than 5.872 Ω, which is the actual reactance to fault location, there is a negative estimation error of -2.45%. When the fault occurs under full-load conditions, for the same fault location the reactance-to-fault estimate is 5.589 Ω. This causes the estimation error to increase to -4.81%. As the error becomes more negative, it can be inferred that under full-load conditions, the estimated value moves further away from the actual value. The same behavior is observed when the fault occurs at node 848. Thus the accuracy of the Takagi method deteriorates with increase in level of load current. There are two reasons for this behavior. Multiple single- and three-phase load taps are present between the monitoring point (Node 800) and the two fault locations. Under full-load conditions, considerable current is drawn by these load branches and hence the lumped load assumption is violated. Also the current I_{sup} defined in (1.17) is not equal to the fault current I_F as the load does not exhibit constant current characteristics.

The positive-sequence reactance method shows a similar trend as the Takagi method. When there is no load current in the system this method gives highly accurate reactance-to-fault estimates with errors below 0.5%. For the full-load case, estimation errors increase and are in the range of -3% to -8.6%. As fault resistance $R_F = 0$ Ω, the slight phase difference between I_F and I_S does not lead to any errors. Inaccuracy in estimation is mainly introduced because the lumped load assumption is not satisfied.

It is to be noted that although accuracy of the Takagi and positive-sequence reactance methods deteriorates under full-load conditions, the estimated reactance-to-fault is within 0.5 Ω to 0.7 Ω of the actual value. Hence even under full-load conditions the performance of both these methods can be

considered acceptable.

The loop reactance method performs exceptionally well under no-load conditions. The estimated reactance-to-fault is almost equal to the actual value at all the fault locations. However there is a drastic reduction in accuracy for the full-load case. Estimation errors are now in the range of 60% to 70%. This is due to the fact that all nodes are located at a considerable distance from the monitoring point. As a result the magnitude of fault current is in the range of 0.9 kA to 1.2 kA. Since the load current is about 420 A/phase, it is nearly 25% to 30% of the fault current and its effect cannot be neglected. Hence the performance of the loop reactance method, which completely ignores load current in its derivation, is affected severely.

For the balanced-load method, estimation errors under full-load conditions are 4% to 30% higher than those under no-load conditions. This is because the full-load case violates the lumped load assumption and also renders the balanced-load representation invalid. This method is more sensitive to the level of unbalance in the system rather than the magnitude of load current.

The load current in a practical distribution system is substantial. As a result, for faults located far away from the monitoring location, the magnitude of fault current is comparable to the load current. It would be advisable to use the Takagi or positive-sequence reactance methods for such systems, because their performance is not affected significantly by the level of load current. Since system load has a severe impact on the accuracy of the loop reactance method, it should be used on lightly loaded systems. The balanced-load method is suitable for use on systems serving heavy but balanced three-phase loads.

6.2 Summary of Sensitivity Analysis of Impedance-based Methods

Ideally, it is expected that estimation results of all the impedance-based methods should be completely free from errors. This would be possible if there are no circuit modeling and measurement errors. Also, the fault current magnitude should be considerably higher than the load current. In such a case all the assumptions made by the impedance-based methods are satisfied. However, in a practical distribution system, measurement and modeling errors can occur simultaneously. The system may be serving a low, moderate or heavy load when a fault occurs. Hence it is necessary to understand the cumulative effect of all error sources on the four impedance-based methods.

Inaccurate modeling of phase conductor distances, conductor sizes and phase to neutral conductor distances does not severely impact fault location estimates of Takagi and positive-sequence reactance methods. Modeling errors in earth resistivity can cause the estimation errors to increase or decrease by 2% to 5% depending upon whether the modeled earth resistivity value is more than or less than the accurate value. In spite of the fact that the uniform line impedance assumption made by these methods is violated in a practical distribution system, the estimation results are only marginally affected. Measurement errors do affect these methods causing the fault location estimates to vary by 5% to 6%. This variation can be positive or negative depending upon the sign of the phase angle errors and the relative magnitude of CT and VT ratio errors. Increase in level of load current can cause the estimation errors to increase by 5% to 8%. To account for the combined effect of all these errors, the actual reactance to fault location is expected to be within $\pm 10\%$ of the estimate given by these methods. Thus if the Takagi method or the

positive-sequence reactance method estimates the reactance-to-fault to be 10 Ω, it is reasonable to expect that the actual value of reactance-to-fault lies between 9 Ω to 11 Ω.

The loop reactance method is insensitive to modeling errors. However it is extremely sensitive to the magnitude of load current in the system. Although it can estimate the reactance to fault location with almost 100% accuracy under no-load conditions, estimation errors increase drastically as the level of load current rises. When this method is used to conduct fault location on a full-load model of the IEEE 34 Node Test Feeder, the estimation errors are in the range of 10% to 70%. The full-load model is designed such that the load current is nearly equal to 50% of the fault current when faults occur far away from the monitoring station. This is done so as to account for the worst case scenario. In a practical system the magnitude of load current is not so high. For such systems, load current can lead to 15% to 25% errors in estimation. Additionally, ratio and phase angle errors in CTs and VTs cause errors of 8% to 30% in estimation of fault location. It is important to note that this method always overestimates the reactance-to-fault. The actual reactance to fault location is within -30% of the estimated value. Negative sign indicates that the actual reactance to fault location is always lesser than the value estimated by this method.

Like the loop reactance method, the balanced-load method is also unaffected due to errors in circuit modeling. However unbalanced load currents can cause the fault location estimates of the balanced-load method to be overestimated by 7% to 25%. Measurement errors can cause the estimation results to vary by 6% to 7%. This method also consistently overestimates fault location. The actual fault location is expected to be within -30% of the estimated

value.

Sensitivity analysis conclusively proves that the Takagi and positive-sequence reactance methods are better suited for use on distribution circuits as compared to the loop reactance and balanced-load methods. Even though the Takagi and positive-sequence reactance methods incorrectly assume line impedances to be uniform and exhibit a slight sensitivity to modeling errors, the fault location estimates obtained by these methods are robust. The loop reactance method and the balanced-load method are insensitive to modeling errors. However this advantage is overshadowed by the fact that both methods are considerably sensitive to measurement errors and level of load current in the system.

Appendices

Appendix A

Specifications of the Modified IEEE 34 Node Test Feeder

Table A.1: Line Segment Lengths and Configurations (Part A)

From Node	To Node	Length (miles)	Configuration
800	802	0.49	300
802	806	0.33	300
806	808	0.62	300
808	810	1.10	303
808	812	0.62	300
812	814	0.62	300
814	850	0.00	301
816	818	0.32	302
816	824	0.62	301
818	820	1.00	302
820	822	1.00	302
824	826	0.57	303
824	828	0.16	301
828	830	0.62	301
830	854	0.10	301
832	858	0.63	301
832	888	0.00	Transformer

Table A.2: Line Segment Lengths and Configurations (Part B)

From Node	To Node	Length (miles)	Configuration
834	860	0.90	301
834	842	0.72	301
836	840	0.90	301
836	862	0.05	301
842	844	0.90	301
844	846	0.90	301
846	848	0.90	301
850	816	0.06	301
852	832	0.002	301
854	856	1.00	303
854	852	0.62	301
858	864	0.30	303
858	834	0.62	301
860	836	0.90	301
862	838	0.92	304
888	890	0.62	300

Table A.3: Spot Loads in the Modified IEEE 34 Node Test Feeder

Node	Load Model	Ph-1 (kW)	Ph-1 (kVAr)	Ph-2 (kW)	Ph-2 (kVAr)	Ph-3 (kW)	Ph-3 (kVAr)
860	Y-PQ	100	80	100	80	100	80
840	Y-I	700	800	700	800	700	800
844	Y-Z	1000	780	1000	780	1000	780
848	D-PQ	20	16	20	16	20	16
890	D-I	800	400	800	400	800	400
830	D-Z	10	5	10	5	25	10
Total		344	224	344	224	359	229

Table A.4: Distributed Loads in the Modified IEEE 34 Node Test Feeder

From Node	To Node	Load Model	Ph-1 (kW)	Ph-1 (kVAr)	Ph-2 (kW)	Ph-2 (kVAr)	Ph-3 (kW)	Ph-3 (kVAr)
802	806	Y-PQ	0	0	30	15	25	14
808	810	Y-I	0	0	16	8	0	0
818	820	Y-Z	34	17	0	0	0	0
820	822	Y-PQ	135	70	0	0	0	0
816	824	D-I	0	0	5	2	0	0
824	826	Y-I	0	0	40	20	0	0
824	828	Y-PQ	0	0	0	0	4	2
828	830	Y-PQ	7	3	0	0	0	0
854	856	Y-PQ	0	0	4	2	0	0
832	858	D-Z	7	3	2	1	6	3
858	864	Y-PQ	2	1	0	0	0	0
858	834	D-PQ	26.7	13.3	26.7	13.3	26.7	13.3
834	860	D-Z	16	8	20	10	110	55
860	836	D-PQ	30	15	10	6	42	22
836	840	D-I	18	9	22	11	0	0
862	838	Y-PQ	0	0	28	14	0	0
842	844	Y-PQ	9	5	0	0	0	0
844	846	Y-PQ	0	0	25	12	20	11
846	848	Y-PQ	0	0	23	11	0	0
Total			262	133	240	120	220	114

Appendix B

Comprehensive Results for Effect of Circuit Model Errors on Fault Location Estimates

Table B.1: Reactance-to-fault estimates for the Takagi and positive-sequence reactance methods (Increase in phase conductor distances)

A: Takagi method					**B: Positive-sequence reactance method**				
Fault at node:	**Actual positive seq. reactance (ohm)**	**Estimated positive seq. reactance (ohm)**	**Error with incorrect circuit model (%)**	**Error for reference case (%)**	**Fault at node:**	**Actual positive seq. reactance (ohm)**	**Estimated positive seq. reactance (ohm)**	**Error with incorrect circuit model (%)**	**Error for reference case (%)**
814	2.230	2.120	-4.94	-6.68	814	2.230	2.293	2.84	1.42
830	3.459	3.352	-3.10	-4.77	830	3.459	3.509	1.44	0.05
860	5.872	5.673	-3.39	-4.81	860	5.872	5.758	-1.94	-3.05
848	7.992	7.327	-8.31	-9.53	848	7.992	7.374	-7.73	-8.62
808	1.197	1.145	-4.34	-6.22	808	1.197	1.237	3.31	1.80
832	4.066	3.959	-2.62	-4.25	832	4.066	4.105	0.97	-0.34
840	7.386	6.906	-6.50	-7.75	840	7.386	6.931	-6.15	-7.07
844	6.478	6.198	-4.33	-5.70	844	6.478	6.276	-3.12	-4.16

Table B.2: Reactance-to-fault estimates for the Takagi and positive-sequence reactance methods (Decrease in phase conductor distances)

A: Takagi method					**B: Positive-sequence reactance method**				
Fault at node:	**Actual positive seq. reactance (ohm)**	**Estimated positive seq. reactance (ohm)**	**Error with incorrect circuit model (%)**	**Error for reference case (%)**	**Fault at node:**	**Actual positive seq. reactance (ohm)**	**Estimated positive seq. reactance (ohm)**	**Error with incorrect circuit model (%)**	**Error for reference case (%)**
814	2.230	2.022	-9.33	-6.68	814	2.230	2.216	-0.61	1.42
830	3.459	3.208	-7.24	-4.77	830	3.459	3.393	-1.92	0.05
860	5.872	5.466	-6.91	-4.81	860	5.872	5.598	-4.66	-3.05
848	7.992	7.086	-11.33	-9.53	848	7.992	7.202	-9.89	-8.62
808	1.197	1.090	-8.96	-6.22	808	1.197	1.192	-0.41	1.80
832	4.066	3.796	-6.64	-4.25	832	4.066	3.973	-2.27	-0.34
840	7.386	6.676	-9.61	-7.75	840	7.386	6.763	-8.43	-7.07
844	6.478	5.978	-7.71	-5.70	844	6.478	6.109	-5.69	-4.16

Table B.3: Reactance-to-fault estimates for the Takagi and positive-sequence reactance methods (Increase in conductor GMR)

A: Takagi method					**B: Positive-sequence reactance method**				
Fault at node:	**Actual positive seq. reactance (ohm)**	**Estimated positive seq. reactance (ohm)**	**Error with incorrect circuit model (%)**	**Error for reference case (%)**	**Fault at node:**	**Actual positive seq. reactance (ohm)**	**Estimated positive seq. reactance (ohm)**	**Error with incorrect circuit model (%)**	**Error for reference case (%)**
814	2.230	2.053	-7.93	-6.68	814	2.230	2.253	1.01	1.42
830	3.459	3.252	-5.97	-4.77	830	3.459	3.447	-0.35	0.05
860	5.872	5.524	-5.93	-4.81	860	5.872	5.673	-3.39	-3.05
848	7.992	7.147	-10.58	-9.53	848	7.992	7.282	-8.88	-8.62
808	1.197	1.108	-7.44	-6.22	808	1.197	1.213	1.34	1.80
832	4.066	3.845	-5.43	-4.25	832	4.066	4.035	-0.77	-0.34
840	7.386	6.736	-8.80	-7.75	840	7.386	6.842	-7.36	-7.07
844	6.478	6.038	-6.80	-5.70	844	6.478	6.187	-4.49	-4.16

Table B.4: Reactance-to-fault estimates for the Takagi and positive-sequence reactance methods (Decrease in conductor GMR)

A: Takagi method					B: Positive-sequence reactance method				
Fault at node:	**Actual positive seq. reactance (ohm)**	**Estimated positive seq. reactance (ohm)**	**Error with incorrect circuit model (%)**	**Error for reference case (%)**	**Fault at node:**	**Actual positive seq. reactance (ohm)**	**Estimated positive seq. reactance (ohm)**	**Error with incorrect circuit model (%)**	**Error for reference case (%)**
814	2.230	2.113	-5.26	-6.68	814	2.230	2.274	1.98	1.42
830	3.459	3.344	-3.33	-4.77	830	3.459	3.481	0.63	0.05
860	5.872	5.668	-3.47	-4.81	860	5.872	5.720	-2.59	-3.05
848	7.992	7.331	-8.27	-9.53	848	7.992	7.332	-8.26	-8.62
808	1.197	1.140	-4.74	-6.22	808	1.197	1.226	2.38	1.80
832	4.066	3.951	-2.82	-4.25	832	4.066	4.074	0.19	-0.34
840	7.386	6.906	-6.49	-7.75	840	7.386	6.891	-6.70	-7.07
844	6.478	6.195	-4.37	-5.70	844	6.478	6.236	-3.74	-4.16

Table B.5: Reactance-to-fault estimates for the Takagi and positive-sequence reactance methods (Increase in phase to neutral conductor distances)

A: Takagi method					B: Positive-sequence reactance method				
Fault at node:	**Actual positive seq. reactance (ohm)**	**Estimated positive seq. reactance (ohm)**	**Error with incorrect circuit model (%)**	**Error for reference case (%)**	**Fault at node:**	**Actual positive seq. reactance (ohm)**	**Estimated positive seq. reactance (ohm)**	**Error with incorrect circuit model (%)**	**Error for reference case (%)**
814	2.230	2.059	-7.66	-6.68	814	2.230	2.236	0.27	1.42
830	3.459	3.264	-5.62	-4.77	830	3.459	3.421	-1.10	0.05
860	5.872	5.553	-5.44	-4.81	860	5.872	5.637	-4.00	-3.05
848	7.992	7.195	-9.98	-9.53	848	7.992	7.245	-9.34	-8.62
808	1.197	1.110	-7.24	-6.22	808	1.197	1.204	0.54	1.80
832	4.066	3.861	-5.04	-4.25	832	4.066	4.005	-1.49	-0.34
840	7.386	6.778	-8.24	-7.75	840	7.386	6.805	-7.86	-7.07
844	6.478	6.072	-6.26	-5.70	844	6.478	6.150	-5.06	-4.16

Table B.6: Reactance-to-fault estimates for the Takagi and positive-sequence reactance methods (Decrease in phase to neutral conductor distances)

A: Takagi method					B: Positive-sequence reactance method				
Fault at node:	**Actual positive seq. reactance (ohm)**	**Estimated positive seq. reactance (ohm)**	**Error with incorrect circuit model (%)**	**Error for reference case (%)**	**Fault at node:**	**Actual positive seq. reactance (ohm)**	**Estimated positive seq. reactance (ohm)**	**Error with incorrect circuit model (%)**	**Error for reference case (%)**
814	2.230	2.107	-5.53	-6.68	814	2.230	2.294	2.89	1.42
830	3.459	3.331	-3.71	-4.77	830	3.459	3.513	1.56	0.05
860	5.872	5.635	-4.04	-4.81	860	5.872	5.764	-1.84	-3.05
848	7.992	7.274	-8.99	-9.53	848	7.992	7.378	-7.68	-8.62
808	1.197	1.138	-4.92	-6.22	808	1.197	1.237	3.35	1.80
832	4.066	3.934	-3.25	-4.25	832	4.066	4.110	1.09	-0.34
840	7.386	6.857	-7.16	-7.75	840	7.386	6.936	-6.09	-7.07
844	6.478	6.155	-4.99	-5.70	844	6.478	6.281	-3.03	-4.16

Table B.7: Reactance-to-fault estimates for the Takagi and positive-sequence reactance methods (Increase in earth resistivity)

A: Takagi method					B: Positive-sequence reactance method				
Fault at node:	**Actual positive seq. reactance (ohm)**	**Estimated positive seq. reactance (ohm)**	**Error with incorrect circuit model (%)**	**Error for reference case (%)**	**Fault at node:**	**Actual positive seq. reactance (ohm)**	**Estimated positive seq. reactance (ohm)**	**Error with incorrect circuit model (%)**	**Error for reference case (%)**
814	2.230	2.000	-10.33	-6.68	814	2.230	2.171	-2.65	1.42
830	3.459	3.180	-8.08	-4.77	830	3.459	3.330	-3.72	0.05
860	5.872	5.436	-7.41	-4.81	860	5.872	5.513	-6.12	-3.05
848	7.992	7.064	-11.61	-9.53	848	7.992	7.102	-11.14	-8.62
808	1.197	1.076	-10.14	-6.22	808	1.197	1.165	-2.63	1.80
832	4.066	3.765	-7.39	-4.25	832	4.066	3.904	-3.98	-0.34
840	7.386	6.652	-9.94	-7.75	840	7.386	6.668	-9.71	-7.07
844	6.478	5.950	-8.14	-5.70	844	6.478	6.019	-7.08	-4.16

Table B.8: Reactance-to-fault estimates for the Takagi and positive-sequence reactance methods (Decrease in earth resistivity)

A: Takagi method					**B: Positive-sequence reactance method**				
Fault at node:	**Actual positive seq. reactance (ohm)**	**Estimated positive seq. reactance (ohm)**	**Error with incorrect circuit model (%)**	**Error for reference case (%)**	**Fault at node:**	**Actual positive seq. reactance (ohm)**	**Estimated positive seq. reactance (ohm)**	**Error with incorrect circuit model (%)**	**Error for reference case (%)**
814	2.230	2.180	-2.25	-6.68	814	2.230	2.374	6.47	1.42
830	3.459	3.434	-0.73	-4.77	830	3.459	3.624	4.77	0.05
860	5.872	5.772	-1.70	-4.81	860	5.872	5.913	0.70	-3.05
848	7.992	7.425	-7.09	-9.53	848	7.992	7.546	-5.58	-8.62
808	1.197	1.181	-1.32	-6.22	808	1.197	1.284	7.27	1.80
832	4.066	4.049	-0.42	-4.25	832	4.066	4.234	4.14	-0.34
840	7.386	7.004	-5.17	-7.75	840	7.386	7.098	-3.89	-7.07
844	6.478	6.298	-2.77	-5.70	844	6.478	6.438	-0.62	-4.16

Appendix C

Comprehensive Results for Effect of the Uniform Line Impedance Assumption on Fault Location Estimates

Table C.1: Reactance-to-fault estimates for the Takagi and positive-sequence reactance method (System with Uniform Line Impedances)

A: Takagi method					**B: Positive-sequence reactance method**				
Fault at node:	**Actual positive seq. reactance (ohm)**	**Estimated positive seq. reactance (ohm)**	**Error with homogen. system model (%)**	**Error for reference case (%)**	**Fault at node:**	**Actual positive seq. reactance (ohm)**	**Estimated positive seq. reactance (ohm)**	**Error with homogen. system model (%)**	**Error for reference case (%)**
814	2.254	2.235	-0.87	-6.68	814	2.254	2.217	-1.66	1.42
830	3.484	3.463	-0.60	-4.77	830	3.484	3.431	-1.54	0.05
860	5.897	5.790	-1.81	-4.81	860	5.897	5.689	-3.52	-3.05
848	8.017	7.462	-6.92	-9.53	848	8.017	7.318	-8.71	-8.62
808	1.211	1.201	-0.88	-6.22	808	1.211	1.193	-1.50	1.80
832	4.090	4.072	-0.44	-4.25	832	4.090	4.029	-1.50	-0.34
840	7.411	7.028	-5.17	-7.75	840	7.411	6.866	-7.36	-7.07
844	6.502	6.325	-2.74	-5.70	844	6.502	6.217	-4.40	-4.16

Appendix D

Comprehensive Results for Effect of CT Measurement Errors on Fault Location Estimates

D.1 Effect of CT Measurement Errors

Table D.1: Reactance-to-fault estimates for the Takagi and positive-sequence reactance methods (6% CT ratio error)

A: Takagi method					**B: Positive-sequence reactance method**				
Fault at node:	**Actual positive seq. reactance (ohm)**	**Estimated positive seq. reactance (ohm)**	**Error with inaccurate current meas. (%)**	**Error for reference case (%)**	**Fault at node:**	**Actual positive seq. reactance (ohm)**	**Estimated positive seq. reactance (ohm)**	**Error with inaccurate current meas. (%)**	**Error for reference case (%)**
814	2.230	2.221	-0.39	-6.68	814	2.230	2.420	8.52	1.42
830	3.459	3.529	1.99	-4.77	830	3.459	3.719	7.48	0.05
860	5.872	6.026	2.65	-4.81	860	5.872	6.164	5.01	-3.05
848	7.992	7.821	-2.12	-9.53	848	7.992	7.944	-0.57	-8.62
808	1.197	1.197	-0.27	-6.22	808	1.197	1.300	8.37	1.80
832	4.066	4.177	2.64	-4.25	832	4.066	4.361	7.15	-0.34
840	7.386	7.369	-0.29	-7.75	840	7.386	7.461	0.97	-7.07
844	6.478	6.592	1.73	-5.70	844	6.478	6.731	3.87	-4.16

Table D.2: Reactance-to-fault estimates for the loop reactance and balanced-load methods (6% CT ratio error)

A: Loop reactance method					**B: Balanced-load method**				
Fault at node:	**Actual loop reactance (ohm)**	**Estimated loop reactance (ohm)**	**Error with inaccurate current meas. (%)**	**Error for reference case (%)**	**Fault at node:**	**Actual positive seq. reactance (ohm)**	**Estimated positive seq. reactance (ohm)**	**Error with inaccurate current meas. (%)**	**Error for reference case (%)**
814	3.605	4.613	27.96	18.22	814	2.230	3.065	37.45	29.21
830	5.684	8.278	45.64	32.47	830	3.459	4.645	34.24	26.22
860	9.753	18.078	85.36	62.62	860	5.872	7.179	22.30	14.92
848	13.332	27.034	102.77	72.69	848	7.992	9.132	14.29	7.41
808	1.935	2.271	17.37	9.26	808	1.197	1.729	44.06	35.76
832	6.705	10.400	55.11	39.99	832	4.066	5.421	33.20	25.33
840	12.313	24.923	102.41	73.16	840	7.386	8.456	14.43	7.62
844	10.78	20.668	91.72	66.65	844	6.478	7.847	21.10	13.87

Table D.3: Reactance-to-fault estimates for the Takagi and positive-sequence reactance methods (1^0 phase angle error in CTs)

A: Takagi method					**B: Positive-sequence reactance method**				
Fault at node:	**Actual positive seq. reactance (ohm)**	**Estimated positive seq. reactance (ohm)**	**Error with inaccurate current meas. (%)**	**Error for reference case (%)**	**Fault at node:**	**Actual positive seq. reactance (ohm)**	**Estimated positive seq. reactance (ohm)**	**Error with inaccurate current meas. (%)**	**Error for reference case (%)**
814	2.230	2.046	-8.26	-6.68	814	2.230	2.204	-1.16	1.42
830	3.459	3.231	-6.62	-4.77	830	3.459	3.358	-2.95	0.05
860	5.872	5.466	-6.88	-4.81	860	5.872	5.494	-6.41	-3.05
848	7.992	7.066	-11.56	-9.53	848	7.992	7.033	-11.97	-8.62
808	1.197	1.104	-8.03	-6.22	808	1.197	1.188	-1.04	1.80
832	4.066	3.816	-6.24	-4.25	832	4.066	3.924	-3.58	-0.34
840	7.386	6.654	-9.96	-7.75	840	7.386	6.608	-10.59	-7.07
844	6.478	5.974	-7.81	-5.70	844	6.478	5.987	-7.61	-4.16

Table D.4: Reactance-to-fault estimates for the loop reactance and balanced-load methods (1^0 phase angle error in CTs)

A: Loop reactance method					**B: Balanced-load method**				
Fault at node:	**Actual loop reactance (ohm)**	**Estimated loop reactance (ohm)**	**Error with inaccurate current meas. (%)**	**Error for reference case (%)**	**Fault at node:**	**Actual positive seq. reactance (ohm)**	**Estimated positive seq. reactance (ohm)**	**Error with inaccurate current meas. (%)**	**Error for reference case (%)**
814	3.605	4.175	15.81	18.22	814	2.230	2.829	26.86	29.21
830	5.684	7.335	29.05	32.47	830	3.459	4.271	23.44	26.22
860	9.753	15.140	55.24	62.62	860	5.872	6.568	11.90	14.92
848	13.332	21.494	61.22	72.69	848	7.992	8.346	4.45	7.41
808	1.935	2.075	7.24	9.26	808	1.197	1.597	33.12	35.76
832	6.705	9.111	35.89	39.99	832	4.066	4.979	22.33	25.33
840	12.313	19.972	62.20	73.16	840	7.386	7.725	4.54	7.62
844	10.78	17.076	58.40	66.65	844	6.478	7.178	10.77	13.87

Table D.5: Reactance-to-fault estimates for the Takagi and positive-sequence reactance methods (-1^0 phase angle error in CTs)

A: Takagi method					**B: Positive-sequence reactance method**				
Fault at node:	**Actual positive seq. reactance (ohm)**	**Estimated positive seq. reactance (ohm)**	**Error with inaccurate current meas. (%)**	**Error for reference case (%)**	**Fault at node:**	**Actual positive seq. reactance (ohm)**	**Estimated positive seq. reactance (ohm)**	**Error with inaccurate current meas. (%)**	**Error for reference case (%)**
814	2.230	2.113	-5.24	-6.68	814	2.230	2.319	4.00	1.42
830	3.459	3.354	-3.06	-4.77	830	3.459	3.564	3.02	0.05
860	5.872	5.705	-2.81	-4.81	860	5.872	5.890	0.34	-3.05
848	7.992	7.381	-7.62	-9.53	848	7.992	7.570	-5.26	-8.62
808	1.197	1.141	-4.92	-6.22	808	1.197	1.249	4.09	1.80
832	4.066	3.967	-2.53	-4.25	832	4.066	4.178	2.65	-0.34
840	7.386	6.961	-5.81	-7.75	840	7.386	7.115	-3.72	-7.07
844	6.478	6.236	-3.77	-5.70	844	6.478	6.426	-0.83	-4.16

Table D.6: Reactance-to-fault estimates for the loop reactance and balanced-load methods (-1^0 phase angle error in CTs)

A: Loop reactance method					**B: Balanced-load method**				
Fault at node:	**Actual loop reactance (ohm)**	**Estimated loop reactance (ohm)**	**Error with inaccurate current meas. (%)**	**Error for reference case (%)**	**Fault at node:**	**Actual positive seq. reactance (ohm)**	**Estimated positive seq. reactance (ohm)**	**Error with inaccurate current meas. (%)**	**Error for reference case (%)**
814	3.605	4.339	20.35	18.22	814	2.230	2.933	31.51	29.21
830	5.684	7.719	35.80	32.47	830	3.459	4.460	28.90	26.22
860	9.753	16.511	69.30	62.62	860	5.872	6.926	17.99	14.92
848	13.332	24.501	83.78	72.69	848	7.992	8.819	10.38	7.41
808	1.935	2.153	11.25	9.26	808	1.197	1.652	37.68	35.76
832	6.705	9.651	43.93	39.99	832	4.066	5.211	28.04	25.33
840	12.313	22.611	83.63	73.16	840	7.386	8.170	10.55	7.62
844	10.78	18.813	74.52	66.65	844	6.478	7.572	16.86	13.87

Table D.7: Reactance-to-fault estimates for the Takagi and positive-sequence reactance methods (6% ratio error and 1^0 phase angle error in CTs)

A: Takagi method					**B: Positive-sequence reactance method**				
Fault at node:	**Actual positive seq. reactance (ohm)**	**Estimated positive seq. reactance (ohm)**	**Error with inaccurate current meas. (%)**	**Error for reference case (%)**	**Fault at node:**	**Actual positive seq. reactance (ohm)**	**Estimated positive seq. reactance (ohm)**	**Error with inaccurate current meas. (%)**	**Error for reference case (%)**
814	2.230	2.185	-2.01	-6.68	814	2.230	2.358	5.75	1.42
830	3.459	3.463	0.11	-4.77	830	3.459	3.608	4.30	0.05
860	5.872	5.897	0.43	-4.81	860	5.872	5.950	1.33	-3.05
848	7.992	7.651	-4.27	-9.53	848	7.992	7.653	-4.23	-8.62
808	1.197	1.177	-1.70	-6.22	808	1.197	1.267	5.88	1.80
832	4.066	4.096	0.75	-4.25	832	4.066	4.225	3.91	-0.34
840	7.386	7.203	-2.47	-7.75	840	7.386	7.187	-2.70	-7.07
844	6.478	6.451	-0.41	-5.70	844	6.478	6.494	0.24	-4.16

Table D.8: Reactance-to-fault estimates for the loop reactance and balanced-load methods (6% ratio error and 1^0 phase angle error in CTs)

A: Loop reactance method					**B: Balanced-load method**				
Fault at node:	**Actual loop reactance (ohm)**	**Estimated loop reactance (ohm)**	**Error with inaccurate current meas. (%)**	**Error for reference case (%)**	**Fault at node:**	**Actual positive seq. reactance (ohm)**	**Estimated positive seq. reactance (ohm)**	**Error with inaccurate current meas. (%)**	**Error for reference case (%)**
814	3.605	4.523	25.46	18.22	814	2.230	3.010	34.96	29.21
830	5.684	8.062	41.84	32.47	830	3.459	4.544	31.36	26.22
860	9.753	17.245	76.82	62.62	860	5.872	6.988	19.00	14.92
848	13.332	25.056	87.94	72.69	848	7.992	8.879	11.10	7.41
808	1.935	2.229	15.20	9.26	808	1.197	1.699	41.97	35.76
832	6.705	10.092	50.52	39.99	832	4.066	5.297	30.28	25.33
840	12.313	23.211	88.51	73.16	840	7.386	8.218	11.27	7.62
844	10.78	19.590	81.72	66.65	844	6.478	7.636	17.88	13.87

Table D.9: Reactance-to-fault estimates for the Takagi and positive-sequence reactance methods (6% ratio error and -1^0 phase angle error in CTs)

A: Takagi method					**B: Positive-sequence reactance method**				
Fault at node:	**Actual positive seq. reactance (ohm)**	**Estimated positive seq. reactance (ohm)**	**Error with inaccurate current meas. (%)**	**Error for reference case (%)**	**Fault at node:**	**Actual positive seq. reactance (ohm)**	**Estimated positive seq. reactance (ohm)**	**Error with inaccurate current meas. (%)**	**Error for reference case (%)**
814	2.230	2.256	1.17	-6.68	814	2.230	2.481	11.24	1.42
830	3.459	3.592	3.85	-4.77	830	3.459	3.828	10.67	0.05
860	5.872	6.146	4.68	-4.81	860	5.872	6.375	8.56	-3.05
848	7.992	7.976	-0.19	-9.53	848	7.992	8.229	2.97	-8.62
808	1.197	1.216	1.61	-6.22	808	1.197	1.333	11.37	1.80
832	4.066	4.255	4.65	-4.25	832	4.066	4.495	10.57	-0.34
840	7.386	7.522	1.84	-7.75	840	7.386	7.731	4.67	-7.07
844	6.478	6.724	3.80	-5.70	844	6.478	6.964	7.51	-4.16

Table D.10: Reactance-to-fault estimates for the loop reactance and balanced-load methods (6% ratio error and -1^0 phase angle error in CTs)

A: Loop reactance method					**B: Balanced-load method**				
Fault at node:	**Actual loop reactance (ohm)**	**Estimated loop reactance (ohm)**	**Error with inaccurate current meas. (%)**	**Error for reference case (%)**	**Fault at node:**	**Actual positive seq. reactance (ohm)**	**Estimated positive seq. reactance (ohm)**	**Error with inaccurate current meas. (%)**	**Error for reference case (%)**
814	3.605	4.700	30.37	18.22	814	2.230	3.120	39.90	29.21
830	5.684	8.486	49.29	32.47	830	3.459	4.744	37.16	26.22
860	9.753	18.870	93.48	62.62	860	5.872	7.368	25.48	14.92
848	13.332	28.912	116.86	72.69	848	7.992	9.382	17.39	7.41
808	1.935	2.312	19.50	9.26	808	1.197	1.758	46.83	35.76
832	6.705	10.696	59.52	39.99	832	4.066	5.544	36.35	25.33
840	12.313	26.548	115.61	73.16	840	7.386	8.691	17.67	7.62
844	10.78	21.691	101.21	66.65	844	6.478	8.056	24.36	13.87

D.2 Effect of VT Measurement Errors

Table D.11: Reactance-to-fault estimates for the Takagi and positive-sequence reactance methods (5% ratio error in VTs)

A: Takagi method					**B: Positive-sequence reactance method**				
Fault at node:	**Actual positive seq. reactance (ohm)**	**Estimated positive seq. reactance (ohm)**	**Error with inaccurate voltage meas. (%)**	**Error for reference case (%)**	**Fault at node:**	**Actual positive seq. reactance (ohm)**	**Estimated positive seq. reactance (ohm)**	**Error with inaccurate voltage meas. (%)**	**Error for reference case (%)**
814	2.230	1.976	-11.39	-6.68	814	2.230	2.149	-3.63	1.42
830	3.459	3.129	-9.57	-4.77	830	3.459	3.289	-4.95	0.05
860	5.872	5.309	-9.55	-4.81	860	5.872	5.409	-7.86	-3.05
848	7.992	6.868	-14.04	-9.53	848	7.992	6.939	-13.15	-8.62
808	1.197	1.066	-11.13	-6.22	808	1.197	1.158	-3.53	1.80
832	4.066	3.698	-9.13	-4.25	832	4.066	3.849	-5.42	-0.34
840	7.386	6.472	-12.42	-7.75	840	7.386	6.521	-11.77	-7.07
844	6.478	5.803	-10.44	-5.70	844	6.478	5.898	-8.98	-4.16

Table D.12: Reactance-to-fault estimates for the loop reactance and balanced-load methods (5% ratio error in VTs)

A: Loop reactance method					**B: Balanced-load method**				
Fault at node:	**Actual loop reactance (ohm)**	**Estimated loop reactance (ohm)**	**Error with inaccurate voltage measure. (%)**	**Error for reference case (%)**	**Fault at node:**	**Actual positive seq. reactance (ohm)**	**Estimated positive seq. reactance (ohm)**	**Error with inaccurate voltage meas. (%)**	**Error for reference case (%)**
814	3.605	4.045	12.21	18.22	814	2.230	2.716	21.81	29.21
830	5.684	7.154	25.86	32.47	830	3.459	4.119	19.05	26.22
860	9.753	15.049	54.30	62.62	860	5.872	6.368	8.48	14.92
848	13.332	21.880	64.12	72.69	848	7.992	8.117	1.59	7.41
808	1.935	2.009	3.80	9.26	808	1.197	1.534	27.79	35.76
832	6.705	8.917	32.99	39.99	832	4.066	4.811	18.20	25.33
840	12.313	20.255	64.50	73.16	840	7.386	7.507	1.58	7.62
844	10.78	17.066	58.31	66.65	844	6.478	6.967	7.52	13.87

Table D.13: Reactance-to-fault estimates for the Takagi and positive-sequence reactance methods (1^0 phase angle error in VTs)

A: Takagi method					**B: Positive-sequence reactance method**				
Fault at node:	**Actual positive seq. reactance (ohm)**	**Estimated positive seq. reactance (ohm)**	**Error with inaccurate voltage meas. (%)**	**Error for reference case (%)**	**Fault at node:**	**Actual positive seq. reactance (ohm)**	**Estimated positive seq. reactance (ohm)**	**Error with inaccurate voltage meas. (%)**	**Error for reference case (%)**
814	2.230	2.115	-5.17	-6.68	814	2.230	2.319	3.99	1.42
830	3.459	3.356	-3.00	-4.77	830	3.459	3.562	2.96	0.05
860	5.872	5.706	-2.79	-4.81	860	5.872	5.880	0.16	-3.05
848	7.992	7.381	-7.62	-9.53	848	7.992	7.551	-5.50	-8.62
808	1.197	1.142	-4.88	-6.22	808	1.197	1.249	4.09	1.80
832	4.066	3.969	-2.47	-4.25	832	4.066	4.174	2.56	-0.34
840	7.386	6.960	-5.82	-7.75	840	7.386	7.097	-3.96	-7.07
844	6.478	6.237	-3.75	-5.70	844	6.478	6.414	-1.03	-4.16

Table D.14: Reactance-to-fault estimates for the loop reactance and balanced-load methods (1^0 phase angle error in VTs)

A: Loop reactance method					**B: Balanced-load method**				
Fault at node:	**Actual loop reactance (ohm)**	**Estimated loop reactance (ohm)**	**Error with inaccurate voltage measure. (%)**	**Error for reference case (%)**	**Fault at node:**	**Actual positive seq. reactance (ohm)**	**Estimated positive seq. reactance (ohm)**	**Error with inaccurate voltage measure. (%)**	**Error for reference case (%)**
814	3.605	4.329	20.09	18.22	814	2.230	2.943	31.99	29.21
830	5.684	7.676	35.04	32.47	830	3.459	4.477	29.38	26.22
860	9.753	16.212	66.22	62.62	860	5.872	6.949	18.37	14.92
848	13.332	23.656	77.44	72.69	848	7.992	8.844	10.69	7.41
808	1.935	2.150	11.12	9.26	808	1.197	1.659	38.21	35.76
832	6.705	9.576	42.82	39.99	832	4.066	5.230	28.50	25.33
840	12.313	21.892	77.79	73.16	840	7.386	8.196	10.91	7.62
844	10.78	18.400	70.69	66.65	844	6.478	7.596	17.22	13.87

Table D.15: Reactance-to-fault estimates for the Takagi and positive-sequence reactance methods (-1^0 phase angle error in VTs)

A: Takagi method					**B: Positive-sequence reactance method**				
Fault at node:	**Actual positive seq. reactance (ohm)**	**Estimated positive seq. reactance (ohm)**	**Error with inaccurate voltage measure. (%)**	**Error for reference case (%)**	**Fault at node:**	**Actual positive seq. reactance (ohm)**	**Estimated positive seq. reactance (ohm)**	**Error with inaccurate voltage measure. (%)**	**Error for reference case (%)**
814	2.230	2.045	-8.31	-6.68	814	2.230	2.205	-1.14	1.42
830	3.459	3.230	-6.64	-4.77	830	3.459	3.360	-2.88	0.05
860	5.872	5.470	-6.81	-4.81	860	5.872	5.506	-6.21	-3.05
848	7.992	7.076	-11.44	-9.53	848	7.992	7.056	-11.70	-8.62
808	1.197	1.103	-8.06	-6.22	808	1.197	1.188	-1.03	1.80
832	4.066	3.815	-6.26	-4.25	832	4.066	3.929	-3.48	-0.34
840	7.386	6.664	-9.82	-7.75	840	7.386	6.628	-10.31	-7.07
844	6.478	5.979	-7.73	-5.70	844	6.478	6.002	-7.38	-4.16

Table D.16: Reactance-to-fault estimates for the loop reactance and balanced-load methods (-1^0 phase angle error in VTs)

A: Loop reactance method					**B: Balanced-load method**				
Fault at node:	**Actual loop reactance (ohm)**	**Estimated loop reactance (ohm)**	**Error with inaccurate voltage measure. (%)**	**Error for reference case (%)**	**Fault at node:**	**Actual positive seq. reactance (ohm)**	**Estimated positive seq. reactance (ohm)**	**Error with inaccurate voltage measure. (%)**	**Error for reference case (%)**
814	3.605	4.185	16.10	18.22	814	2.230	2.818	26.37	29.21
830	5.684	7.383	29.89	32.47	830	3.459	4.254	22.95	26.22
860	9.753	15.466	58.58	62.62	860	5.872	6.545	11.50	14.92
848	13.332	22.400	68.02	72.69	848	7.992	8.321	4.14	7.41
808	1.935	2.078	7.38	9.26	808	1.197	1.591	32.58	35.76
832	6.705	9.193	37.11	39.99	832	4.066	4.960	21.87	25.33
840	12.313	20.745	68.48	73.16	840	7.386	7.699	4.17	7.62
844	10.78	17.523	62.55	66.65	844	6.478	7.154	10.40	13.87

Table D.17: Reactance-to-fault estimates for the Takagi and positive-sequence reactance methods (5% ratio error and 1^0 phase angle error in VTs)

A: Takagi method					**B: Positive-sequence reactance method**				
Fault at node:	**Actual positive seq. reactance (ohm)**	**Estimated positive seq. reactance (ohm)**	**Error with inaccurate voltage measure. (%)**	**Error for reference case (%)**	**Fault at node:**	**Actual positive seq. reactance (ohm)**	**Estimated positive seq. reactance (ohm)**	**Error with inaccurate voltage measure. (%)**	**Error for reference case (%)**
814	2.230	2.009	-9.91	-6.68	814	2.230	2.203	-1.21	1.42
830	3.459	3.188	-7.82	-4.77	830	3.459	3.384	-2.16	0.05
860	5.872	5.421	-7.68	-4.81	860	5.872	5.586	-4.87	-3.05
848	7.992	7.012	-12.26	-9.53	848	7.992	7.173	-10.24	-8.62
808	1.197	1.084	-9.40	-6.22	808	1.197	1.187	-0.87	1.80
832	4.066	3.771	-7.25	-4.25	832	4.066	3.966	-2.47	-0.34
840	7.386	6.612	-10.48	-7.75	840	7.386	6.742	-8.71	-7.07
844	6.478	5.925	-8.54	-5.70	844	6.478	6.093	-5.94	-4.16

Table D.18: Reactance-to-fault estimates for the loop reactance and balanced-load methods (5% ratio error and 1^0 phase angle error in VTs)

A: Loop reactance method					**B: Balanced-load method**				
Fault at node:	**Actual loop reactance (ohm)**	**Estimated loop reactance (ohm)**	**Error with inaccurate voltage measure. (%)**	**Error for reference case (%)**	**Fault at node:**	**Actual positive seq. reactance (ohm)**	**Estimated positive seq. reactance (ohm)**	**Error with inaccurate voltage measure. (%)**	**Error for reference case (%)**
814	3.605	4.110	14.01	18.22	814	2.230	2.776	24.46	29.21
830	5.684	7.290	28.25	32.47	830	3.459	4.224	22.11	26.22
860	9.753	15.400	57.90	62.62	860	5.872	6.558	11.69	14.92
848	13.332	22.470	68.54	72.69	848	7.992	8.365	4.67	7.41
808	1.935	2.040	5.43	9.26	808	1.197	1.565	30.77	35.76
832	6.705	9.100	35.72	39.99	832	4.066	4.938	21.45	25.33
840	12.313	20.800	68.93	73.16	840	7.386	7.742	4.82	7.62
844	10.78	17.480	62.15	66.65	844	6.478	7.176	10.77	13.87

Table D.19: Reactance-to-fault estimates for the Takagi and positive-sequence reactance methods (5% ratio error and -1^0 phase angle error in VTs)

A: Takagi method					**B: Positive-sequence reactance method**				
Fault at node:	**Actual positive seq. reactance (ohm)**	**Estimated positive seq. reactance (ohm)**	**Error with inaccurate voltage measure. (%)**	**Error for reference case (%)**	**Fault at node:**	**Actual positive seq. reactance (ohm)**	**Estimated positive seq. reactance (ohm)**	**Error with inaccurate voltage measure. (%)**	**Error for reference case (%)**
814	2.230	1.942	-12.89	-6.68	814	2.230	2.094	-6.08	1.42
830	3.459	3.069	-11.29	-4.77	830	3.459	3.192	-7.71	0.05
860	5.872	5.197	-11.50	-4.81	860	5.872	5.230	-10.93	-3.05
848	7.992	6.722	-15.88	-9.53	848	7.992	6.703	-16.13	-8.62
808	1.197	1.048	-12.44	-6.22	808	1.197	1.128	-5.75	1.80
832	4.066	3.625	-10.85	-4.25	832	4.066	3.732	-8.21	-0.34
840	7.386	6.331	-14.28	-7.75	840	7.386	6.297	-14.75	-7.07
844	6.478	5.680	-12.32	-5.70	844	6.478	5.702	-11.98	-4.16

Table D.20: Reactance-to-fault estimates for the loop reactance and balanced-load methods (5% ratio error and -1^0 phase angle error in VTs)

A: Loop reactance method					**B: Balanced-load method**				
Fault at node:	**Actual loop reactance (ohm)**	**Estimated loop reactance (ohm)**	**Error with inaccurate voltage measure. (%)**	**Error for reference case (%)**	**Fault at node:**	**Actual positive seq. reactance (ohm)**	**Estimated positive seq. reactance (ohm)**	**Error with inaccurate voltage measure. (%)**	**Error for reference case (%)**
814	3.605	3.976	10.29	18.22	814	2.230	2.656	19.12	29.21
830	5.684	7.014	23.39	32.47	830	3.459	4.013	16.01	26.22
860	9.753	14.693	50.65	62.62	860	5.872	6.175	5.17	14.92
848	13.332	21.280	59.62	72.69	848	7.992	7.867	-1.56	7.41
808	1.935	1.974	2.00	9.26	808	1.197	1.501	25.41	35.76
832	6.705	8.734	30.26	39.99	832	4.066	4.682	15.15	25.33
840	12.313	19.707	60.05	73.16	840	7.386	7.269	-1.58	7.62
844	10.78	16.647	54.42	66.65	844	6.478	6.756	4.30	13.87

D.3 Combined Effect of CT and VT Measurement Errors

Table D.21: Reactance-to-fault estimates (6% ratio error, 1^0 phase angle error in CTs AND 5% ratio error, 1^0 phase angle error in VTs)

A: Takagi method					**B: Positive-sequence reactance method**				
Fault at node:	**Actual positive seq. reactance (ohm)**	**Estimated positive seq. reactance (ohm)**	**Error with inaccurate current and vtg. meas. (%)**	**Error for reference case (%)**	**Fault at node:**	**Actual positive seq. reactance (ohm)**	**Estimated positive seq. reactance (ohm)**	**Error with inaccurate current and vtg. meas. (%)**	**Error for reference case (%)**
814	2.230	2.112	-5.31	-6.68	814	2.230	2.298	3.07	1.42
830	3.459	3.354	-3.02	-4.77	830	3.459	3.530	2.06	0.05
860	5.872	5.724	-2.53	-4.81	860	5.872	5.844	-0.48	-3.05
848	7.992	7.426	-7.08	-9.53	848	7.992	7.524	-5.85	-8.62
808	1.197	1.137	-4.98	-6.22	808	1.197	1.235	3.20	1.80
832	4.066	3.970	-2.35	-4.25	832	4.066	4.139	1.80	-0.34
840	7.386	6.996	-5.28	-7.75	840	7.386	7.068	-4.31	-7.07
844	6.478	6.261	-3.34	-5.70	844	6.478	6.379	-1.52	-4.16

Table D.22: Reactance-to-fault estimates (6% ratio error, 1^0 phase angle error in CTs AND 5% ratio error, 1^0 phase angle error in VTs)

A: Loop reactance method					**B: Balanced-load method**				
Fault at node:	**Actual loop reactance (ohm)**	**Estimated loop reactance (ohm)**	**Error with inaccurate current and vtg. meas. (%)**	**Error for reference case (%)**	**Fault at node:**	**Actual positive seq. reactance (ohm)**	**Estimated positive seq. reactance (ohm)**	**Error with inaccurate current and vtg. meas. (%)**	**Error for reference case (%)**
814	3.605	4.371	21.25	18.22	814	2.230	2.901	30.11	29.21
830	5.684	7.813	37.45	32.47	830	3.459	4.400	27.20	26.22
860	9.753	16.789	72.15	62.62	860	5.872	6.799	15.79	14.92
848	13.332	24.516	83.89	72.69	848	7.992	8.662	8.39	7.41
808	1.935	2.155	11.36	9.26	808	1.197	1.638	36.86	35.76
832	6.705	9.790	46.01	39.99	832	4.066	5.138	26.37	25.33
840	12.313	22.697	84.34	73.16	840	7.386	8.015	8.51	7.62
844	10.78	19.094	77.13	66.65	844	6.478	7.437	14.81	13.87

Table D.23: Reactance-to-fault estimates (6% ratio error, 1^0 phase angle error in CTs AND 5% ratio error, -1^0 phase angle error in VTs)

A: Takagi method					**B: Positive-sequence reactance method**				
Fault at node:	**Actual positive seq. reactance (ohm)**	**Estimated positive seq. reactance (ohm)**	**Error with inaccurate current and vtg. meas. (%)**	**Error for reference case (%)**	**Fault at node:**	**Actual positive seq. reactance (ohm)**	**Estimated positive seq. reactance (ohm)**	**Error with inaccurate current and vtg. meas. (%)**	**Error for reference case (%)**
814	2.230	2.039	-8.54	-6.68	814	2.230	2.181	-2.18	1.42
830	3.459	3.224	-6.79	-4.77	830	3.459	3.323	-3.92	0.05
860	5.872	5.479	-6.69	-4.81	860	5.872	5.460	-7.02	-3.05
848	7.992	7.108	-11.05	-9.53	848	7.992	7.015	-12.22	-8.62
808	1.197	1.098	-8.27	-6.22	808	1.197	1.172	-2.06	1.80
832	4.066	3.811	-6.26	-4.25	832	4.066	3.887	-4.40	-0.34
840	7.386	6.688	-9.44	-7.75	840	7.386	6.585	-10.84	-7.07
844	6.478	5.994	-7.47	-5.70	844	6.478	5.956	-8.05	-4.16

Table D.24: Reactance-to-fault estimates (6% ratio error, 1^0 phase angle error in CTs AND 5% ratio error, -1^0 phase angle error in VTs)

A: Loop reactance method					**B: Balanced-load method**				
Fault at node:	**Actual loop reactance (ohm)**	**Estimated loop reactance (ohm)**	**Error with inaccurate current and vtg. meas. (%)**	**Error for reference case (%)**	**Fault at node:**	**Actual positive seq. reactance (ohm)**	**Estimated positive seq. reactance (ohm)**	**Error with inaccurate current and vtg. meas. (%)**	**Error for reference case (%)**
814	3.605	4.221	17.09	18.22	814	2.230	2.773	24.34	29.21
830	5.684	7.503	32.00	32.47	830	3.459	4.172	20.62	26.22
860	9.753	15.971	63.75	62.62	860	5.872	6.387	8.77	14.92
848	13.332	23.083	73.14	72.69	848	7.992	8.128	1.70	7.41
808	1.935	2.080	7.48	9.26	808	1.197	1.569	31.06	35.76
832	6.705	9.382	39.93	39.99	832	4.066	4.862	19.58	25.33
840	12.313	21.397	73.77	73.16	840	7.386	7.506	1.63	7.62
844	10.78	18.121	68.10	66.65	844	6.478	6.986	7.84	13.87

Table D.25: Reactance-to-fault estimates (6% ratio error, -1^0 phase angle error in CTs AND 5% ratio error, 1^0 phase angle error in VTs)

A: Takagi method					**B: Positive-sequence reactance method**				
Fault at node:	**Actual positive seq. reactance (ohm)**	**Estimated positive seq. reactance (ohm)**	**Error with inaccurate current and vtg. meas. (%)**	**Error for reference case (%)**	**Fault at node:**	**Actual positive seq. reactance (ohm)**	**Estimated positive seq. reactance (ohm)**	**Error with inaccurate current and vtg. meas. (%)**	**Error for reference case (%)**
814	2.230	2.177	-2.36	-6.68	814	2.230	2.413	8.22	1.42
830	3.459	3.474	0.43	-4.77	830	3.459	3.737	8.04	0.05
860	5.872	5.952	1.37	-4.81	860	5.872	6.243	6.31	-3.05
848	7.992	7.721	-3.38	-9.53	848	7.992	8.065	0.92	-8.62
808	1.197	1.174	-1.91	-6.22	808	1.197	1.297	8.34	1.80
832	4.066	4.117	1.25	-4.25	832	4.066	4.393	8.04	-0.34
840	7.386	7.286	-1.35	-7.75	840	7.386	7.579	2.61	-7.07
844	6.478	6.511	0.51	-5.70	844	6.478	6.821	5.31	-4.16

Table D.26: Reactance-to-fault estimates (6% ratio error, -1^0 phase angle error in CTs AND 5% ratio error, 1^0 phase angle error in VTs)

A: Loop reactance method					**B: Balanced-load method**				
Fault at node:	**Actual loop reactance (ohm)**	**Estimated loop reactance (ohm)**	**Error with inaccurate current and vtg. meas. (%)**	**Error for reference case (%)**	**Fault at node:**	**Actual positive seq. reactance (ohm)**	**Estimated positive seq. reactance (ohm)**	**Error with inaccurate current and vtg. meas. (%)**	**Error for reference case (%)**
814	3.605	4.536	25.82	18.22	814	2.230	3.003	34.66	29.21
830	5.684	8.207	44.40	32.47	830	3.459	4.586	32.57	26.22
860	9.753	18.310	87.74	62.62	860	5.872	7.153	21.82	14.92
848	13.332	28.136	111.04	72.69	848	7.992	9.132	14.27	7.41
808	1.935	2.232	15.37	9.26	808	1.197	1.692	41.32	35.76
832	6.705	10.353	54.40	39.99	832	4.066	5.367	32.00	25.33
840	12.313	25.829	109.77	73.16	840	7.386	8.455	14.48	7.62
844	10.78	21.061	95.37	66.65	844	6.478	7.828	20.84	13.87

Appendix E

Comprehensive Results for Effect of Load Current on Fault Location Estimates

Table E.1: Reactance-to-fault estimates for the Takagi and positive-sequence reactance methods (No-load system model)

A: Takagi method					**B: Positive-sequence reactance method**				
Fault at node:	**Actual positive seq. reactance (ohm)**	**Estimated positive seq. reactance (ohm)**	**Error with zero load current (%)**	**Error for reference case (%)**	**Fault at node:**	**Actual positive seq. reactance (ohm)**	**Estimated positive seq. reactance (ohm)**	**Error with zero load current (%)**	**Error for reference case (%)**
814	2.230	2.113	-5.27	-6.68	814	2.230	2.288	2.60	1.42
830	3.459	3.335	-3.62	-4.77	830	3.459	3.509	1.41	0.05
860	5.872	5.726	-2.45	-4.81	860	5.872	5.897	0.45	-3.05
848	7.992	7.833	-1.97	-9.53	848	7.992	7.999	0.12	-8.62
808	1.197	1.135	-5.46	-6.22	808	1.197	1.228	2.33	1.80
832	4.066	3.937	-3.26	-4.25	832	4.066	4.111	1.00	-0.34
840	7.386	7.212	-2.41	-7.75	840	7.386	7.372	-0.24	-7.07
844	6.478	6.334	-2.25	-5.70	844	6.478	6.505	0.38	-4.16

Table E.2: Reactance-to-fault estimates for the Takagi and positive-sequence reactance methods (No-load system model)

A: Loop reactance method					**B: Balanced-load method**				
Fault at node:	**Actual loop reactance (ohm)**	**Estimated loop reactance (ohm)**	**Error with zero load current (%)**	**Error for reference case (%)**	**Fault at node:**	**Actual positive seq. reactance (ohm)**	**Estimated positive seq. reactance (ohm)**	**Error with zero load current (%)**	**Error for reference case (%)**
814	3.605	3.572	-0.92	18.22	814	2.230	2.158	-3.24	29.21
830	5.684	5.652	-0.56	32.47	830	3.459	3.364	-2.77	26.22
860	9.753	9.752	-0.01	62.62	860	5.872	6.240	6.30	14.92
848	13.332	13.389	0.43	72.69	848	7.992	8.249	3.24	7.41
808	1.935	1.916	-0.96	9.26	808	1.197	1.156	-3.64	35.76
832	6.705	6.681	-0.36	39.99	832	4.066	3.961	-2.69	25.33
840	12.313	12.321	0.07	73.16	840	7.386	8.721	18.01	7.62
844	10.78	10.796	0.15	66.65	844	6.478	6.349	-2.02	13.87

Bibliography

[1] Surya Santoso. *Fundamentals of Electric Power Quality.* 2009.

[2] M. Kezunovic and B. Drazenovic-Perunicic. Fault Location. In *Wiley Encyclopedia of Electrical and Electronics Engineering*, 1999.

[3] Distribution Fault Location: Field Data and Analysis. *EPRI, Palo Alto, CA*, 2006.

[4] T. Takagi, Y. Yamakoshi, M. Yamaura, R. Kondow, and T. Matsushima. Development of a New Type Fault Locator Using the One-terminal Voltage and Current Data. In *IEEE Transactions on Power Apparatus and Systems*, 1982.

[5] K. Zimmerman and D. Costello. Impedance-based Fault Location Experience. In *Rural Electric Power Conference, IEEE*, 2006.

[6] A. A. Girgis, C. M. Fallon, and D. L. Lubkeman. A Fault Location Technique for Rural Distribution Feeders. In *IEEE Transactions on Industry Applications*, 1993.

[7] A. L. Dalcastagne and S. L. Zimath. A Study about the Sources of Error of Impedance-based Fault Location Methods. In *Transmission and Distribution Conference and Exposition: Latin America, IEEE/PES*, 2008.

[8] IEEE Guide for Determining Fault Location on AC Transmission and Distribution Lines. *IEEE Std C37.114-2004*, 2005.

[9] W. D. Stevenson Jr. *Elements of Power System Analysis*. 1982.

[10] Y. G. Paithankar and S. R. Bhide. *Fundamentals of Power System Protection*. 2007.

[11] W. H. Kersting. *Distribution System Modeling and Analysis*. 2002.

[12] N. Karnik, S. Das, S. Kulkarni, and S. Santoso. Effect of Load Current on Fault Location Estimates of Impedance-based Methods. In *IEEE PES General Meeting, Detroit*, 2011.

[13] W. H. Kersting. Radial Distribution Test Feeders. In *Power Engineering Society Winter Meeting, IEEE*, 2001.

[14] Manitoba HVDC Research Centre. *Applications of PSCAD/EMTDC*.

[15] Distribution Test Feeder Working Group. IEEE 34 Node Test Feeder. *http://ewh.ieee.org/soc/pes/dsacom/testfeeders/index.html*.

[16] IEEE Standard Requirements for Instrument Transformers. *IEEE Std C57.13-2008*, 2008.

Vita

Neeraj Karnik was born in Pune, India. He obtained a Bachelor of Technology (B. Tech) degree in Electrical Engineering from College of Engineering Pune, in June 2008. After completing his undergraduate education, he worked as a Graduate Engineer Trainee with Schneider Electric India Pvt. Ltd. Since August 2009, he has been working towards his Masters in Electrical Engineering at the University of Texas at Austin under the supervision of Dr. Surya Santoso. He was as an Engineeering Intern at Lower Colorado River Authority (LCRA) in summer 2011. He is currently employed as a Power System Planning Intern at PwrSolutions Inc. in Dallas, TX.

Permanent address: C-7 Shubham Complex, Chinchwad, Pune - 411033, India

This thesis was typed by Neeraj Karnik.